# NAVAL POSTGRADUATE SCHOOL

MONTEREY, CALIFORNIA

# THESIS

INFLUENCE OF ANTARCTIC OSCILLATION ON INTRASEASONAL VARIABILITY OF LARGE-SCALE CIRCULATIONS OVER THE WESTERN NORTH PACIFIC

by

Kenneth R. Burton Jr.

March 2005

| | |
|---|---|
| Thesis Advisor: | Patrick Harr |
| Second Reader: | Russell Elsberry |

Approved for public release; distribution is unlimited.

THIS PAGE INTENTIONALLY LEFT BLANK

| REPORT DOCUMENTATION PAGE | | *Form Approved OMB No. 0704-0188* |
|---|---|---|
| Public reporting burden for this collection of information is estimated to average 1 hour per response, including the time for reviewing instruction, searching existing data sources, gathering and maintaining the data needed, and completing and reviewing the collection of information. Send comments regarding this burden estimate or any other aspect of this collection of information, including suggestions for reducing this burden, to Washington headquarters Services, Directorate for Information Operations and Reports, 1215 Jefferson Davis Highway, Suite 1204, Arlington, VA 22202-4302, and to the Office of Management and Budget, Paperwork Reduction Project (0704-0188) Washington DC 20503. | | |
| 1. AGENCY USE ONLY *(Leave blank)* | 2. REPORT DATE<br>March 2005 | 3. REPORT TYPE AND DATES COVERED<br>Master's Thesis |
| 4. TITLE AND SUBTITLE: Influence of Antarctic Oscillation on intraseasonal variability of large-scale circulations over the western North Pacific. | | 5. FUNDING NUMBERS |
| 6. AUTHOR(S) Kenneth R. Burton Jr. | | |
| 7. PERFORMING ORGANIZATION NAME(S) AND ADDRESS(ES)<br>Naval Postgraduate School<br>Monterey, CA 93943-5000 | | 8. PERFORMING ORGANIZATION REPORT NUMBER |
| 9. SPONSORING /MONITORING AGENCY NAME(S) AND ADDRESS(ES)<br>N/A | | 10. SPONSORING/MONITORING AGENCY REPORT NUMBER |
| 11. SUPPLEMENTARY NOTES The views expressed in this thesis are those of the author and do not reflect the official policy or position of the Department of Defense or the U.S. Government. | | |
| 12a. DISTRIBUTION / AVAILABILITY STATEMENT<br>Approved for public release; distribution is unlimited. | | 12b. DISTRIBUTION CODE |


13. ABSTRACT (maximum 200 words)

This study examines Southern Hemisphere mid-latitude wave variations connected to the Antarctic Oscillation (AAO) to establish connections with the 15- to 25-day wave activity in the western North Pacific monsoon trough region. The AAO index defined from the leading empirical orthogonal functions of 700 hPa height anomalies led to seven distinct circulation patterns that vary in conjunction with the 15- to 25-day monsoon trough mode. For nearly one half of the significant events the onset of 15- to 25-day monsoon trough convective activity coincided with a peak negative AAO index and the peak in monsoon trough convection coincided with a peak positive index. The remaining events either occur when the AAO is not significantly varying or when the AAO-related Southern Hemisphere mid-latitude circulations do not match 15- to 25-day transitions.

When a significant connection occurs between the Southern Hemisphere mid-latitude circulations related to the AAO and the 15- to 25-day wave activity in the western North Pacific monsoon trough, the mechanism is via equatorward Rossby-wave dispersion. When wave energy flux in the Southern Hemisphere is directed zonally, no connection is established between the AAO and the alternating periods of enhanced and reduced convection in the western North Pacific monsoon trough.


| 14. SUBJECT TERMS Antarctic Oscillation, Rossby Wave Dispersion, Large-scale Tropical Circulations, Intraseasonal Variability | | | 15. NUMBER OF PAGES<br>113 |
|---|---|---|---|
| | | | 16. PRICE CODE |
| 17. SECURITY CLASSIFICATION OF REPORT<br>Unclassified | 18. SECURITY CLASSIFICATION OF THIS PAGE<br>Unclassified | 19. SECURITY CLASSIFICATION OF ABSTRACT<br>Unclassified | 20. LIMITATION OF ABSTRACT<br>UL |

NSN 7540-01-280-5500

Standard Form 298 (Rev. 2-89)
Prescribed by ANSI Std. 239-18

THIS PAGE INTENTIONALLY LEFT BLANK

Approved for public release; distribution is unlimited.

# INFLUENCE OF ANTARCTIC OSCILLATION ON INTRASEASONAL VARIABILITY OF LARGE-SCALE CIRCULATIONS OVER THE WESTERN NORTH PACIFIC

Kenneth R. Burton Jr.
Captain, United States Air Force
B.S., Metropolitan State College of Denver, 1998

Submitted in partial fulfillment of the
requirements for the degree of

MASTER OF SCIENCE IN METEOROLOGY

from the

NAVAL POSTGRADUATE SCHOOL
March 2005

Author: Kenneth R. Burton Jr.

Approved by: Patrick Harr
Thesis Advisor

Russell Elsberry
Second Reader

Philip Durkee
Chairman, Department of Meteorology

THIS PAGE INTENTIONALLY LEFT BLANK

# ABSTRACT

This study examines Southern Hemisphere mid-latitude wave variations connected to the Antarctic Oscillation (AAO) to establish connections with the 15- to 25-day wave activity in the western North Pacific monsoon trough region. The AAO index defined from the leading empirical orthogonal functions of 700 hPa height anomalies led to seven distinct circulation patterns that vary in conjunction with the 15- to 25-day monsoon trough mode. For nearly one half of the significant events the onset of 15- to 25-day monsoon trough convective activity coincided with a peak negative AAO index and the peak in monsoon trough convection coincided with a peak positive index. The remaining events either occur when the AAO is not significantly varying or when the AAO-related Southern Hemisphere mid-latitude circulations do not match 15- to 25-day transitions.

When a significant connection occurs between the Southern Hemisphere mid-latitude circulations related to the AAO and the 15- to 25-day wave activity in the western North Pacific monsoon trough, the mechanism is via equatorward Rossby-wave dispersion. When wave energy flux in the Southern Hemisphere is directed zonally, no connection is established between the AAO and the alternating periods of enhanced and reduced convection in the western North Pacific monsoon trough.

THIS PAGE INTENTIONALLY LEFT BLANK

# TABLE OF CONTENTS


I. INTRODUCTION ..... 1
A. OBJECTIVE ..... 1
B. BACKGROUND ..... 2
1. 15- to 25-day Oscillation ..... 2
2. Antarctic Oscillation ..... 7
3. Synopsis ..... 8

II. METHODOLOGY ..... 11
A. DATA ..... 11
B. EMPIRICAL ORTHOGONAL FUNCTION ANALYSIS ..... 11
C. AAO DAILY INDICES ..... 11

III. ANALYSIS ..... 13
A. EOF SPATIAL ANALYSIS ..... 13
1. Background ..... 13
2. Results ..... 13
*a. AAO Structure ..... 13*
*b. EOF 2 Structure ..... 15*
*c. EOF 3 Structure ..... 17*
B. EOF TEMPORAL ANALYSIS ..... 18
1. AAO Daily Index ..... 18
2. AAO Variance ..... 20
3. AAO Persistence ..... 21
4. AAO Spectral Analysis ..... 22
C. 15- TO 25-DAY FILTERED EOF ANALYSIS ..... 23
1. AAO 15- to 25-Day Filtered ..... 24
2. EOF 2 15- to 25-Day Filtered ..... 25
3. EOF 3 15- to 25-Day Filtered ..... 26
4. AAO 15- to 25-Day Zonal Wind Composites ..... 27
D. AAO AND THE 15-TO 25-DAY OSCILLATION ..... 33
1. Frequency Distribution ..... 33
2. Single Event Analysis of the AAO Coinciding with the 15- to 25-Day Oscillation ..... 35
E. COMPOSITES ..... 42
1. 850 hPa Winds and OLR (Group A4) ..... 43
*a. Phase 1 ..... 44*
*b. Phase 2 ..... 46*
*c. Phase 3 ..... 47*
*d. Phase 4 ..... 49*
*e. Phase 5 ..... 51*
*f. Phase 6 ..... 53*
*g. Phase 7 ..... 54*

*h. Phase 8* ..... *55*
2. 200 hPa Winds and OLR (Group A4) ..... 57
*a. Phase 3* ..... *57*
*b. Phase 6* ..... *59*
3. Group C Composites ..... 60
*a. Phase 2* ..... *60*
*b. Phase 6* ..... *63*
4. Group A5 Composites ..... 64
*a. Phase 3* ..... *65*
*b. Phase 7* ..... *67*
5. Group B4 Composites ..... 68
*a. Phase 1* ..... *68*
*b. Phase 5* ..... *70*
6. Group N Composites ..... 72
*a. Phase 3* ..... *72*
7. Group P Composites ..... 74
*a. Phase 2* ..... *74*
*b. Phase 3* ..... *76*

IV. SUMMARY AND CONCLUSION ..... 79
A. SUMMARY ..... 79
B. RELATIONSHIP OF THE AAO AND THE 15- TO 25-DAY OSCILLATION ..... 80
C. HOW THE AAO NEGATIVE TO POSITVE TO NEGATIVE INDEX COINCIDES WITH THE 15- TO 25-DAY WAVE EVENT ..... 83
D. FUTURE STUDY ..... 87

APPENDIX ..... 89

LIST OF REFERENCES ..... 91

INITIAL DISTRIBUTION LIST ..... 93

# LIST OF FIGURES


Figure 1.1 Example of a time series of two SVD coefficients (dark blue and light blue lines) that are approximately in quadrature. Four phases (labeled A- D) are defined based on 90° phase divisions and eight phases (labeled 1- 8) are defined based on 45° phase divisions. Typical 850 hPa wind anomalies over the monsoon trough region of the western North Pacific are defined by the red line (from Delk 2004). ..... 3

Figure 1.2 Mode 2 heterogeneous correlation map for 850 hPa u- and v-correlation coefficients (streamlines, no units) and OLR-correlation coefficients (shaded, no units). Only significant values are plotted (from Delk 2004). ..... 4

Figure 1.3 Tropical cyclone formation location (dots) and tracks (solid lines) for phases 1-2 of the active 15- to 25-day cycle (from Delk 2004)..... 5

Figure 1.4 Tropical cyclone formation location (dots) and tracks (solid lines) for phases 3-4 of the active 15- to 25-day cycle (from Delk 2004)..... 6

Figure 1.5 Tropical cyclone formation location (dots) and tracks (solid lines) for phases 5-6 of the active 15- to 25-day cycle (from Delk 2004)..... 6

Figure 1.6 Tropical cyclone formation location (dots) and tracks (solid lines) for phases 7-8 of the active 15- to 25-day cycle (from Delk 2004)..... 7

Figure 3.1 700 hPa height anomalies (m) from 1979-2003 regressed onto the leading EOF pattern of 700 hPa heights. Contour interval is 5 m. Negative contours are dashed. ..... 14

Figure 3.2 Similar to Figure 3.1 except for the second EOF pattern of 700 hPa heights. ..... 16

Figure 3.3 Similar to Figure 3.1 except for the second EOF pattern of 700 hPa heights. ..... 17

Figure 3.4 Daily time series from 1979-1983 of the AAO index defined as the leading PC of the 700 hPa height anomaly EOF analysis. ..... 19

Figure 3.5 NCEP/CPC monthly time series from 1979-2005 of the AAO index defined as the leading PC of 700 hPa height anomaly EOF analysis. (from NCEP/CPC website 2005) ..... 19

Figure 3.6 Monthly variance (unitless) of the AAO index defined as the leading PC of the 700 hPa height anomaly EOF analysis from 1979-2003. ... 20

Figure 3.7 Box and Whisker diagrams for time persistence (days) for both significant AAO positive and significant AAO negative indices from 1979-2003. The box in the middle of the diagram is bounded by the upper and lower quartiles, and thus locates the central 50% of the data. The center bar through each box represents the persistence median. The whiskers extend away from the box to the two extreme values. ..... 22

Figure 3.8 Fourier power spectrum (solid line) of the daily AAO index defined as the leading PC of the 700 hPa height anomaly EOF analysis from 1979-2003. Upper dashed line (green) is the 99% confidence spectrum and lower dashed line (red) equals the red noise spectrum. ..... 23
Figure 3.9 700 hPa height anomalies (m) from 1979-2003 regressed onto the leading EOF pattern of 15- to 25-day filtered 700 hPa heights. Contour interval is 5 m. Negative contours are dashed. ..... 25
Figure 3.10 Similar to Figure 3.9 except for the second EOF pattern of 700 hPa heights. ..... 26
Figure 3.11 Similar to Figure 3.9 except for the second EOF pattern of 700 hPa heights. ..... 27
Figure 3.12 Composite of average daily 200 hPa zonal winds (m/s) filtered at 15- to 25-days from 1979-2000 for AAO positive days (top) and AAO negative days (bottom). Contour interval is 10 m/s. ..... 28
Figure 3.13 Composite of average daily 200 hPa zonal wind anomalies (m/s) filtered at 15- to 25-days from 1979-2000 for AAO positive days (top) and AAO negative days (bottom). Contour interval is 1 m/s. Negative anomaly contours are dashed. ..... 30
Figure 3.14 Similar to Figure 3.12, except for 850 hPa zonal winds. ..... 31
Figure 3.15 Similar to Figure 3.13, except for 850 hPa zonal winds. ..... 32
Figure 3.16 Frequency distribution for positive values of the AAO index of 15- to 25-day filtered 700 hPa heights for each phase of the 15- to 25-day oscillation from Mar– Oct from 1979-2000. ..... 34
Figure 3.17 Similar to Figure 3.16, except for negative values of the AAO index. . 34
Figure 3.18 Plot of significant daily AAO index versus 15- to 25-day phase as representative of group A. ..... 37
Figure 3.19 Same as Figure 3.18, except as representative of group B. ..... 37
Figure 3.20 Same as Figure 3.18, except as representative of group P. ..... 38
Figure 3.21 Same as Figure 3.18, except as representative of group N. ..... 38
Figure 3.22 Plot of daily AAO index versus 15- to 25-day phase as representative of group C, which does not meet any significant AAO criteria. ..... 39
Figure 3.23 Average daily AAO index values for each 15- to 25-day phase from Mar-Oct between 1979-2000. ..... 39
Figure 3.24 Average daily AAO index values for groups A4 (dashed black) and A5 (solid red) during the 15- to 25-day phase cycle from Mar-Oct between 1979-2000. Vertical bars indicate the standard deviation of the AAO index. ..... 41
Figure 3.25 Similar to Figure 3.24, except for groups B4 and B6. ..... 42
Figure 3.26 Phase 1 composite of 850 hPa streamfunction anomalies (contour interval, $10^6$ $m^2$ $s^{-1}$), significant wind anomalies (arrows) in m $s^{-1}$ (scale at bottom), and OLR anomalies (shaded) in W $m^{-2}$ for group A4. ..... 44

Figure 3.27 Phase 2 composite of 850 hPa streamfunction anomalies (contour interval, $10^6$ $m^2$ $s^{-1}$), significant wind anomalies (arrows) in m $s^{-1}$ (scale at bottom), and OLR anomalies (shaded) in W $m^{-2}$ for group A4. ..... 45
Figure 3.28 Phase 3 composite of 850 hPa streamfunction anomalies (contour interval, $10^6$ $m^2$ $s^{-1}$), significant wind anomalies (arrows) in m $s^{-1}$ (scale at bottom), and OLR anomalies (shaded) in W $m^{-2}$ for group A4. ..... 47
Figure 3.29 Phase 4 composite of 850 hPa streamfunction anomalies (contour interval, $10^6$ $m^2$ $s^{-1}$), significant wind anomalies (arrows) in m $s^{-1}$ (scale at bottom), and OLR anomalies (shaded) in W $m^{-2}$ for group A4. ..... 49
Figure 3.30 Phase 5 composite of 850 hPa streamfunction anomalies (contour interval, $10^6$ $m^2$ $s^{-1}$), significant wind anomalies (arrows) in m $s^{-1}$ (scale at bottom), and OLR anomalies (shaded) in W $m^{-2}$ for group A4. ..... 51
Figure 3.31 Phase 6 composite of 850 hPa streamfunction anomalies (contour interval, $10^6$ $m^2$ $s^{-1}$), significant wind anomalies (arrows) in m $s^{-1}$ (scale at bottom), and OLR anomalies (shaded) in W $m^{-2}$ for group A4. ..... 52
Figure 3.32 Phase 7 composite of 850 hPa streamfunction anomalies (contour interval, $10^6$ $m^2$ $s^{-1}$), significant wind anomalies (arrows) in m $s^{-1}$ (scale at bottom), and OLR anomalies (shaded) in W $m^{-2}$ for group A4. ..... 54
Figure 3.33 Phase 8 composite of 850 hPa streamfunction anomalies (contour interval, $10^6$ in $m^2$ $s^{-1}$), significant wind anomalies (arrows) in m $s^{-1}$ (scale at bottom), and OLR anomalies (shaded) in W $m^{-2}$ for group A4. ..... 55
Figure 3.34 Phase 3 composite of 200 hPa streamfunction anomalies (contour interval, $10^6$ in $m^2$ $s^{-1}$), significant wind anomalies (arrows) in m $s^{-1}$ (scale at bottom), and OLR anomalies (shaded) in W $m^{-2}$ for group A4. ..... 57
Figure 3.35 Phase 6 composite of 200 hPa streamfunction anomalies (contour interval, $10^6$ in $m^2$ $s^{-1}$), significant wind anomalies (arrows) in m $s^{-1}$ (scale at bottom), and OLR anomalies (shaded) in W $m^{-2}$ for group A4. ..... 59
Figure 3.36 Phase 2 composite of 850 hPa streamfunction anomalies (contour interval, $10^6$ $m^2$ $s^{-1}$), significant wind anomalies (arrows) in m $s^{-1}$ (scale at bottom), and OLR anomalies (shaded) in W $m^{-2}$ for group C. ..... 60
Figure 3.37 Phase 2 composite of 200 hPa streamfunction anomalies (contour interval, $10^6$ $m^2$ $s^{-1}$), significant wind anomalies (arrows) in m $s^{-1}$ (scale at bottom), and OLR anomalies (shaded) in W $m^{-2}$ for group C. ..... 62

Figure 3.38 Phase 6 composite of 850 hPa streamfunction anomalies (contour interval, $10^6$ $m^2$ $s^{-1}$), significant wind anomalies (arrows) in m $s^{-1}$ (scale at bottom), and OLR anomalies (shaded) in W $m^{-2}$ for group C. ..... 63
Figure 3.39 Phase 6 composite of 200 hPa streamfunction anomalies (contour interval, $10^6$ $m^2$ $s^{-1}$), significant wind anomalies (arrows) in m $s^{-1}$ (scale at bottom), and OLR anomalies (shaded) in W $m^{-2}$ for group C. ..... 64
Figure 3.40 Phase 3 composite of 850 hPa streamfunction anomalies (contour interval, $10^6$ $m^2$ $s^{-1}$), significant wind anomalies (arrows) in m $s^{-1}$ (scale at bottom), and OLR anomalies (shaded) in W $m^{-2}$ for group A5. ..... 65
Figure 3.41 Phase 7 composite of 850 hPa streamfunction anomalies (contour interval, $10^6$ in $m^2$ $s^{-1}$), significant wind anomalies (arrows) in m $s^{-1}$ (scale at bottom), and OLR anomalies (shaded) in W $m^{-2}$ for group A5. ..... 67
Figure 3.42 Phase 1 composite of 850 hPa streamfunction anomalies (contour interval, $10^6$ in $m^2$ $s^{-1}$), significant wind anomalies (arrows) in m $s^{-1}$ (scale at bottom), and OLR anomalies (shaded) in W $m^{-2}$ for group B4. ..... 69
Figure 3.43 Phase 5 composite of 850 hPa streamfunction anomalies (contour interval, $10^6$ $m^2$ $s^{-1}$), significant wind anomalies (arrows) in m $s^{-1}$ (scale at bottom), and OLR anomalies (shaded) in W $m^{-2}$ for group B4. ..... 70
Figure 3.44 Phase 3 composite of 850 hPa streamfunction anomalies (contour interval, $10^6$ $m^2$ $s^{-1}$), significant wind anomalies (arrows) in m $s^{-1}$ (scale at bottom), and OLR anomalies (shaded) in W $m^{-2}$ for group N. ..... 71
Figure 3.45 Phase 6 composite of 850 hPa streamfunction anomalies (contour interval, $10^6$ $m^2$ $s^{-1}$), significant wind anomalies (arrows) in m $s^{-1}$ (scale at bottom), and OLR anomalies (shaded) in W $m^{-2}$ for group N. ..... 73
Figure 3.46 Phase 2 composite of 850 hPa streamfunction anomalies (contour interval, $10^6$ $m^2$ $s^{-1}$), significant wind anomalies (arrows) in m $s^{-1}$ (scale at bottom), and OLR anomalies (shaded) in W $m^{-2}$ for group P. ..... 74
Figure 3.47 Phase 3 composite of 850 hPa streamfunction anomalies (contour interval, $10^6$ $m^2$ $s^{-1}$), significant wind anomalies (arrows) in m $s^{-1}$ (scale at bottom), and OLR anomalies (shaded) in W $m^{-2}$ for group P. ..... 76

Figure 3.48 Schematic of anomalous wave activity with equatorward propagation in the Southern Hemisphere related to the AAO transition from a negative to positive index (top) during phases 1-3 of the 15- to 25-day cycle and from a positive to negative index (bottom) during phases 5-7 of the 15- to 25-day cycle. This evolution is representative of group A4. Vector lengths indicate relative strength of the anomalous zonal winds in the subtropics (ST) and polar regions. Maximum westerly anomaly is highlighted in red and maximum easterly anomaly is highlighted in blue..... 86
Figure A1 Daily time series from 1984-1988 of the AAO index defined as the leading PC of the 700 hPa height anomaly EOF analysis. ..... 89
Figure A2 Daily time series from 1989-1993 of the AAO index defined as the leading PC of the 700 hPa height anomaly EOF analysis. ..... 89
Figure A3 Daily time series from 1994-1998 of the AAO index defined as the leading PC of the 700 hPa height anomaly EOF analysis. ..... 90
Figure A4 Daily time series from 1999-2003 of the AAO index defined as the leading PC of the 700 hPa height anomaly EOF analysis. ..... 90

THIS PAGE INTENTIONALLY LEFT BLANK

# LIST OF TABLES

Table 3.1 Phase frequencies in number of days of the 15- to 25-day cycle that occurred during each observed group from May-October between during 1979-2000. ..... 43

THIS PAGE INTENTIONALLY LEFT BLANK

# ACKNOWLEDGMENTS

I would like to extend my most sincere appreciation to Professor Pat Harr whose vision and leadership were instrumental in developing this project. Pat, I'm truly grateful for your devoted time and unwavering patience. I wish you the best of luck to you in your future accomplishments.

My continued thanks to Professors Russ Elsberry and Tom Murphree, the zealous passion you have for your respective fields of expertise has been truly inspiring.

To my family, I would not have been able to accomplish this task without you. I am truly blessed to have you in my life. Thank you for your unquestioned love and support.

THIS PAGE INTENTIONALLY LEFT BLANK

# I. INTRODUCTION

## A. OBJECTIVE

The joint U.S. meteorological and oceanographic (METOC) community has shown an explicit interest in improving long-range forecasting capabilities to leverage military operational readiness. The Air Force Weather Strategic Plan and Vision (2004) describes a transformation in how the U.S. and coalition forces will be required to operate in the future. More specifically, we can expect to operate over a full spectrum of operations with a global focus in which situational awareness and decision superiority will be critical at all levels of operational command. One core process outlined in this transformation is the ability to predict and exploit meteorological impacts to military operations on extended time scales.

Due to the long lead-time requirements associated with the planning of various types of military-related operations (e.g., training, exercises, equipment, and troop movement), extended-range forecasts of severe weather are a key component of the planning process. In particular, military operations in the tropical latitudes are highly susceptible to tropical cyclone impacts. Therefore, long-range tropical cyclone forecasting is an intricate challenge facing Navy/Air Force forecasters today. In this case, long-range forecasts encompass time periods greater than five days. Furthermore, the forecast parameters may not be related to an individual tropical cyclone but related to the general level of tropical cyclone activity.

Numerous factors (e.g., scarcity of observations over large ocean basins, various scales of motion present in the tropics, inadequate numerical model resolution, and limited computing power) have made it difficult to completely understand the dynamical processes involved with tropical cyclone formation, especially at extended ranges. Several studies have documented a tendency for tropical cyclone activity to cluster in time, which suggests that large-scale environmental factors may be involved.

The objective of this study is to investigate the role of the Southern Hemisphere Annular Mode known as Antarctic Oscillation (AAO) in modulating intraseasonal wave activity in the western North Pacific during boreal summer. More specifically, the AAO is examined for potential impacts on the Northern Hemisphere 15- to 25-day oscillation that has been shown to modulate tropical cyclone genesis in the western Pacific monsoon trough region (Delk 2004).

## B. BACKGROUND

### 1. 15- to 25-day Oscillation

Delk (2004) identified a statistically significant relationship between 15- to 25-day wave activity and tropical cyclone occurrence in the western North Pacific. Using singular value decomposition (SVD) (Bretherton et al. 1992) of OLR and 850 hPa winds, she identified 15- to 25-day large-scale wave patterns in the western North Pacific during Northern Hemisphere summer. Each period of the 15- to 25-day cycle is divided into eight phases that are 45° apart (Figure 1.1). Individual phase composites were constructed from the leading two SVD modes to define the structural characteristics of the wave patterns. An active period of the 15- to 25-day oscillation is defined when the SVD mode 2 leads SVD mode 1 by 90°.

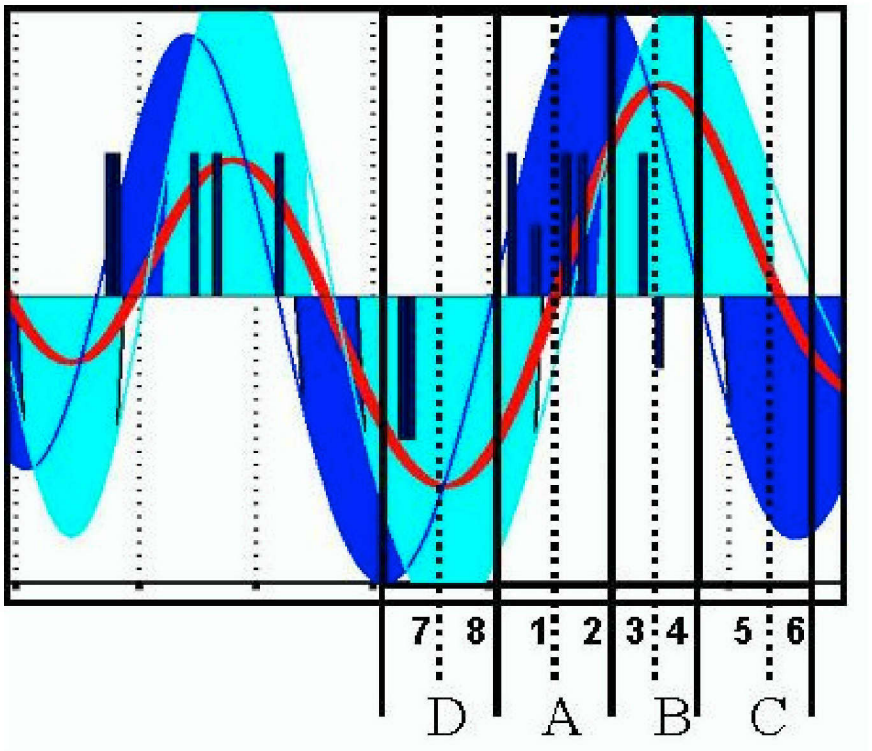


Figure 1.1 Example of a time series of two SVD coefficients (dark blue and light blue lines) that are approximately in quadrature. Four phases (labeled A- D) are defined based on 90° phase divisions and eight phases (labeled 1- 8) are defined based on 45° phase divisions. Typical 850 hPa wind anomalies over the monsoon trough region of the western North Pacific are defined by the red line (from Delk 2004).

The structural characteristics of the SVD mode 2 wave patterns (Figure 1.2) were examined with respect to westward-moving equatorial Rossby waves. These waves were related to enhanced deep convection over the tropical western North Pacific and their propagation into the mid-latitudes. The anomalous heating was responsible for a Rossby-wave response into the western North Pacific mid-latitudes. Delk focused primarily on the contributions of OLR anomalies and zonal wind anomalies that originated over the Philippine Sea. Over the western North Pacific, the wind signature of the 15- to 25-day mode is such that equatorial westerly zonal wind anomalies increase in amplitude and become a part of an enhanced monsoon trough. A connection also appears with a Southern Hemisphere mid-latitude wave train, which may be related to the equatorward penetration of wave energy that then contributes to

the perturbation growth and to areas of anomalous convection over the equatorial western Pacific (Delk 2004). The leading SVD modes were used to identify several wave-like patterns that are related to covariability in equatorial convection and anomalous circulations in the tropics, subtropics, and mid-latitudes. Delk documented that these anomalous wave patterns are related to tropical cyclone activity in the western North Pacific.

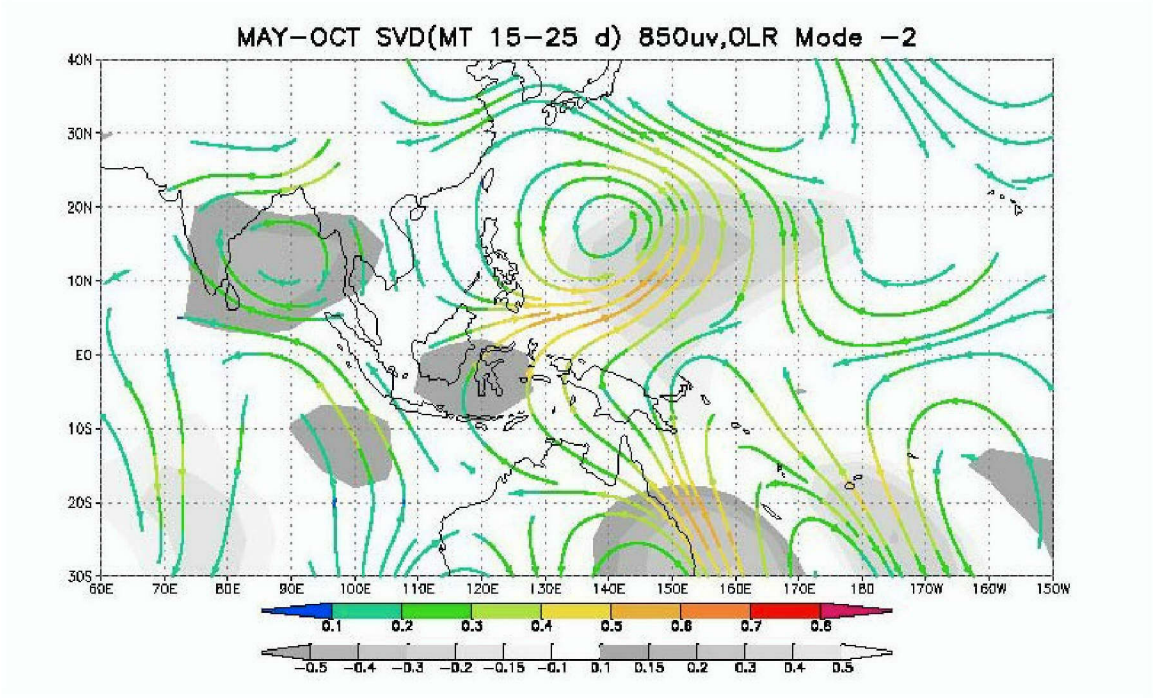


Figure 1.2 Mode 2 heterogeneous correlation map for 850 hPa u- and v-correlation coefficients (streamlines, no units) and OLR-correlation coefficients (shaded, no units). Only significant values are plotted (from Delk 2004).

Tropical cyclone activity was examined by Delk (2004) in relation to the circulation patterns that existed for various phases of the active 15- to 25-day cycle. More than 60% of the tropical cyclones that occurred in the western North Pacific between 1979-2000 formed during the first four phases of the 15- to 25-day cycle (Figures 1.3 - 1.6). Over half of these cyclones formed in the monsoon trough region defined between the equator and 20° N and 120° E to 150° E (Delk 2004). The circulations during the 15- to 25-day cycle not only affected the frequency of tropical cyclone formation, but also impacted the formation location. When anomalous circulation cells associated with enhanced and reduced

convective activity propagated from the southeast to northwest in the western North Pacific, tropical cyclone formation locations shifted accordingly. Note a northward shift in tropical cyclone formation location from phase 1-8 exists. During phase 8, formations reappear over the southeast portion of the domain as the next 15- to 25-day cycle is about to begin.

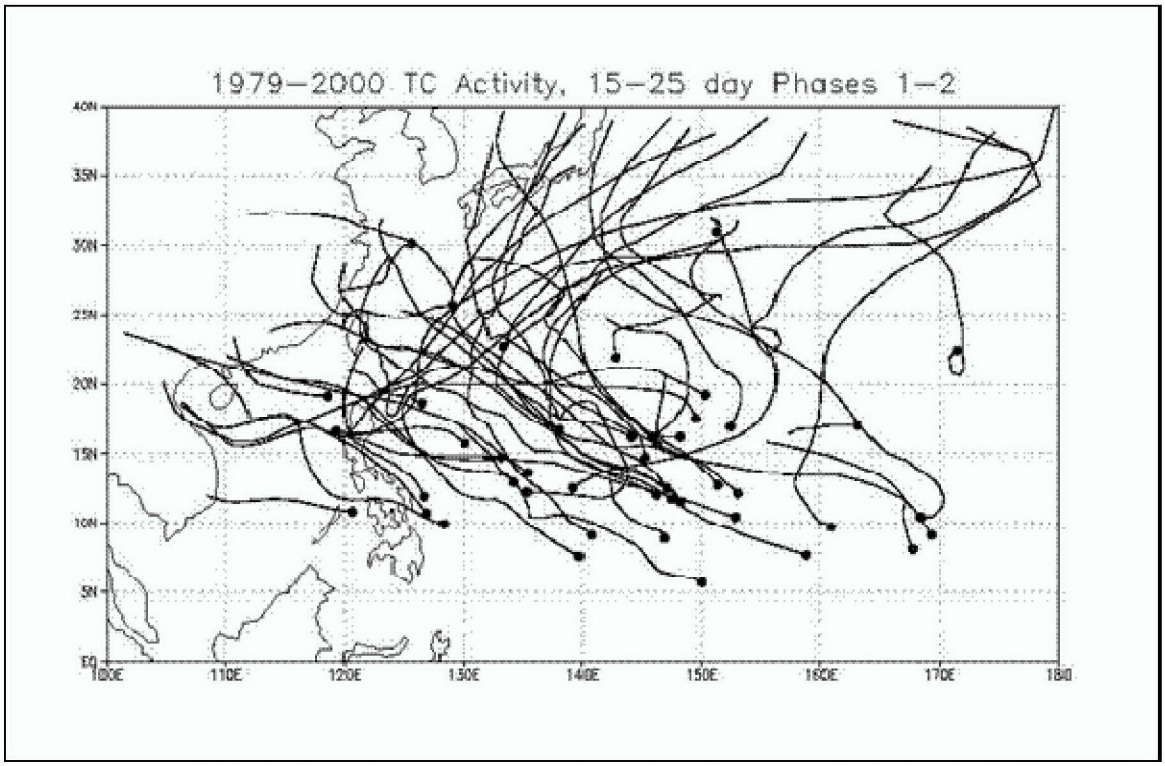


Figure 1.3 Tropical cyclone formation location (dots) and tracks (solid lines) for phases 1-2 of the active 15- to 25-day cycle (from Delk 2004).

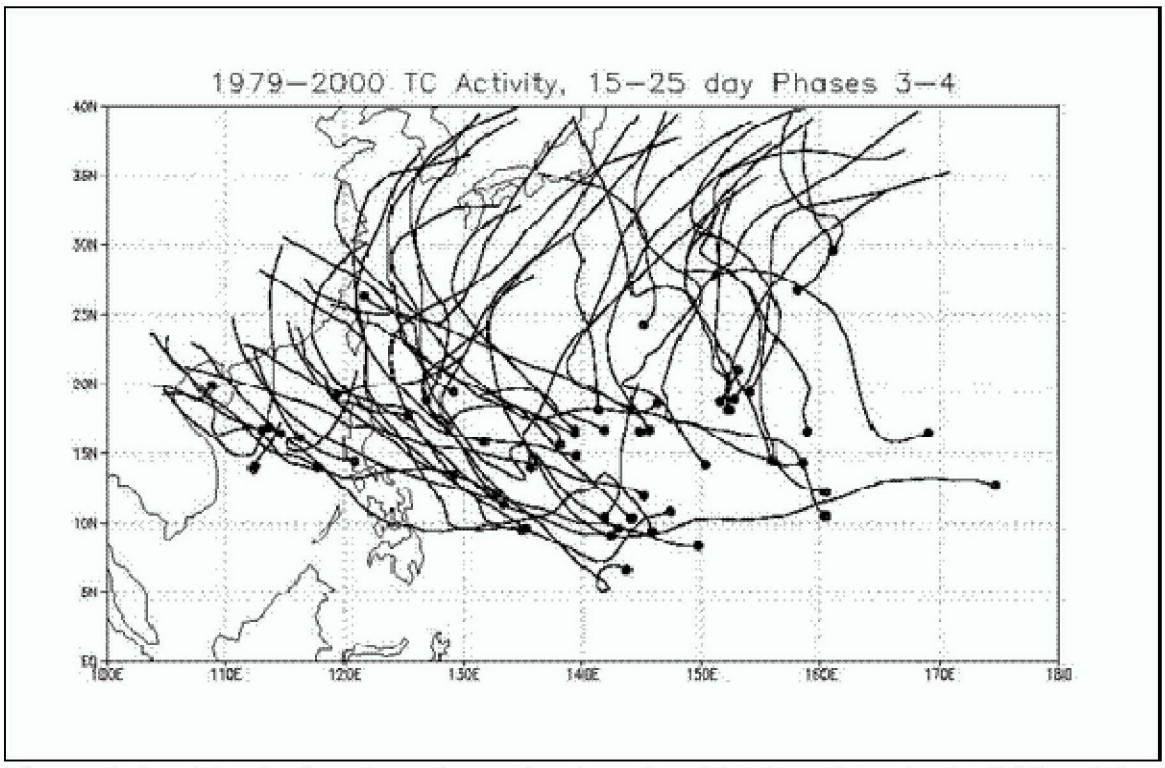


Figure 1.4 Tropical cyclone formation location (dots) and tracks (solid lines) for phases 3-4 of the active 15- to 25-day cycle (from Delk 2004).

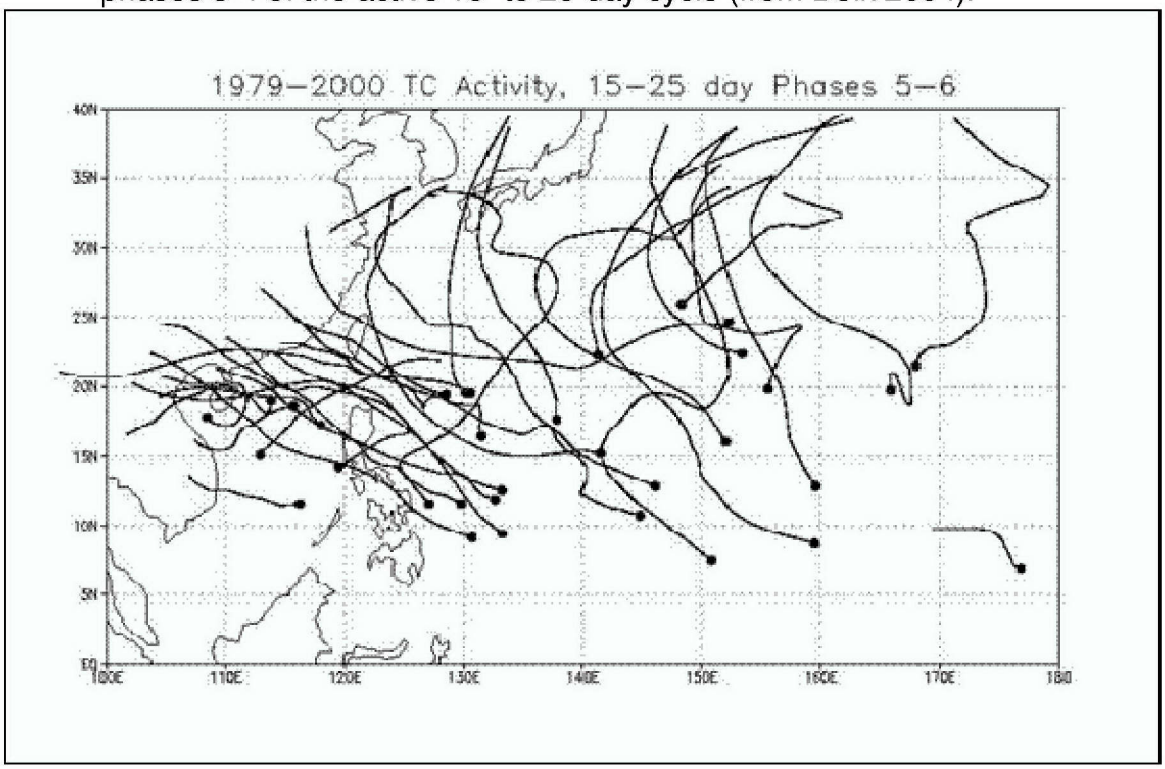


Figure 1.5 Tropical cyclone formation location (dots) and tracks (solid lines) for phases 5-6 of the active 15- to 25-day cycle (from Delk 2004).

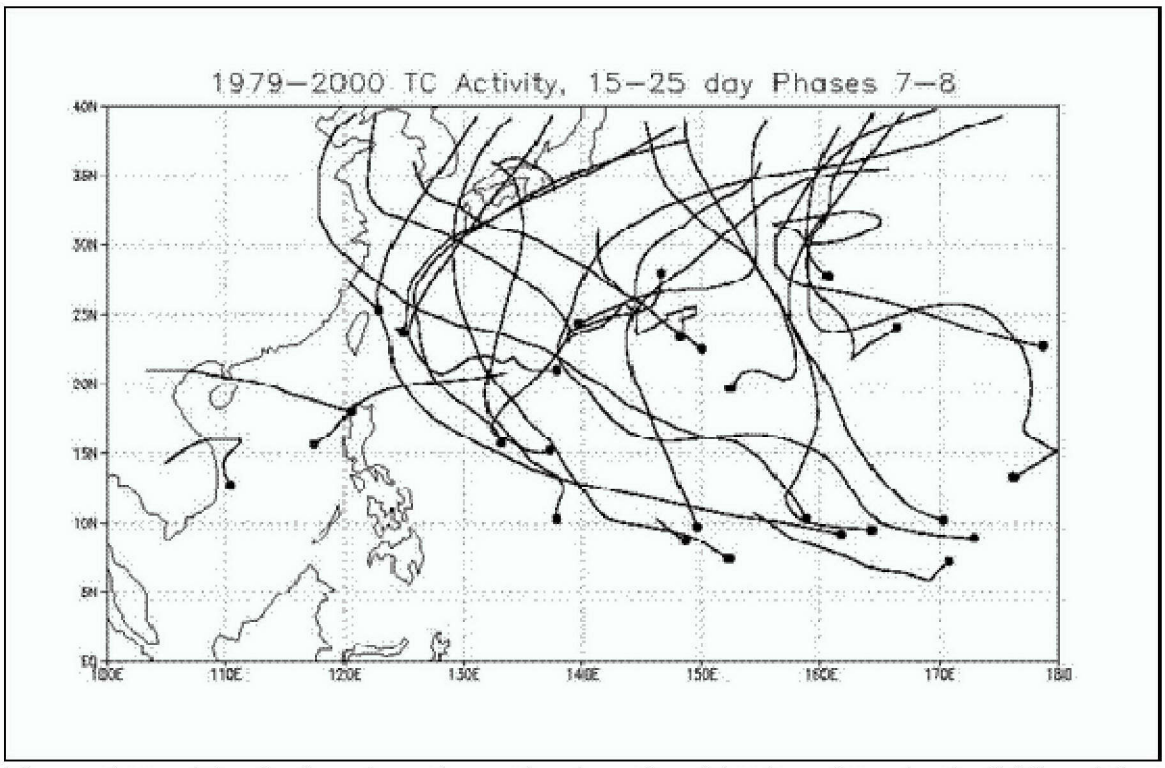


Figure 1.6 Tropical cyclone formation location (dots) and tracks (solid lines) for phases 7-8 of the active 15- to 25-day cycle (from Delk 2004).

### 2. Antarctic Oscillation

The Antarctic Oscillation (AAO) is an annular mode that exists throughout the year and is the leading mode of planetary-scale circulation variability in the Southern Hemisphere. It can be calculated through empirical orthogonal function (EOF) analysis of various atmospheric variables, which will be discussed later in the Methodology section. Kiladis and Mo (1998) characterize the AAO as a zonally symmetric, equivalent barotropic structure, with opposing zonal-wind anomalies over intervals of roughly 20° latitude that involve an exchange of mass between the mid and high latitudes. The typical structure of the AAO consists of a polar vortex surrounded by a high pressure belt and a pronounced dipole pattern in the zonal wind of the mid-latitudes.

In recent years, the AAO has been documented to have significant impacts on the dynamical processes driving tropospheric weather in the Southern Hemisphere. Xue et al. (2004) found the AAO dominates interannual variability of the Mascarene high, which in turn has direct impacts on the strength

of the Somali jet and Indian monsoon westerlies. Similarly, they documented a correlation between the AAO and the Australian high that results in modulations of the associated cross-equatorial flow that further impact the equatorial trade winds in the tropical western Pacific Ocean.

The AAO also has a direct impact on the variability of the Southern Hemisphere jet structure. Hartman and Lo (1998) found that Southern Hemisphere zonal-mean zonal wind composites have distinct wind structures for high and low index phases of the AAO. In the high index, a jet with dual maxima is present at 200 hPa. The most poleward jet maximum is near 60° S and is slightly stronger than the equatorward jet maximum near 30° S. For a low AAO index, a single broad jet of slightly greater peak winds at 200 hPa is near 40° S (Hartman and Lo 1998). Surface wind patterns were characterized by a single westerly jet maximum that shifted from 55° S during the high AAO index to 47.5° S during the low AAO index. Bals-Elsholz et al. (2001) further suggest that the phase of the AAO is correlated to the wintertime Southern Hemisphere split jet and has opposing effects on the strength of the subtropical jet and the polar-front jet.

Shiogama et al. (2004) and Hartman and Lo (1998) studied Southern Hemisphere wave structures driven by variations in the zonal flow associated with the AAO. Both studies suggested that during the poleward transition of the jet, eddy structures had a southeast-northwest tilt and favored equatorward eddy propagation. During the equatorward transition of the jet eddy structures had a more north-south orientation that favored zonal eddy propagation. Most recently, Thompson and Lorenz (2004) found that annular modes such as the AAO have patterns of variability that extend deep into the tropics and even the subtropics of the opposing hemisphere.

## 3. Synopsis

The working hypothesis in this study is that the Southern Hemisphere wave train (Figure 1.2) that is related to the 15- to 25-day active periods of convection in the western Pacific monsoon trough may be related to the AAO.

Periods of high and low AAO index might then be related to tropical cyclone activity over the tropical western North Pacific.

This thesis concentrates on variability of the AAO as it relates to the active convective phase of the 15- to 25-day oscillation. A primary focus will be to examine how the dynamical processes associated with AAO modulate anomalous circulations in the AAO in the Southern Hemisphere. Periods of 15- to 25-day variability of the AAO will be investigated in reference to concurrent periods of 15- to 25-day wave activity in the western North Pacific monsoon trough region. The concluding section will examine the physical mechanisms that potentially link the AAO to periods of enhanced and reduced convection in the monsoon trough associated with the 15- to 25-day oscillation.

THIS PAGE INTENTIONALLY LEFT BLANK

# II. METHODOLOGY

## A. DATA

The data used for this study are 2.5° latitude by 2.5° longitude global gridded reanalysis fields (Kalnay et al. 1996) from the National Centers for Environmental Prediction/National Center for Atmospheric Research (NCEP/NCAR) for the years 1979-2003. Analyzed fields include heights, winds, temperature, relative humidity, and vertical velocity. Outgoing long-wave radiation (OLR) data (Liebmann et al. 1996) on a 2.5° latitude by 2.5° longitude grid are used as a proxy for deep convection. The daily grid values were averaged over the 25 years to determine the climatological mean annual cycle. Daily anomalies for each field were then calculated by subtracting the daily long-term mean from the raw data. The data fields were filtered with a Lanczos filter (Duchon 1979) to isolate 15- to 25-day disturbances.

## B. EMPIRICAL ORTHOGONAL FUNCTION ANALYSIS

Empirical orthogonal function (EOF) analysis (Lorenz 1956) was used to reduce the dimensionality of circulation patterns of 700 hPa heights in the Southern Hemisphere. The purpose of using the EOF technique was to identify the underlying structure of the AAO with respect to the overall variability in the 25 years of daily data. An advantage of this technique is the ability to extract patterns that explain the maximum variance from a data set and allow for multivariate analysis of meteorological fields in both space and time. For the purpose of this study, an S-mode EOF analysis (Richman 1986) was performed such that the structures of the EOFs were defined in the spatial domain while time was the sampling dimension over which the principal components (PCs) are defined. The PCs define the amount of each EOF structure that is contained in the original daily data set.

## C. AAO DAILY INDICES

Daily AAO indices between 1979-2003 were defined by the EOF PCs as is done by the National Centers for Environmental Prediction/Climate Prediction Center (NCEP/CPC) for monthly data sets. Similar indices calculated by the

NCEP/CPC such as that of the Arctic Oscillation are based on 1000 hPa anomalies. Due to varying terrain in the Antarctic, daily 700 hPa height anomalies are projected onto the leading EOF structure of the AAO in the NCEP/CPC analysis and in this study. These indices were then used to determine the strength and phase of the AAO for the period studied.

# III. ANALYSIS

## A. EOF SPATIAL ANALYSIS

### 1. Background

Large-scale structure and variability of the Southern Hemisphere atmosphere were identified by performing an EOF analysis on 25 years of daily 700 hPa height anomaly data. The NCEP/NCAR reanalysis data were gridded with five degree latitudinal separation between 20°S and 90°S and a 10° longitudinal separation around the globe. The resulting data array is $\mathrm{X}_{M,N}$, where $M$ represents the space domain consisting of 540 grid points (36 points in Lon. x 15 points in Lat.) and $N$ represents the time domain of 9125 daily time steps (25 years x 365 days/year). A covariance matrix, $\mathrm{C} = \mathrm{X}\mathrm{X}^{\mathrm{T}} = \mathrm{C}_{M,M}$, was calculated to determine the degree to which each daily 700 hPa height anomaly is related to every other. The EOF analysis of the covariance matrix resulted in eigenvectors that define the orientation at which the data jointly exhibit a maximum amount of variation. Principal components were then computed by projecting each eigenvector on the original anomaly field. By definition, the first EOF describes the greatest amount of variability and represents the predominant anomalous structure of the data being sampled. Subsequent EOFs are the structures that explain progressively smaller amounts of the variance than the previous EOF.

### 2. Results

EOFs were computed for the Southern Hemisphere poleward of 20° S and the 700 hPa height anomalies were regressed onto the EOF patterns. Each regression plot indicates a significant spatial structure in the 700 hPa height anomalies and has the same units as the anomaly field. The first three EOFs explain approximately 33% of the variance in the original data set.

#### *a. AAO Structure*

The leading EOF of 700 hPa height anomalies in the Southern Hemisphere (Figure 3.1) explains 22% of the total variance. This structure is similar to the leading EOF of the Southern Hemisphere 850 hPa heights depicted

in Thompson and Wallace (2000) and to the loading pattern of the AAO as described by the Climate Prediction Center (CPC)

(http://www.cpc.ncep.noaa.gov/products/precip/CWlink/daily_ao_index/aao/aao.loading.html).

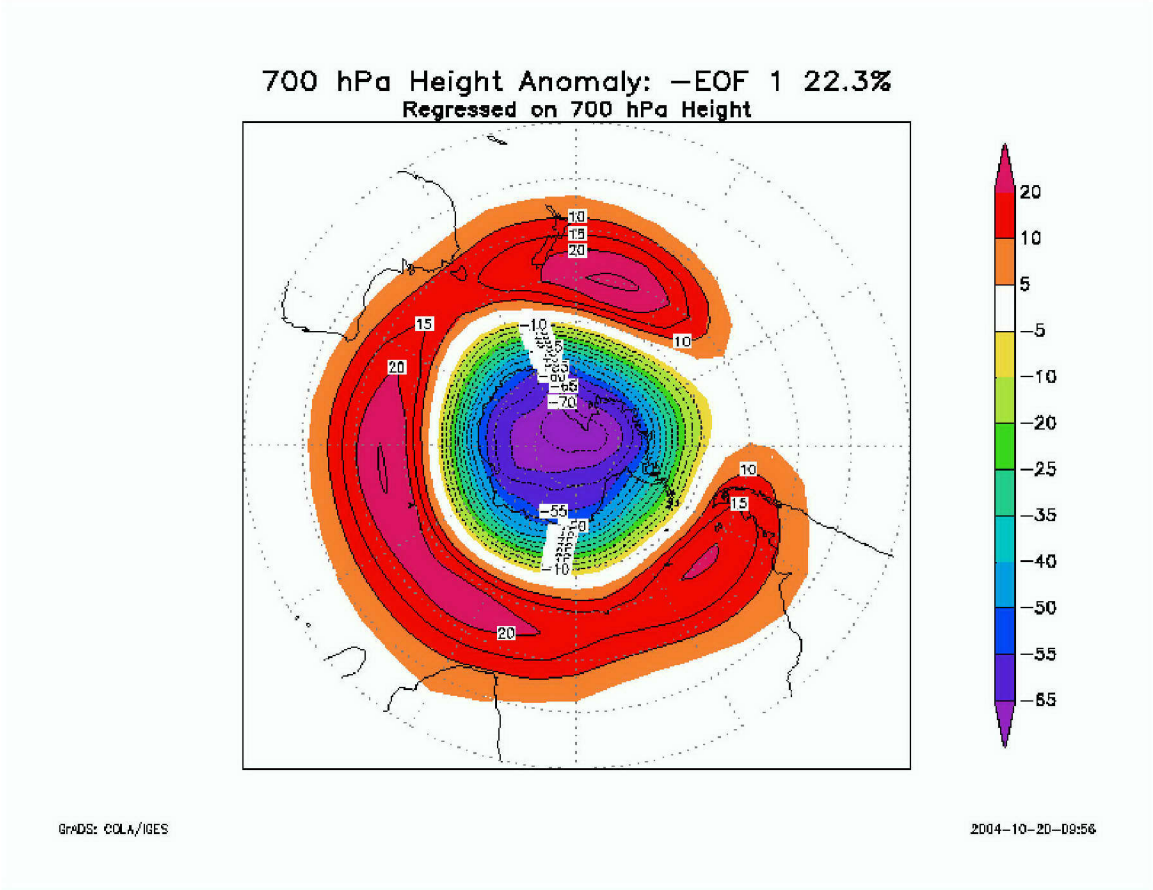


Figure 3.1 700 hPa height anomalies (m) from 1979-2003 regressed onto the leading EOF pattern of 700 hPa heights. Contour interval is 5 m. Negative contours are dashed.

The variability in the geopotential height field is zonally symmetric with a large polarity between the polar latitudes (> 60°S) and the mid-latitudes (45°- 60°S). The AAO is characteristic of a meridional seesaw of pressure anomalies between the polar region and the mid-latitudes that results in strengthening and weakening flow patterns. Figure 3.1 depicts the “high index” polarity (Thompson and Lorenz 2004) and from here forth will be referred to as the positive phase of the AAO. An anomalous polar vortex exists over Antarctica with a minimum

height anomaly of -70 m over the South Pole. An area of anomalous positive height anomalies between 45°- 60°S surrounds the polar low. Three positive height anomaly centers are depicted in the annular mode with maximum height anomalies of +25 meters over the central South Indian Ocean, South Pacific Ocean east of New Zealand, and South Atlantic Ocean near the Falkland Islands. The increased pressure gradient between the mid-latitude and polar regions during the positive phase of the AAO results in anomalously strong westerly zonal flow. In the negative phase of the AAO (not shown), anomalously high geopotential 700 hPa heights are found near the pole and are surrounded by a belt of anomalously low geopotential heights in the mid-latitudes. The weakened gradient between the polar region and mid-latitudes results in weaker than normal westerly zonal flow. Therefore, the AAO forcing of the dominant zonal flow in the Southern Hemisphere mid-latitudes is likely to have numerous impacts on modulating mid-latitude weather.

*b. EOF 2 Structure*

The second EOF (Figure 3.2) has a separate spatial structure of 700 hPa height anomalies in the Southern Hemisphere that explains 6% of the total variance. This pattern bears no resemblance to the annular mode of EOF 1 as it consists of an apparent anomalous Rossby-wave train that covers much of the Southern Hemisphere mid-latitudes. The wave train appears as a zonal wave number three with three positive height anomaly centers and three negative height anomaly centers The strongest 700 hPa height anomalies (+90 m) are centered over the central South Pacific along the Antarctic Circle. The area of increased height anomalies is surrounded by significant height falls (-35 m) east of New Zealand and (-50 m) over the Antarctic Peninsula. These results were similar to Kiladis and Mo (1998) who linked the source of this wave train to the strengthening or weakening of the South Pacific trough east of New Zealand with an opposing anomaly to the north of western Antarctica. They also indicated anomalous downstream centers exist north of the Antarctic Peninsula and along the east coast of South America. Similar to the leading EOF, EOF 2 is present throughout the year and is most common in the winter months. This anomalous

structure has a strong connection to atmospheric variability on both interannual timescales, associated with El Nino Southern Oscillation (ENSO) events, and intraseasonal timescales (Kiladis 1998).

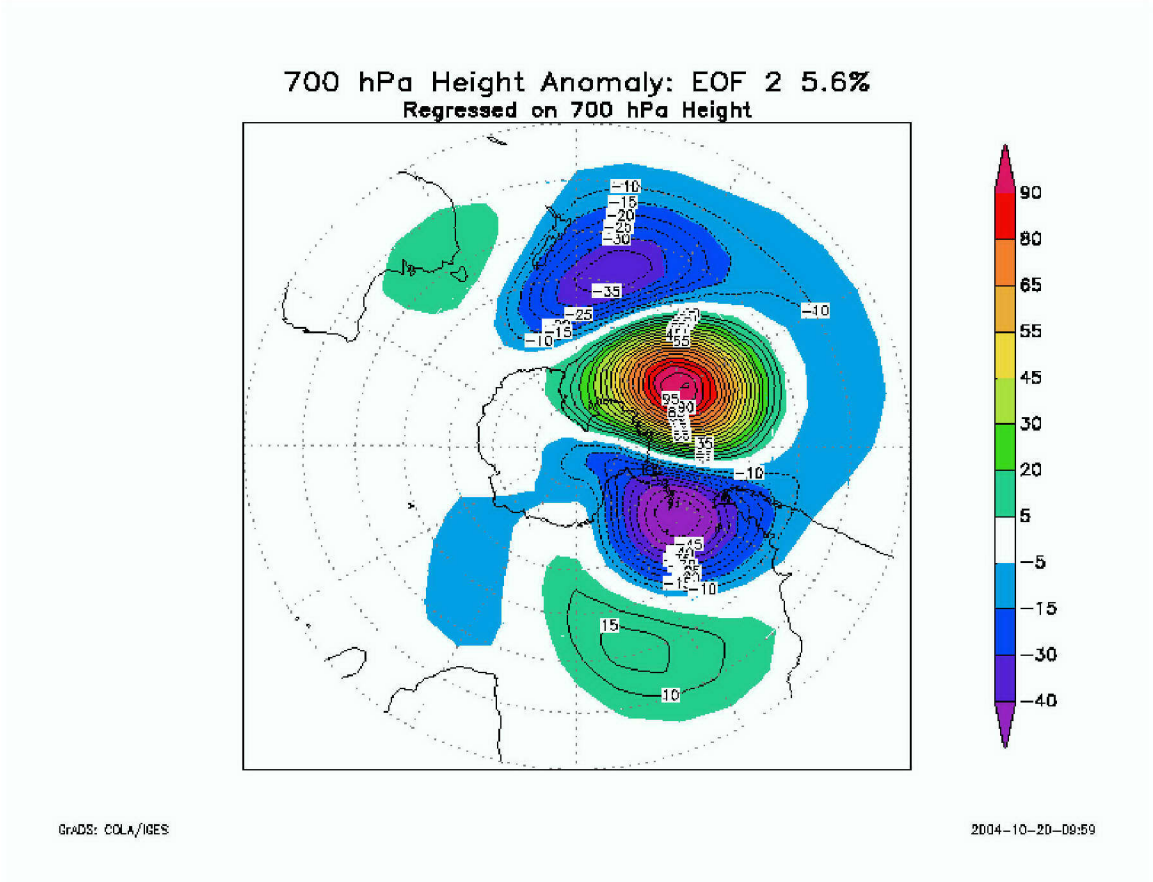


Figure 3.2 Similar to Figure 3.1 except for the second EOF pattern of 700 hPa heights.

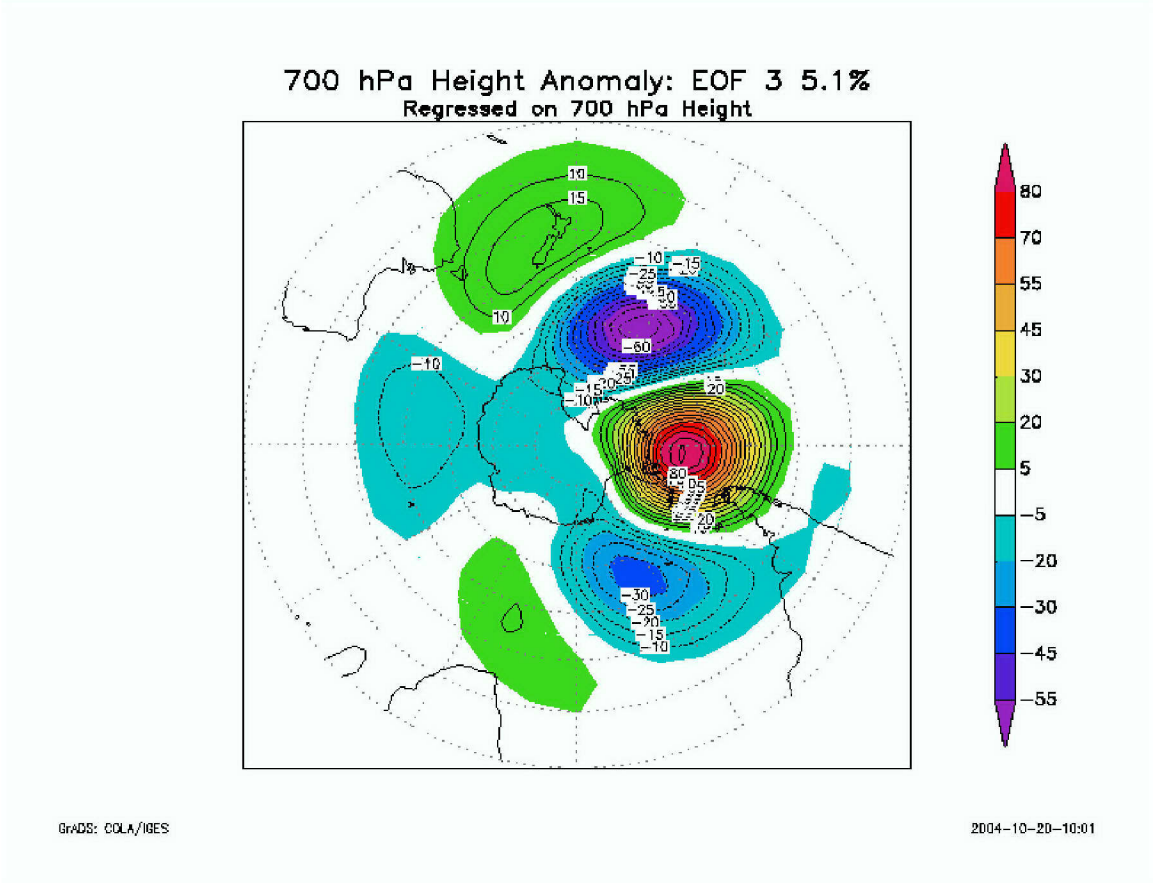


Figure 3.3 Similar to Figure 3.1 except for the second EOF pattern of 700 hPa heights.

### *c. EOF 3 Structure*

The third EOF (Figure 3.3) is similar to EOF 2 in that it depicts a Rossby-wave pattern in the 700 hPa height anomalies that explains 5% of the total variance. Although the wave train appears as a zonal wave number three, the strongest 700 hPa height anomalies (+80 m) are now centered over the Antarctic Peninsula. Adjacent areas of negative height anomalies (-60 m) are over the central South Pacific Ocean and (-30 m) over the South Atlantic Ocean. The pattern similarities between EOF2 and EOF3 are such that anomalous height centers are approximately in quadrature with comparable magnitudes. These characteristics are an indication of Rossby-wave propagation through the Southern Hemisphere mid-latitudes that has an eastward phase speed from a source region over the South Pacific Ocean.

## B. EOF TEMPORAL ANALYSIS

To assess the connection between the AAO and intraseasonal oscillations on a 15- to 25-day timescale, daily AAO indices had to be calculated. Daily AAO indices were constructed by projecting the daily 700 hPa height anomalies poleward of 20°S onto the loading pattern of each EOF. Indices were normalized by the overall variance as defined by the eigenvalues of the EOF analysis. Positive index anomalies are related to the EOF pattern depicted in Figure 3.1 of the leading EOF. A negative index is representative of the opposite pattern depicted in Figure 3.1.

### 1. AAO Daily Index

Unfiltered daily AAO index values were plotted for years 1979-2003 to indicate both duration and magnitude of 700 hPa geopotential height anomalies contributing to the dominant AAO structure. The daily time series displayed in Figure 3.4 indicate alternating periods of positive or negative phases of the AAO from 1979-1983. Complete daily time series for 1984-2003 are shown in the appendix. Significant positive (negative) values of AAO index were defined when the index value was greater (less than) one standard deviation, which is 1.0017. This analysis of the AAO daily time series identified periods of significant AAO activity between 1979-2003 which will be used as to determine the potential linkage between the AAO and the 15- to 25-day mode. Note that daily AAO indices calculated in this study compared quite well with monthly AAO indices derived by the NCEP/CPC (Figure 3.5).

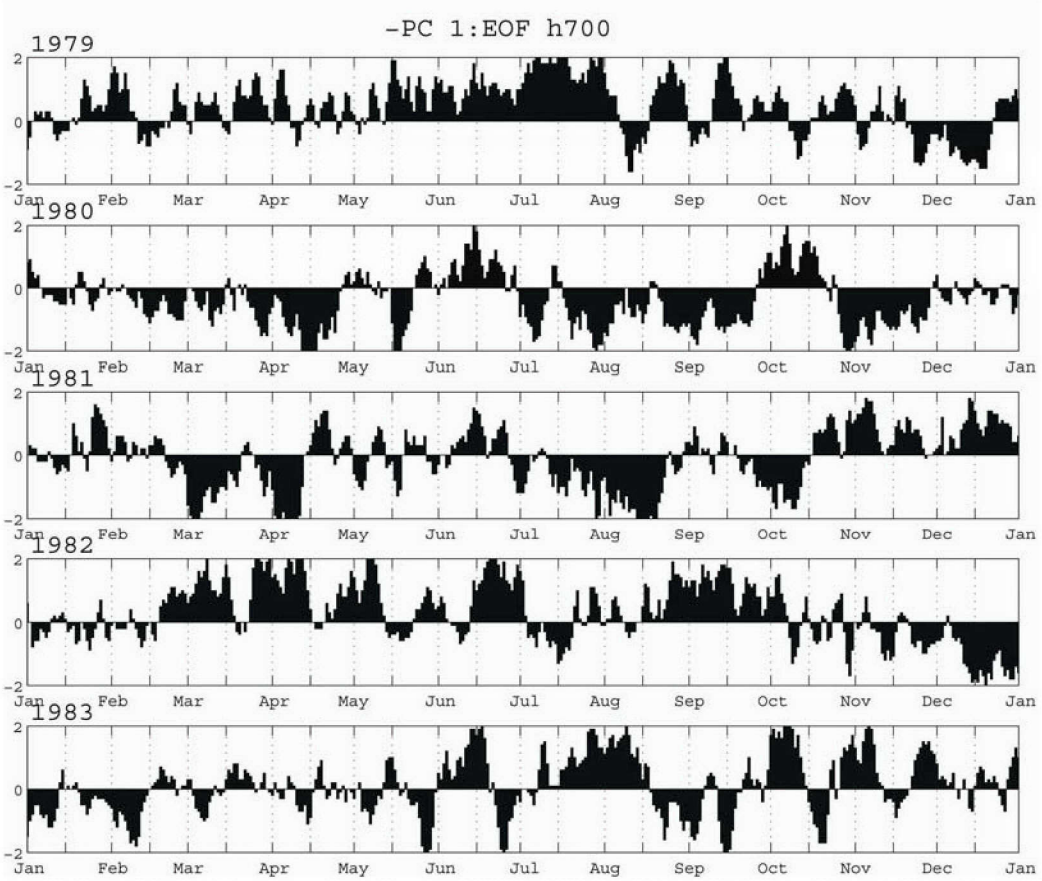


Figure 3.4 Daily time series from 1979-1983 of the AAO index defined as the leading PC of the 700 hPa height anomaly EOF analysis.

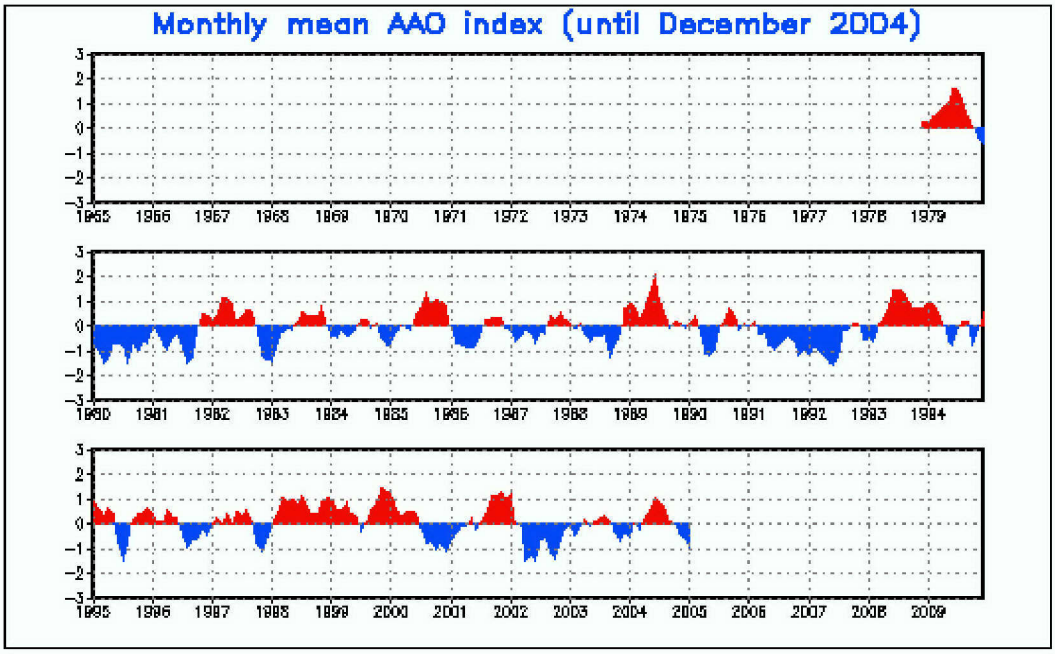


Figure 3.5 NCEP/CPC monthly time series from 1979-2005 of the AAO index defined as the leading PC of 700 hPa height anomaly EOF analysis. (from NCEP/CPC website 2005)

2. AAO Variance

Monthly variances of the daily AAO index were examined to determine the seasonal nature of the AAO for the years 1979-2003 (Figure 3.6). The maximum variability in the AAO occurred between the months of May and October. In fact, the average monthly variance between Jan-Mar is nearly doubled in both May-Jul and Aug-Oct time periods. The largest individual variability was coexistent with the peak of the austral winter in July. These results are consistent with those of Thompson and Wallace (2000) who recorded higher amplitudes during the Southern Hemisphere cold season from May-Oct. In fact, the AAO index varies most during the Northern Hemisphere summer months for which Delk (2004) observed a Southern Hemisphere wave-train that possibly impacts the 15- to 25-mode in the western North Pacific Ocean. Such variations in the strength and duration of the AAO during this period will be examined for potential modulation of the 15- to 25-day convective cycle of the monsoon trough.

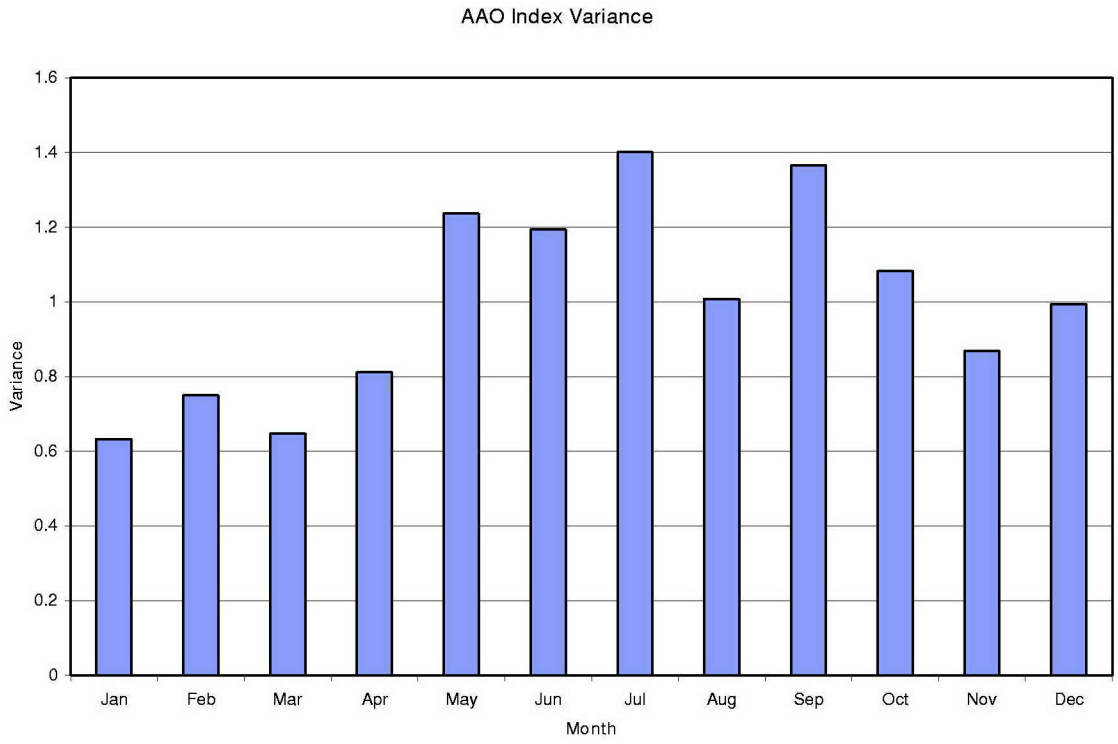


Figure 3.6 Monthly variance (unitless) of the AAO index defined as the leading PC of the 700 hPa height anomaly EOF analysis from 1979-2003.

### 3. AAO Persistence

AAO indices were examined for episodes of persistent positive and negative events indicating the time scales of significant AAO forcing events. An AAO positive (negative) day was defined when the AAO index value was greater (less) than or equal to one standard deviation. Persistence was defined as the total number of consecutive days in an AAO positive (negative) regime. To categorize persistent events, consecutive events were viewed as independent episodes when separated by two or more days. In general, the relative frequency of persistent events decreased rapidly as the duration of events increased. The median persistence for both AAO positive and AAO negative events was 3 days. A total of 1323 days with a significant AAO positive index were included in 227 independent events, so that the mean persistence time for AAO positive events was 4.54 days. For AAO negative events, there were a total of 1351 days included in 208 independents events with a mean persistence time of 4.16 days. A Box and Whisker diagram (Figure 3.7) was constructed to present a quick comparison between the AAO positive and AAO negative persistence distributions. Most AAO events have durations between two and seven days in length, which might suggest that the AAO has a strong connection to synoptic disturbances. Extreme values on the order of 25 to 30 days implicate possible monthly or seasonal forcing of the AAO.

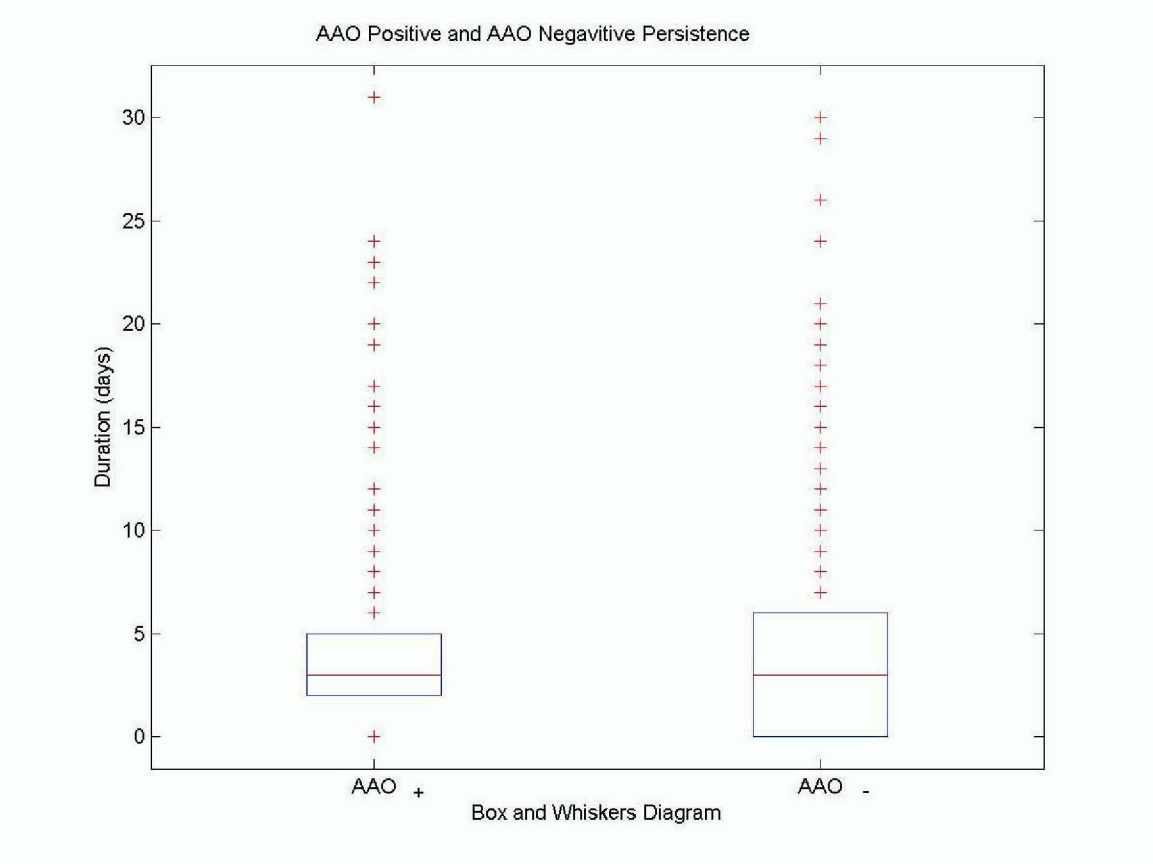


Figure 3.7 Box and Whisker diagrams for time persistence (days) for both significant AAO positive and significant AAO negative indices from 1979-2003. The box in the middle of the diagram is bounded by the upper and lower quartiles, and thus locates the central 50% of the data. The center bar through each box represents the persistence median. The whiskers extend away from the box to the two extreme values.

## 4. AAO Spectral Analysis

A Fourier transform was performed on the original AAO time series data to examine the frequency oscillation of AAO variance. The Fourier power spectrum (Figure 3.8) of the first EOF of 700 hPa anomalies shows significant variance on interannual, annual, and intraseasonal scales. Several studies discuss the role of the AAO on the variability of the atmosphere on interannual scales due to the El Nino Southern Oscillation (Kiladis and Mo 1998), and intraseasonal scales greater than 30 days due to the Madden-Julian Oscillation (Miller et al. 2003, Thompson et al. 2000). However, little attention has been given to intraseasonal variability in the 15- to 25-day range, which also has significant spectral power in Figure 3.8 and might correspond with the 15- to 25-day wave frequency of the

monsoon trough (Delk 2004). In the following section, the AAO structure will be examined with respect to its variability over 15- to 25-day time scales.

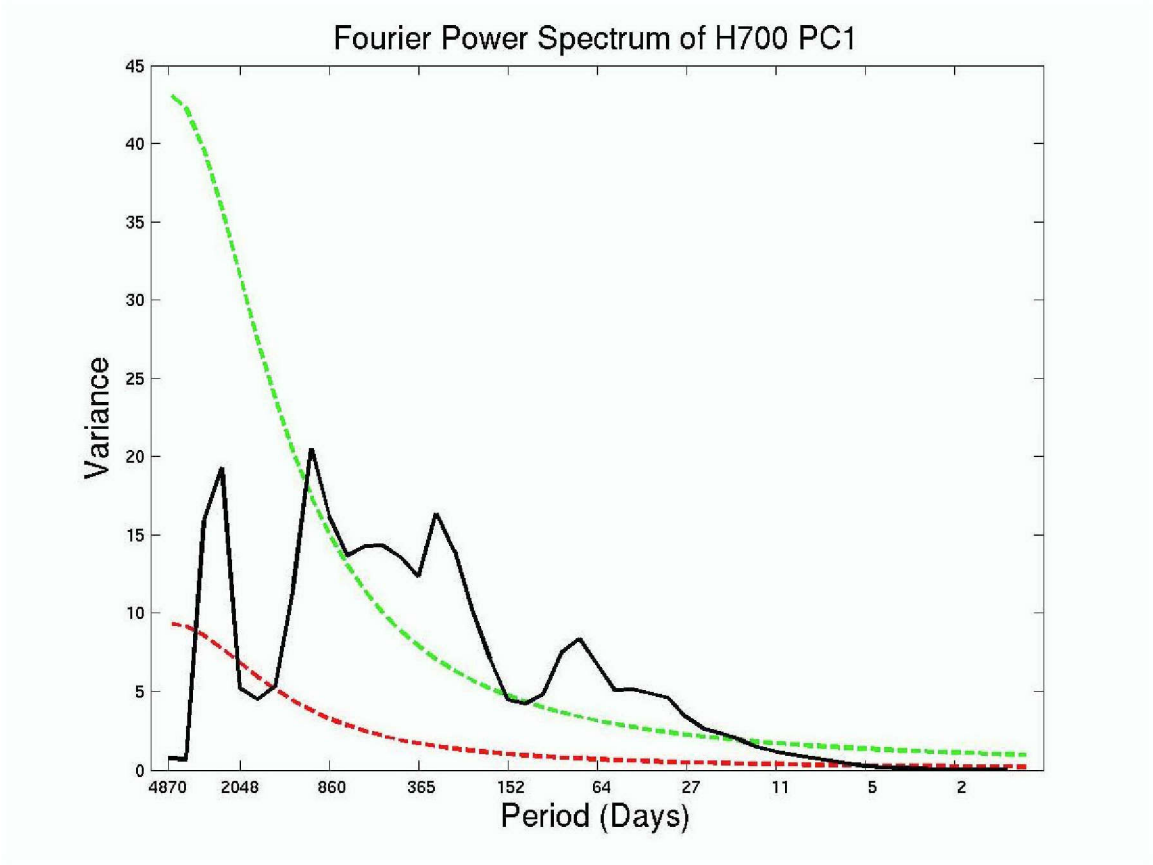


Figure 3.8 Fourier power spectrum (solid line) of the daily AAO index defined as the leading PC of the 700 hPa height anomaly EOF analysis from 1979-2003. Upper dashed line (green) is the 99% confidence spectrum and lower dashed line (red) equals the red noise spectrum.

## C. 15- TO 25-DAY FILTERED EOF ANALYSIS

A second AAO index was computed to highlight intraseasonal variations on the order of 15- to 25-days in the Southern Hemisphere. The original NCEP/NCAR reanalysis 700 hPa geopotential height anomaly data were filtered with a Lanczos filter (Duchon 1979) to retain only variations on the 15- to 25-day timescale. For the case of filtered data, the period 1979-2000 was used to be consistent with the period studied by Delk (2004). An EOF analysis was then performed on the filtered data using the same process described in the beginning of this section. The leading principal component was computed from the filtered

EOFs and the filtered height data to define a 15- to 25-day AAO index. The first three EOF space patterns explained 38% of the total variance.

1. AAO 15- to 25-Day Filtered

The first EOF (Figure 3.9) defines the structure of AAO 15- to 25-day index and explains 19% of the total daily variance. That is, the 15- to 25-day filtered AAO has a similar structure to that of the unfiltered AAO (Figure 3.1). An anomalous polar vortex centered over Antarctica is surrounded by a ring of anomalous positive height anomalies in the mid-latitudes. In this belt of positive height anomalies, three cells are over the south central Indian Ocean, South Pacific Ocean east of New Zealand, and South Atlantic Ocean east of southern South America. The magnitudes of the regressed AAO 15- to 25-day filtered anomalies are 40-50 m smaller over the polar region and 10-15 m smaller in the mid-latitudes than the unfiltered anomalies.

The zonally symmetric structure of the AAO on the 15- to 25-day intraseasonal timescale continues to display strong dynamic support to the strengthening and weakening of mid-latitude westerlies. Therefore, the AAO on the 15- to 25-day timescale is likely to contribute significantly to perturbations in the mid-latitude zonal flow. As an equivalent barotropic structure, the signal of anomalous heights at 700 hPa related to the AAO can be expected to persist vertically throughout the troposphere. In section 4, 850 hPa and 200 hPa zonal winds and zonal wind anomalies will be examined with respect to the phase of the AAO. It is hypothesized that the forcing of the mid-latitude jets in both the upper and lower levels of Southern Hemisphere troposphere play a large part in developing the anomalous mid-latitude wave train documented by Delk (2004) and contribute to the overall strengthening and weakening of the monsoon trough in the Northern Hemisphere.

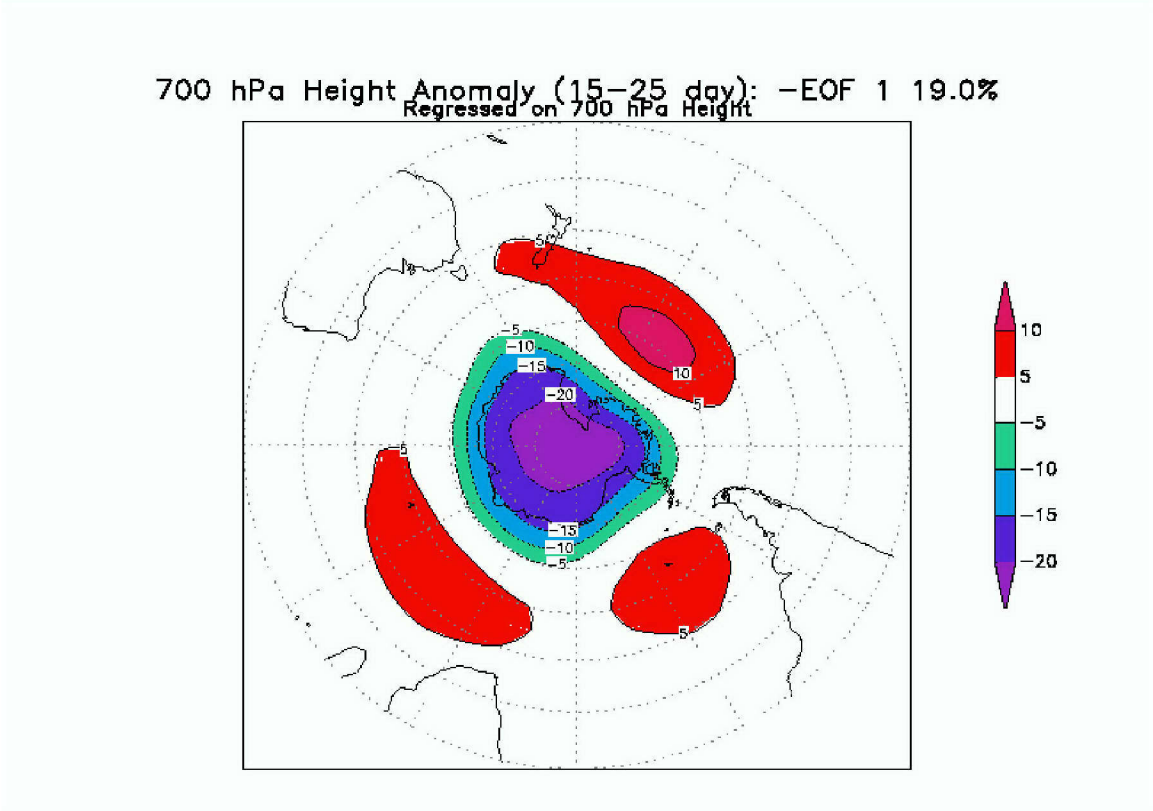


Figure 3.9 700 hPa height anomalies (m) from 1979-2003 regressed onto the leading EOF pattern of 15- to 25-day filtered 700 hPa heights. Contour interval is 5 m. Negative contours are dashed.

2. EOF 2 15- to 25-Day Filtered

The second filtered EOF (Figure 3.10), which explains 10% of the total daily variance, is similar to the unfiltered EOF 2 structure (Figure 3.2) and consists of an anomalous Rossby-wave train that covers much of the Southern Hemisphere mid-latitudes. The wave train appears as a zonally symmetric wave four pattern with alternating anomaly height centers. Kiladis and Mo (1998) found a very similar wave four structure for EOF 2 of 10-50 day filtered Southern Hemisphere 500 hPa geopotential height anomalies from 1973 through 1995. This pattern will lead to significant mass transport between the polar region and lower latitudes with the greatest mass transport in the South Pacific Ocean.

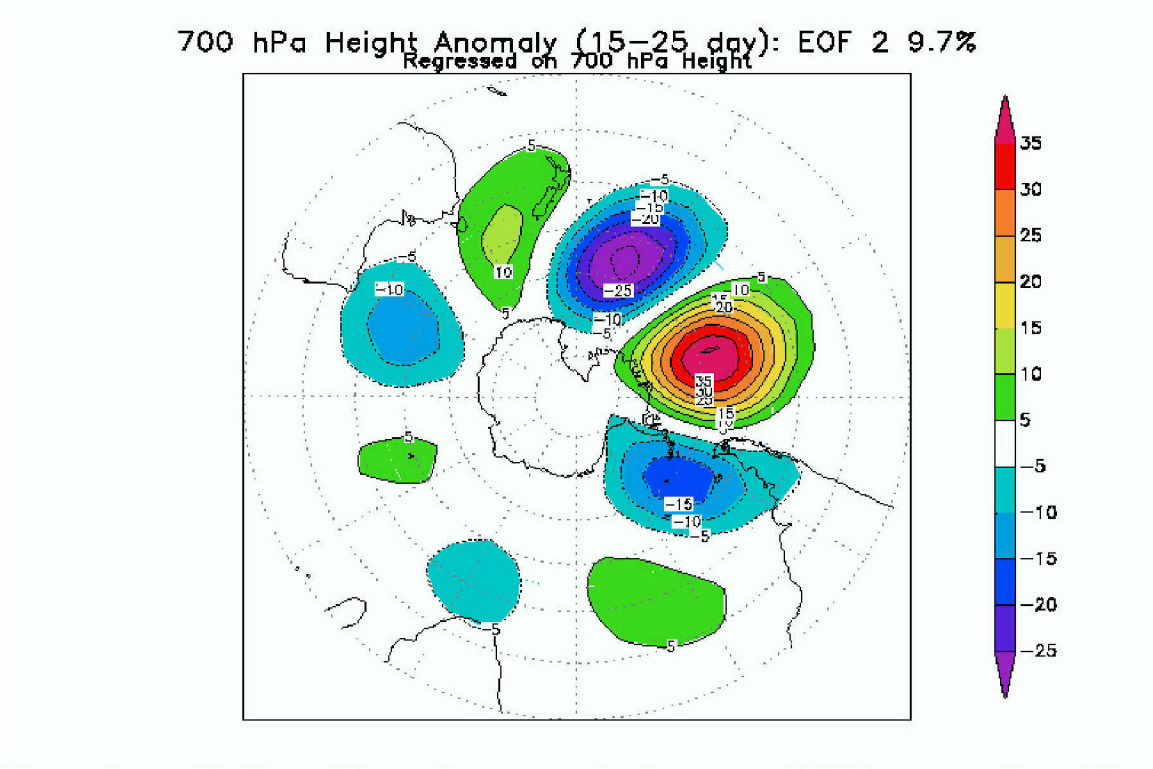


Figure 3.10 Similar to Figure 3.9 except for the second EOF pattern of 700 hPa heights.

3. EOF 3 15- to 25-Day Filtered

The third filtered EOF (Figure 3.11), which explains 9% of the total daily variance, is similar to the structure of EOF 2 of 15- to 25-day filtered height anomalies (Figure 3.10). However, the EOF 3 Rossby-wave pattern in the 700 hPa height anomalies appears to be in spatial quadrature with that of EOF 2. The wave train has a zonal wave four structure with the strongest 700 hPa height anomalies propagating through the South Pacific Ocean. Adjacent wave perturbations are zonally symmetric throughout the mid-latitudes.

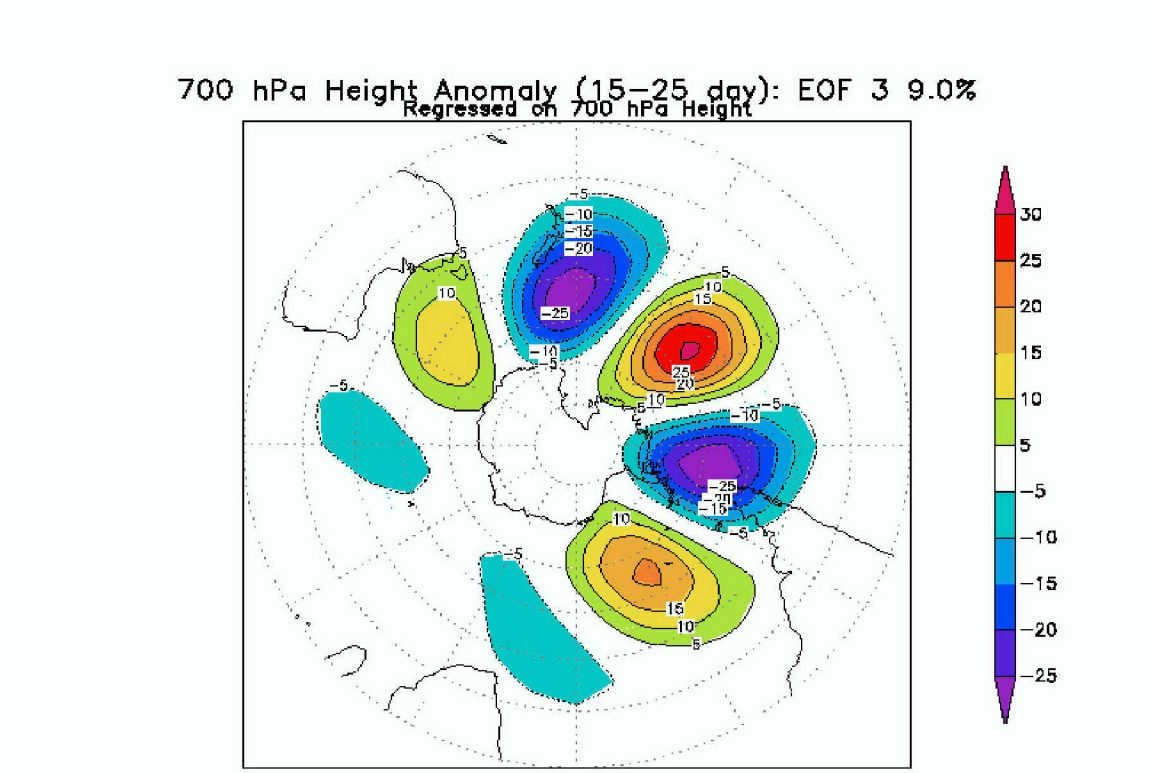


Figure 3.11 Similar to Figure 3.9 except for the second EOF pattern of 700 hPa heights.

4. AAO 15- to 25-Day Zonal Wind Composites

Bals-Elsholz et al. (2001) document the presence of a split jet across the South Pacific Ocean east of Australia as a climatological feature of the Southern Hemisphere upper-level flow during austral winter. To determine the AAO effects on the large-scale, zonal-mean flow in the Southern Hemisphere on a 15- to 25-day time scale, composites of the 850 hPa and 200 hPa zonal winds and their respective anomalies were analyzed. Composites of the u-component of the total wind were derived for both AAO positive and negative index days from March to October between 1979-2000, which are favorable months for tropical cyclone formation in the Northern Hemisphere monsoon trough.

The upper-level composites of 15- to 25-day 200 hPa zonal winds (Figure 3.12) for both AAO positive and negative phases indicate the presence of a split jet south of Australia near 130° E. The equatorward branch of the jet is consistent with the subtropical jet (STJ) centered near 25° S. This jet maximum extends from the central South Indian Ocean into the east-central South Pacific

Ocean. The poleward branch of the split jet is consistent with the polar-front jet (PFJ) centered along 60° S and extends into the eastern South Pacific Ocean south of New Zealand. A zonal wind minimum is apparent over New Zealand between the STJ and the PFJ. The PFJ jet maximum is behind the jet stream split near 50° S south of Madagascar. The jet split appears to be more pronounced during AAO positive events with zonal winds in the poleward branch that extend farther east into the east-central South Pacific and with greater intensity than that of AAO negative events.

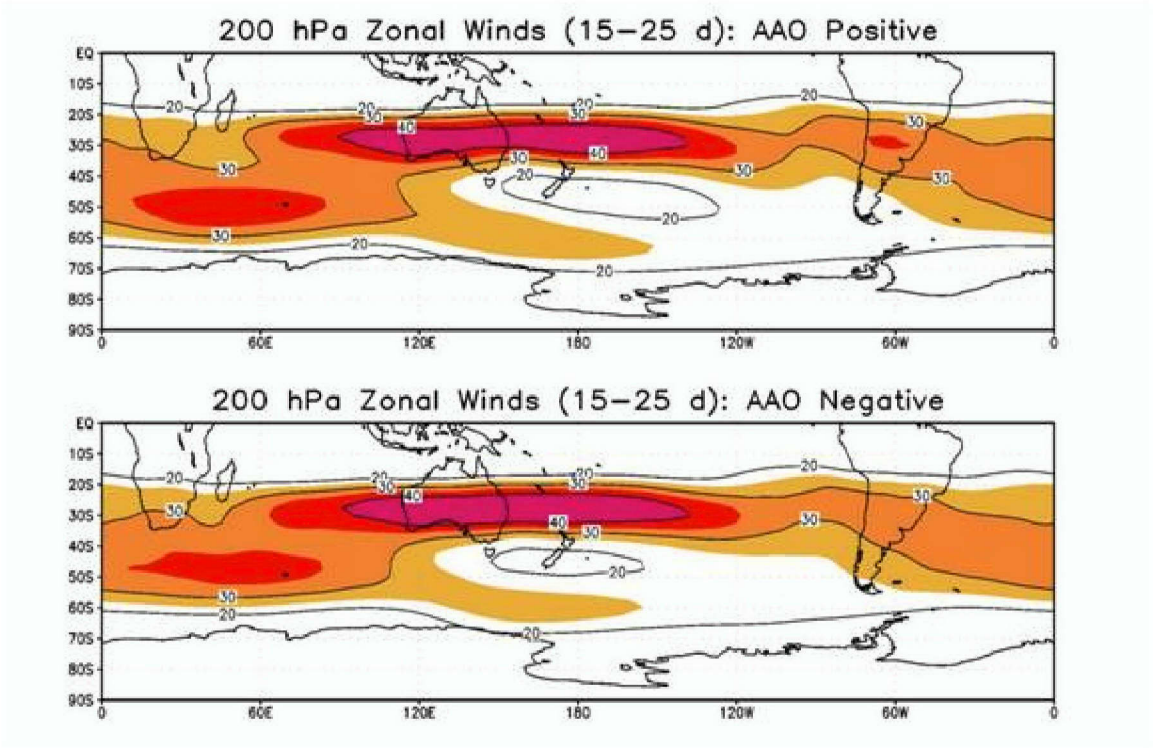


Figure 3.12 Composite of average daily 200 hPa zonal winds (m/s) filtered at 15- to 25-days from 1979-2000 for AAO positive days (top) and AAO negative days (bottom). Contour interval is 10 m/s.

It is apparent in Figure 3.12 that the intensity and spatial scale of the upper-level jet structure vary with the phase of the AAO. Composites of anomalies in the 15- to 25-day zonal wind fields were produced to determine how the upper-level winds for each AAO phase vary relative to the climatological mean jet structure. Upper-level zonal wind anomalies during the positive phase of the AAO (Figure 3.13, top) indicate an anomalously strong PFJ across the

majority of the Southern Hemisphere. Of particular interest to this study is the anomalous westerly zonal wind maximum south of Africa and Madagascar centered around 60° S, since this coincides with the PFJ maximum and is upstream from the equatorial monsoon trough region and is a potential source of wave energy. Likewise, anomalous easterly zonal winds in the subtropics south of Madagascar and eastern Australia indicate a weaker STJ during the positive phase of the AAO. These results are consistent with the enhanced polar vortex structure of the first EOF in Figure 3.9. Bals-Elsholz et al. (2001) defined pronounced split flow in the Southern Hemisphere as having a strengthened PFJ with relatively high cyclonic vorticity poleward of the jet and high anticyclonic vorticity in the velocity minimum between the STJ and the PFJ. Furthermore, Hartman and Lo (1998) related the presence of an anomalous PFJ, which as shown above is related to the positive phase of the AAO, to an anomalous flux of wave energy toward the equator.

Upper-level zonal wind anomalies with a 15- to 25-day period during the negative phase of the AAO (Figure 3.13, bottom) suggest a nearly opposite split jet relationship. In this phase, anomalous easterly winds in the upper latitudes weaken the PFJ and anomalous westerly winds strengthen the STJ upstream of the equatorial monsoon trough region. In this case, the anomalous westerly zonal wind maximum south of Africa and Madagascar shifts equatorward near 35° S. Likewise, anomalous westerly zonal winds in the subtropics over eastern Australia indicate a stronger STJ during the negative phase of the AAO.

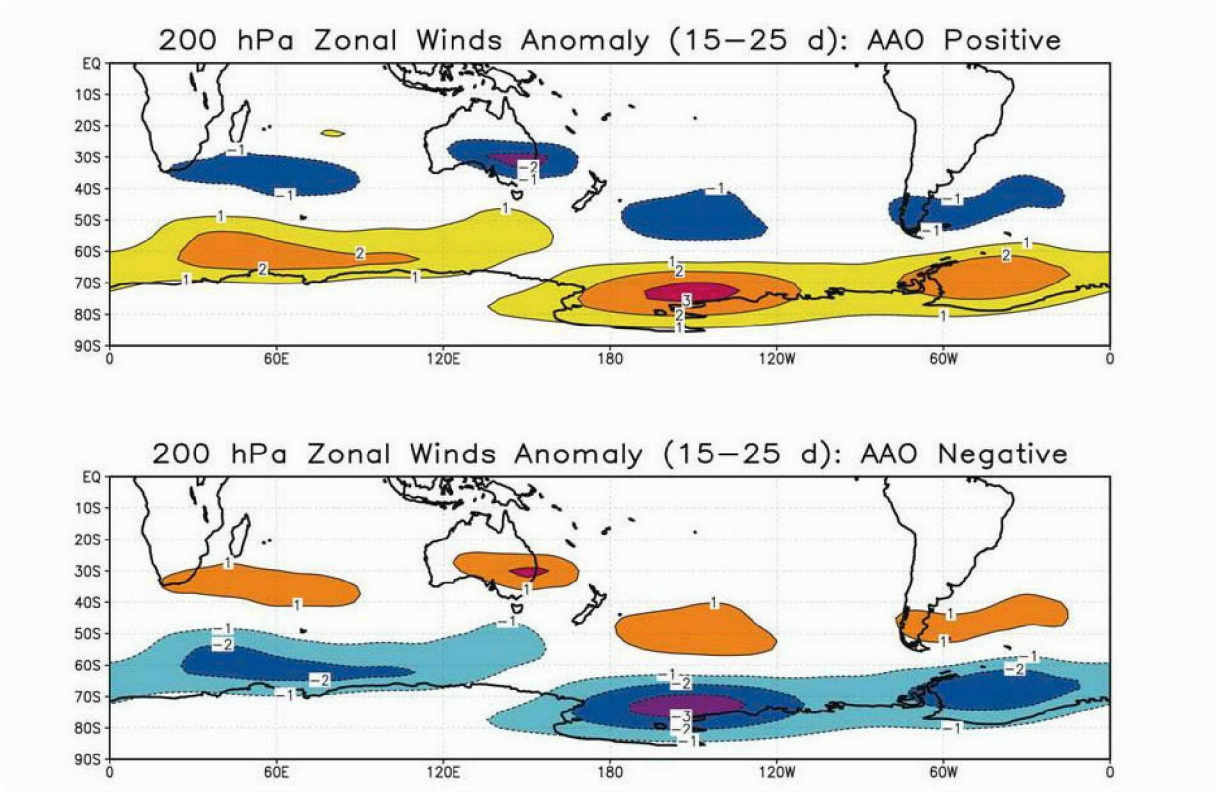


Figure 3.13 Composite of average daily 200 hPa zonal wind anomalies (m/s) filtered at 15- to 25-days from 1979-2000 for AAO positive days (top) and AAO negative days (bottom). Contour interval is 1 m/s. Negative anomaly contours are dashed.

The composites of 15- to 25-day filtered 850 hPa zonal winds (Figure 3.14) for both AAO positive and negative phases indicate the presence of a single jet structure in the mid-latitudes. A low-level zonal jet that extends through most of the Southern Hemisphere is centered along 50° S south of Africa with a zonal wind maximum over the central South Indian Ocean. The jet is more poleward in the central South Pacific Ocean. The 850 hPa zonal jet appears to extend farther east during AAO positive events with greater intensity than that of AAO negative events.

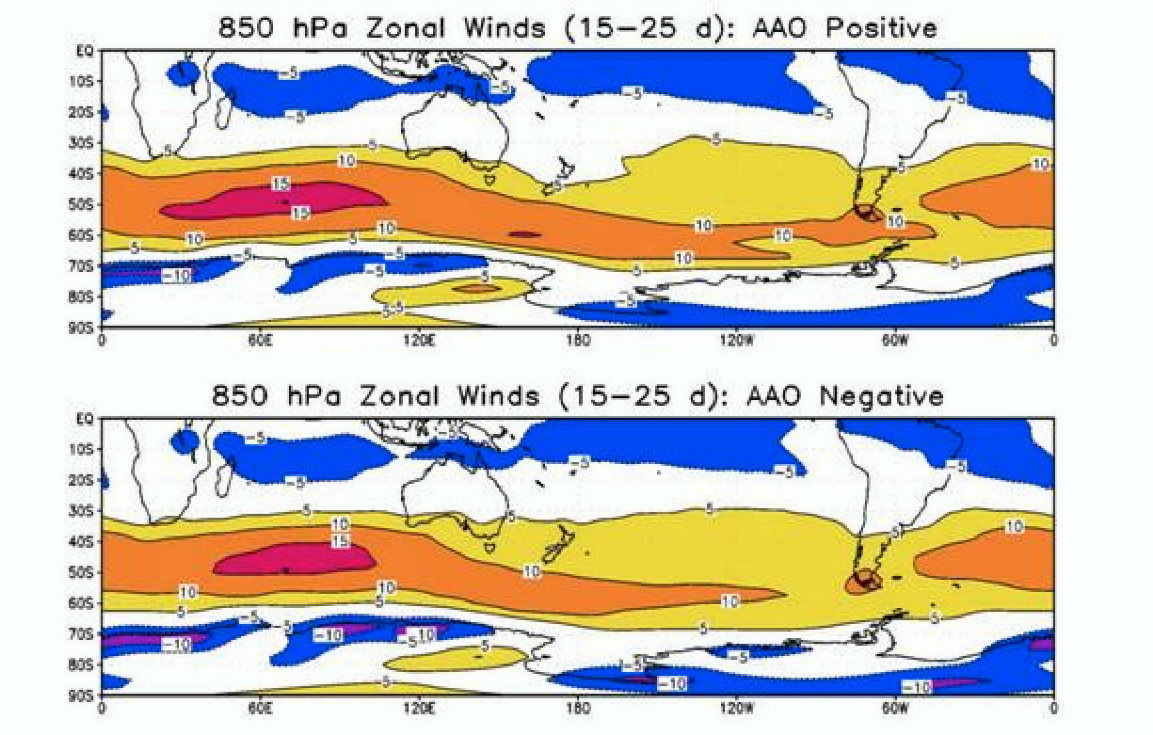


Figure 3.14 Similar to Figure 3.12, except for 850 hPa zonal winds.

Composites of 850 hPa zonal wind anomalies with a 15- to 25-day period (Figure 3.15) indicate the degree of variance from the climatological mean in the low-level jet intensity and spatial coverage. Both the AAO positive and AAO negative events have an equivalent barotropic structure of the AAO (compare with the respective anomalous 200 hPa zonal wind structures in Figure 3.12). During AAO positive events (Figure 3.14, top), anomalous westerly zonal winds over the south Indian Ocean and South Pacific Ocean indicate a poleward shift of the low-level wind maximum and strengthening of the jet. Anomalous easterly zonal winds result in a weaker low-level jet in the mid-latitudes. A nearly opposite 850 hPa zonal wind anomaly structure exists during AAO negative periods (Figure 3.15, bottom). Anomalous westerly zonal winds between 30° S – 40° S suggest an equatorward shift in the low-level jet with increasing westerlies between Africa and Australia, and anomalous easterly zonal winds weakening the poleward extension of the jet.

Hartman and Lo (1998) described the variability of the eddy structure that accompanies zonal flow variations in the Southern Hemisphere similar to those

observed in this study. Using correlation maps of the relative vorticity field, they determined that changes in the composite eddy structure occurred in tandem with the zonal flow oscillation in the lower troposphere. When the jet is displaced poleward, the eddy structures indicated enhanced equatorward propagation. When the jet is displaced equatorward, the eddy structures indicated a more zonal propagation. In this study, the meridional displacement of the 850 hPa jet in the anomaly composites (Figure 3.15) might explain the variance in eddy structures observed during AAO events in connection with the 15- to 25-day mode.

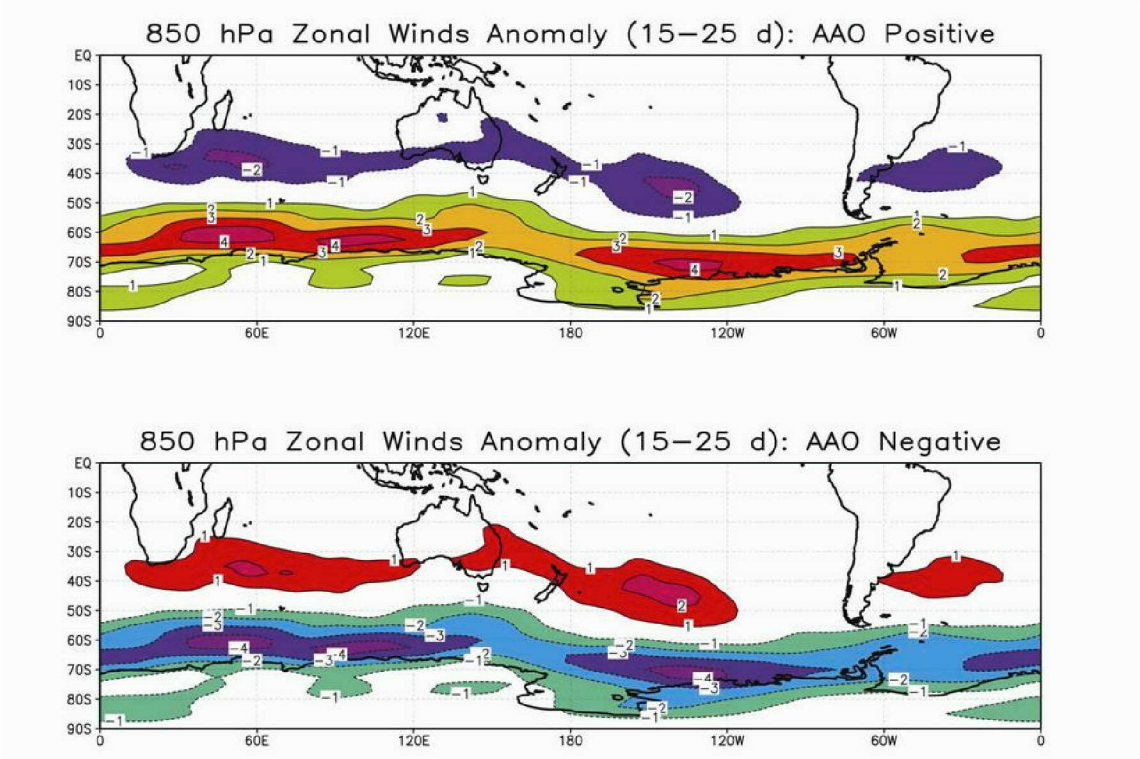


Figure 3.15 Similar to Figure 3.13, except for 850 hPa zonal winds.

In the above analysis section, the AAO has been identified as the leading mode of variability in the Southern Hemisphere circulation, which is dependent on the magnitude of opposing height anomalies between the polar vortex and adjacent mid-latitudes. Temporal analysis of the daily AAO indices have indicated that the maximum variability of the AAO has a seasonal preference that coincides with that of the Northern Hemisphere summer months with significant events typically persisting on sub-weekly time scales. Through Fourier analysis

and filtered EOF analysis, the AAO has been identified as a significant contributor to intraseasonal variations on the order of 15- to 25-days in length. Analysis of 15- to 25-day filtered 200 hPa and 850 hPa zonal winds has verified the AAO has an equivalent barotropic structure with strong dynamical impacts on the jet structure in the Southern Hemisphere, and thus may be connected to the 15- to 25-day cycle of the Northern Hemisphere monsoon trough documented by Delk (2004). The focus of the remainder of this section will be to explore the AAO temporal and spatial relationships with the tropical intraseasonal oscillations of the Northern Hemisphere monsoon trough on the order of 15- to 25-days during boreal summer using daily indices for both the AAO and the 15- to 25-day mode.

## D. AAO AND THE 15-TO 25-DAY OSCILLATION

Given the above analysis of the AAO and height fields, the daily AAO index values for 15- to 25-day filtered 700 hPa height anomalies from May-October for the years 1979-2000 may now be compared with the phases of active 15- to 25-day cycles described by Delk (2004). As illustrated in Figure 1.1, each active period of the 15- to 25-day mode was grouped into eight phases. The phase of the AAO was considered to be positive (negative) when the index value was greater (less) than one standard deviation. Each day meeting the active phase criteria of the 15- to 25-day mode was compared with the corresponding AAO index value for that day.

### 1. Frequency Distribution

A frequency distribution of 15- to 25-day phases for AAO positive events (Figure 3.16) indicates that 60% of the AAO positive days occurred during phases 3, 4, 5, and 6. Between phases 7 through 4 of the 15- to 25-day mode, the frequency of AAO positive days increases and then uniformly decreases. A nearly opposite distribution of AAO negative events exists during the 15- to 25-day mode (Figure 3.17). In general, the number of AAO negative days decreases from phase 1 through phase 5 and then increases through phase 8. In this case, 60% of the AAO negative days occurred during phases 1, 2, 7, and 8 of the 15- to 25-day mode. Based on the analysis of Delk (2004), the middle

phases (3-5) of the 15- to 25-day mode coincide with enhanced convection over the tropical western North Pacific. Based on Figures 3.16 and 3.17, when convection increases in phases 3-5 there is an increase in positive AAO occurrence and a decrease in negative AAO occurrence. Thus, a consistent relationship between high and middle latitude circulation variability in the Southern Hemisphere and equatorial convection is suggested.

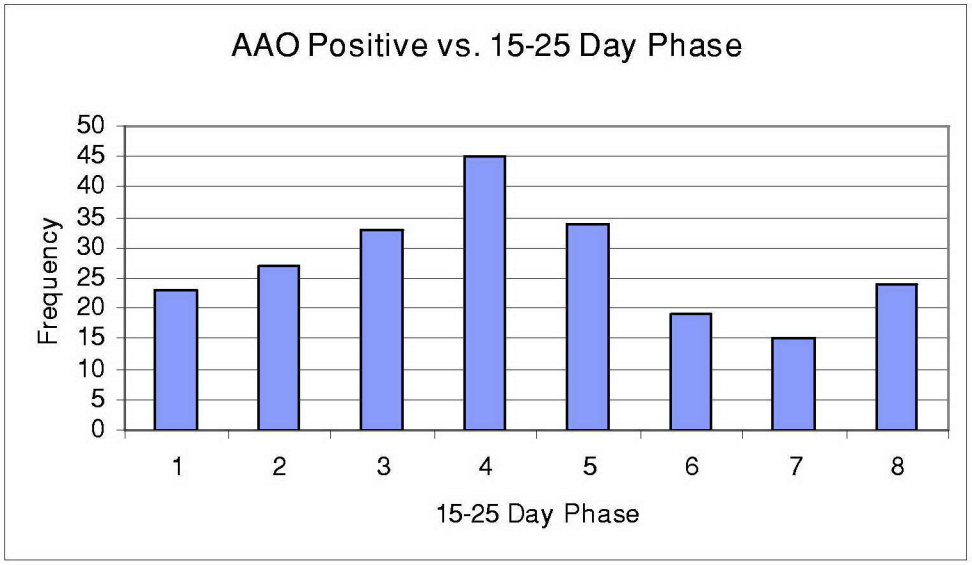


Figure 3.16 Frequency distribution for positive values of the AAO index of 15- to 25-day filtered 700 hPa heights for each phase of the 15- to 25-day oscillation from Mar– Oct from 1979-2000.

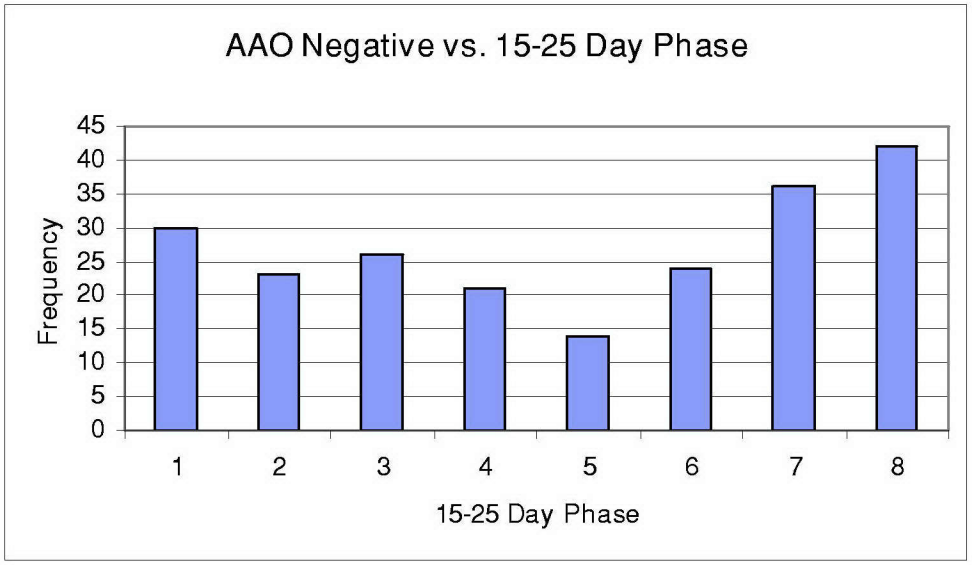


Figure 3.17 Similar to Figure 3.16, except for negative values of the AAO index.

### 2. Single Event Analysis of the AAO Coinciding with the 15- to 25-Day Oscillation

To further investigate the relationship between the 15- to 25-day oscillation of the monsoon trough and the AAO, the above events were examined on a case-by-case basis. During the period of 1979-2000, there were 68 separate 15- to 25-day oscillation events. For each individual event, the phase of the AAO was compared with the corresponding phase of the 15- to 25-day mode. The AAO phase was considered significant and positive (negative) when the index was greater (less) than one standard deviation, which was equal to 1.1775.

Four distinct patterns (A, B, P, N) exist for significant AAO events occurring during the 15- to 25-day mode. Group A appears to have the most common relationship between the AAO and the 15- to 25-day mode and is well correlated with the frequency distribution patterns of the AAO index in Figures 3.16-3.17. Group B occurs less often and has an opposite phase pattern to that of group A. Groups P and N were categorized by their strong positive and negative indices, respectively, of the AAO during the early phases of the 15- to 25-day mode. A fifth group (C) was constructed of cases in which the AAO was neither significantly positive nor negative.

Of the 68 cases, group A, which is represented by one case in Figure 3.18, had the largest number of occurrences (23 cases or 34% of all possible solutions). In group A, a transition from a significant negative AAO occurs during the early stages (phases 1-2) of the 15- to 25-day mode to a significant positive AAO during the middle (phases 3-6) of the 15- to 25-day mode, and then to a significant negative AAO during the end (phases 7-8) of the 15- to 25-day mode. Group B, which was less common (19% of all possible cases), depicts a nearly opposite pattern (Figure 3.19) to that of group A. In group B, a significant positive AAO in the early stages (phases 1-2) of the 15- to 25-day mode transitions to a significant negative AAO in the middle (phases 3-6) of the 15- to 25-day mode, and then transitions back to a significant positive AAO near the end (phase 7-8) of the 15- to 25-day mode. In Group P (Figure 3.20) a significant positive AAO during the early stages (phases 1-3) of the 15- to 25-day

mode then transitions to a significant negative AAO during the end (phases 6-8) of the 15- to 25-day mode. Group P was observed in only 8 of the 68 total cases and thus totaled 12% of all possible solutions. Group N (Figure 3.21) had the least frequent relationship between the AAO and the 15- to 25-day mode and accounted for only 9% of all possible solutions. Group N had a nearly opposite pattern to that of group P, with a significant negative AAO during the early stages (phases 1-3) of the 15- to 25-day mode that transitions to a significant positive AAO during the end (phases 6-8) of the 15- to 25-day mode.

Nearly 75% of all 15- to 25-day cycles observed between the months of March and October from 1979-2000 coincided with significant AAO oscillations. Group C (Figure 3.22) accounted for the remaining 25%. It is interesting to note that while group C was classified as not having a singe day with an AAO index greater than or less than one standard deviation, the general AAO phase pattern for the majority of these (16 of 18) cases display the same phase criteria as one of the other four groups. For example, the AAO index in Figure 3.22 fails to meet the criteria for either significant positive or negative phase, but still resembles the phase pattern of group A (Figure 3.18). Here the group C patterns have a negative AAO index during the beginning (phases 1-2) and ending phases (7-8) of the 15- to 25-day mode and a positive AAO index during the middle phases (3-6) of the 15- to 25-day mode.

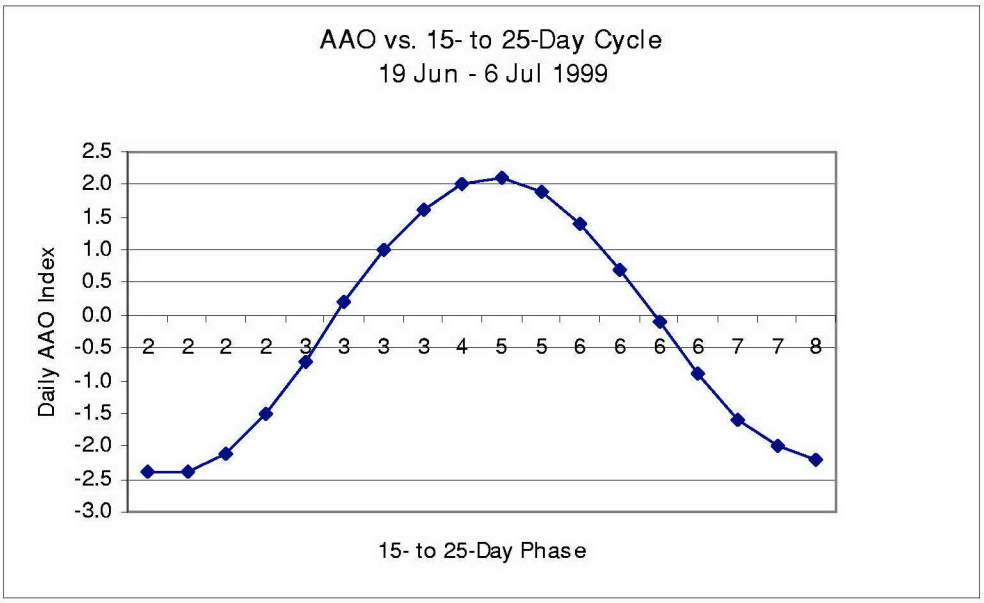


Figure 3.18 Plot of significant daily AAO index versus 15- to 25-day phase as representative of group A.

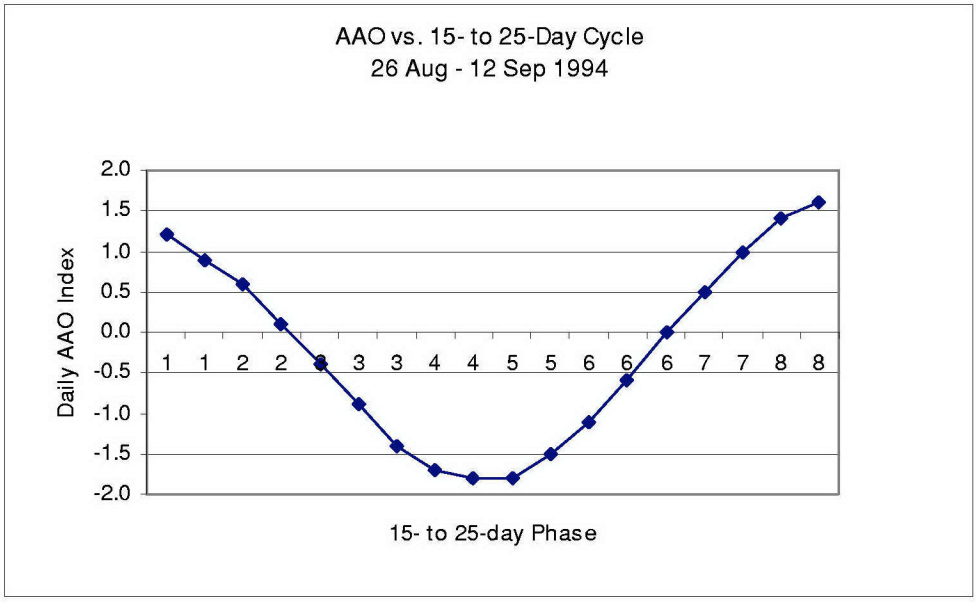


Figure 3.19 Same as Figure 3.18, except as representative of group B.

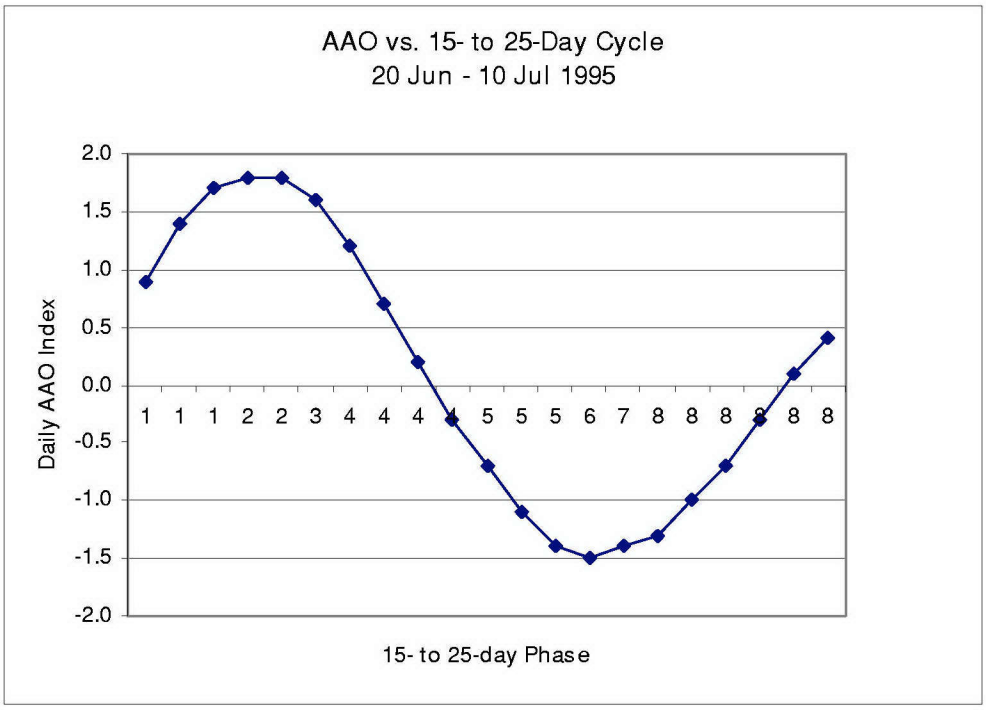


Figure 3.20 Same as Figure 3.18, except as representative of group P.

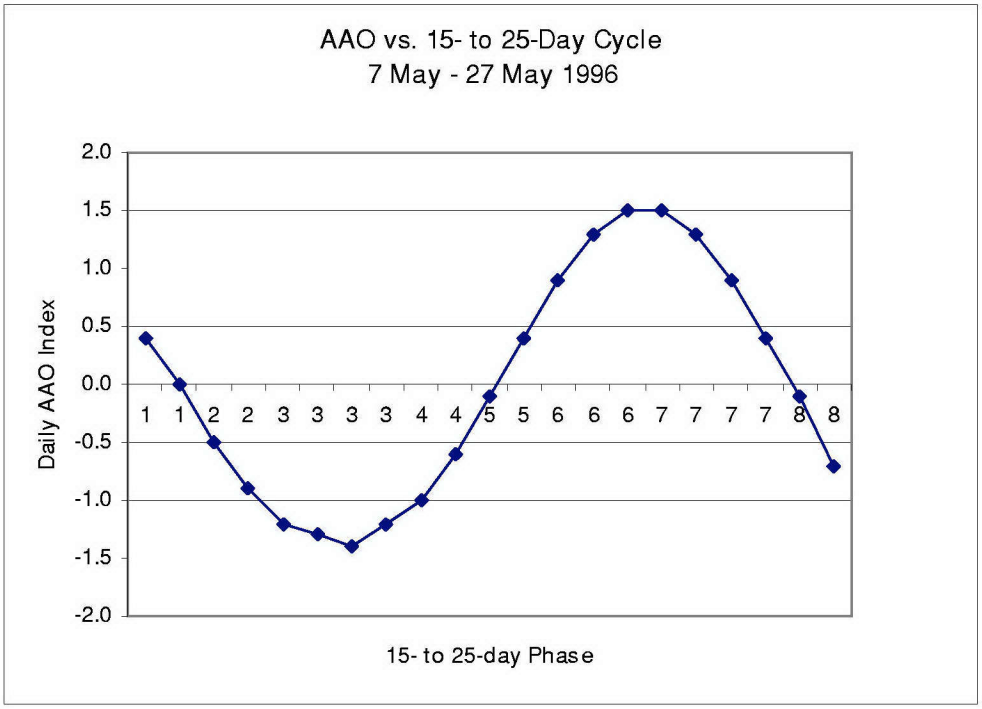


Figure 3.21 Same as Figure 3.18, except as representative of group N.

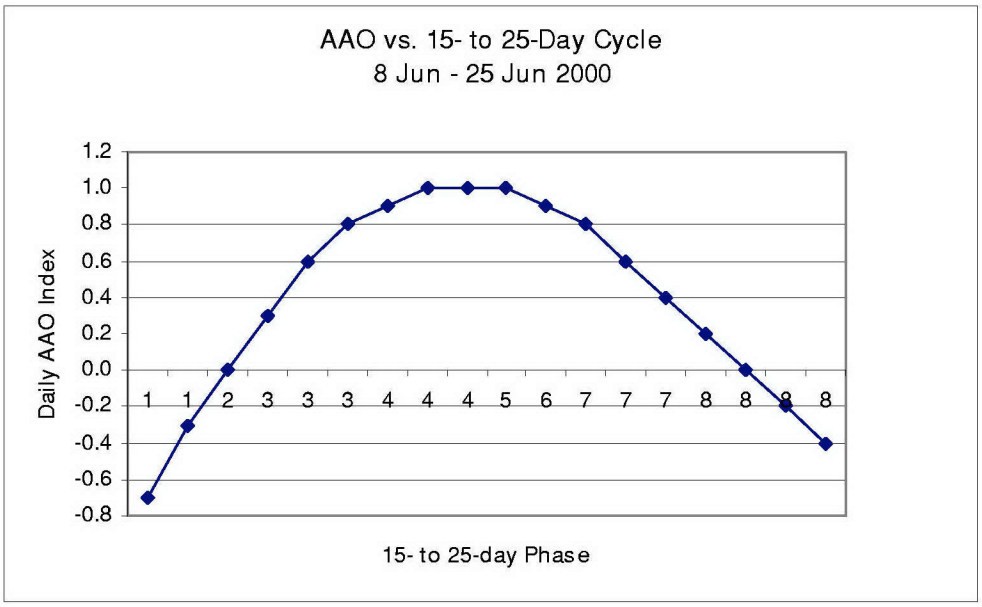


Figure 3.22 Plot of daily AAO index versus 15- to 25-day phase as representative of group C, which does not meet any significant AAO criteria.

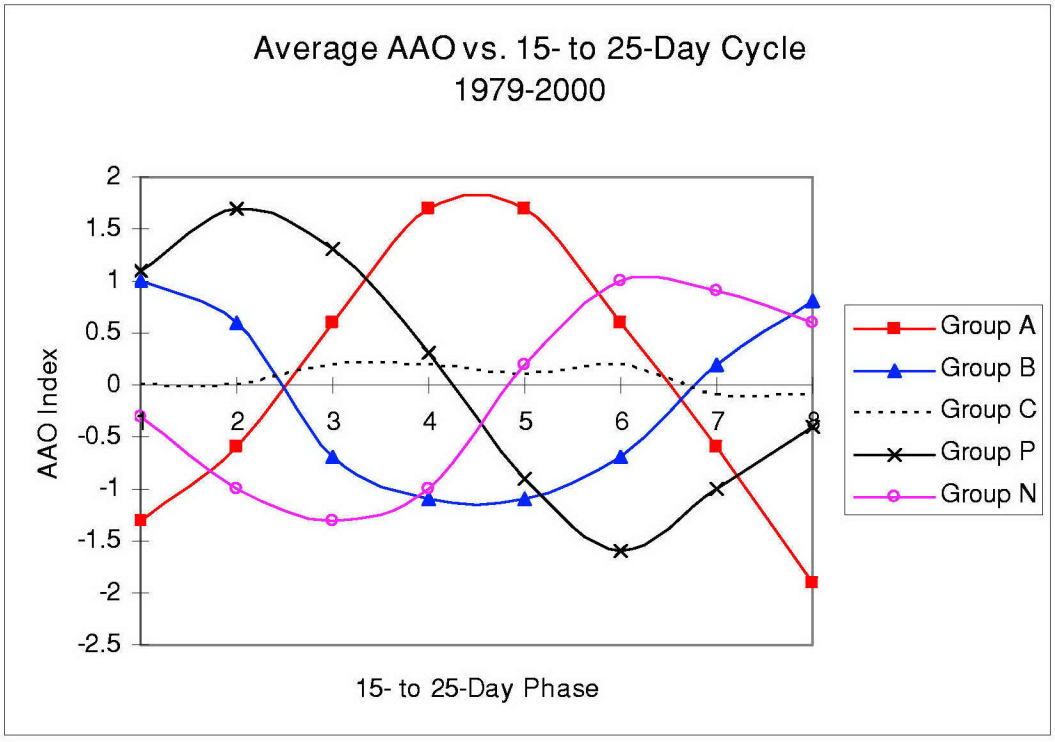


Figure 3.23 Average daily AAO index values for each 15- to 25-day phase from Mar-Oct between 1979-2000.

Daily AAO index values for each group were averaged from 1979-2000 and plotted with their respective phase relationship to the 15- to 25-day mode (Figure 3.23). The phases of the 15- to 25-day mode are defined such that enhanced convection over the monsoon trough region of the western North Pacific peaks at phase 4 (Delk 2004). The groupings above indicate that the peak in convection occurs in conjunction with a variety of AAO conditions. The majority (group A) occurred in association with a change from a significant negative AAO index to a significant positive AAO index, which is related to the AAO index distributions in Figures 3.16 – 3.17.

Examination of the variability associated with the average AAO index curves in Figure 3.23 indicates that between transition phases three and six the variability was much larger than at other phases. It was determined that this variability was related to variations in the timing of the peak AAO. Therefore, group A was separated into sub-groups, A4 and A5. In group A4, the AAO index peaks in phase 4 while group A5 peaks in phase 5. In the original group A data, the AAO index is initially negative, transitions to positive and peaks in phases 3, 4, 5, or 6, and then transitions back to negative. It is apparent from Figure 3.24 that the transition phases of the original group A data, which was a combination of group A4 and group A5, had competing AAO index values. Thus, the signal of the AAO would be weak during these phases. For example, the AAO index in Figure 3.24 is positive during phase 3 of the 15- to 25-day mode in group A4, while the AAO index is negative during the same phase in group A5.

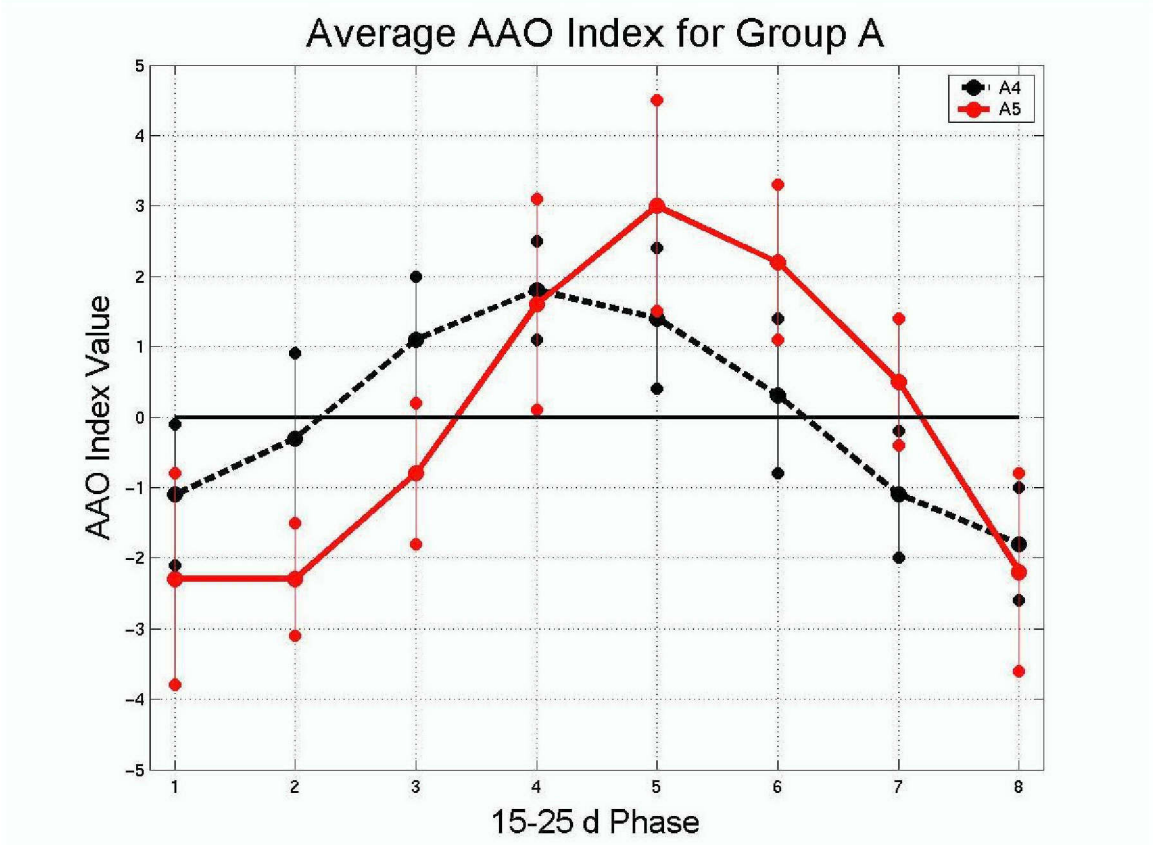


Figure 3.24 Average daily AAO index values for groups A4 (dashed black) and A5 (solid red) during the 15- to 25-day phase cycle from Mar-Oct between 1979-2000. Vertical bars indicate the standard deviation of the AAO index.

Similar to group A, a sub-grouping was developed for the original group B phase relationship between the AAO and the 15- to 25-day cycle. In the original group B data (Figure 3.19), the AAO index is initially positive and then transitions to a peak negative index in phases 3, 4, 5, or 6, and finally transitions back to positive. The AAO index of sub-groups B4 and B6 during the 15- to 25-day mode is shown in Figure 3.25. However, the error bars indicate considerable differences in the respective AAO index values in the transition phases, particularly in phases 2 and 7.

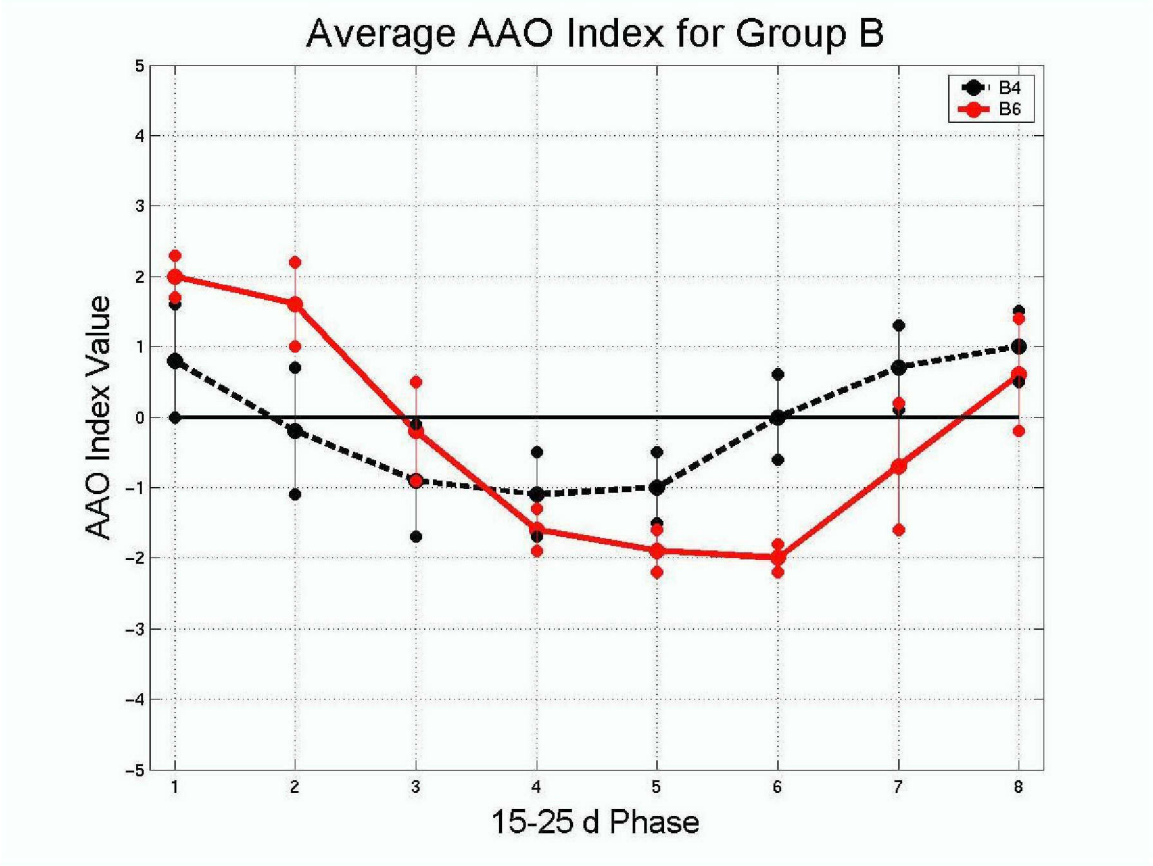


Figure 3.25 Similar to Figure 3.24, except for groups B4 and B6.

## E. COMPOSITES

Composite lower- and upper-level circulation patterns are examined to identify the mechanisms associated with each AAO group during the 15- to 25-day phase that contribute to the enhancement and suppression of the monsoon trough convection. Outgoing Longwave Radiation (OLR) anomaly fields between 30°S and 30°N are used as a proxy for convection in the tropics. For the display of OLR composites, only OLR anomalies that are significantly different from zero are plotted.

Streamfunction anomalies at 850 hPa and 200 hPa are used to identify variations from the climatological mean circulations. For the display of anomalous lower- and upper-level circulation patterns, all streamfunction values are plotted, but only significant wind vectors are displayed. Local significance is determined by a t-test in which the anomaly values are examined to determine if they are significantly different from zero.

| Group | Phase 1 | Phase 2 | Phase 3 | Phase 4 | Phase 5 | Phase 6 | Phase 7 | Phase 8 | Total |
|---|---|---|---|---|---|---|---|---|---|
| A4 | 44 | 43 | 44 | 37 | 38 | 42 | 39 | 38 | 325 |
| A5 | 11 | 8 | 16 | 19 | 8 | 7 | 19 | 15 | 103 |
| B4 | 22 | 16 | 26 | 24 | 17 | 15 | 21 | 25 | 166 |
| B6 | 3 | 11 | 10 | 2 | 4 | 8 | 11 | 4 | 53 |
| N | 10 | 7 | 12 | 22 | 15 | 9 | 13 | 17 | 105 |
| P | 16 | 17 | 21 | 21 | 15 | 17 | 22 | 21 | 150 |
| C | 43 | 37 | 47 | 46 | 39 | 38 | 50 | 50 | 350 |

Table 3.1 Phase frequencies in number of days of the 15- to 25-day cycle that occurred during each observed group from May-October between during 1979-2000.

The number of days that were used in developing each composite is defined in Table 3.1. These data are based on the total number of days in which each phase of the 15- to 25-day cycle occurred for each of the seven groups described in the previous section. The most common of all groups was group C for which the 15- to 25-day cycle of convective activity in the monsoon trough was not found to have any significant connection to the AAO. Group B6 had the fewest common occurrences of 15- to 25-day AAO variability and western North Pacific monsoon trough convective events. Since less than five days met the criteria for phases 1, 4, 5, and 8, this was too small of a sample for compositing and group B6 will not be evaluated for any significant relationship between the AAO and the 15- to 25-day cycle.

Group A4 was the most common of the statistically significant western North Pacific AAO and 15- to 25-day occurrences. For this reason, it will be initially examined to establish the basic framework to which other groups may be compared. It is especially important to compare group A4 and group C, since the latter group does not contain any significant AAO influences.

1. 850 hPa Winds and OLR (Group A4)

For this group, all eight phases of the 15- to 25-day mode will be examined. However, the analysis will concentrate on the transition phases of each group as they represent a basic change in the structure of the monsoon trough as documented by Delk (2004).

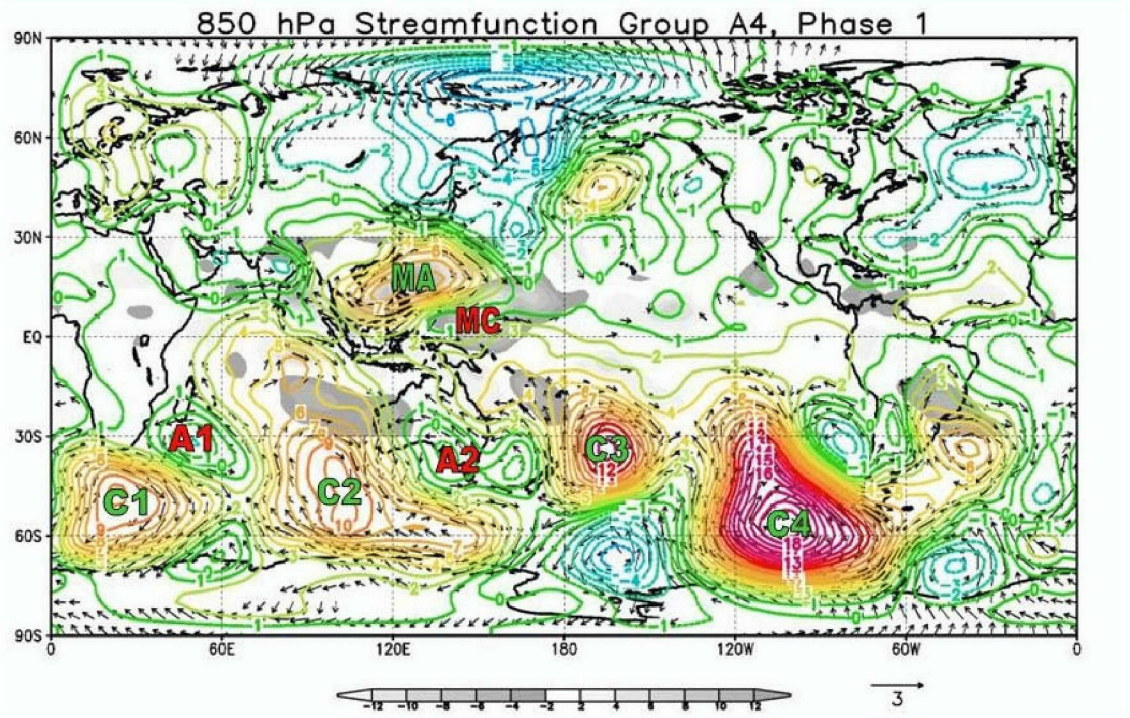


Figure 3.26 Phase 1 composite of 850 hPa streamfunction anomalies (contour interval, $10^6$ $m^2$ $s^{-1}$), significant wind anomalies (arrows) in m $s^{-1}$ (scale at bottom), and OLR anomalies (shaded) in W $m^{-2}$ for group A4.

*a. Phase 1*

In phase 1 (Figure 3.26), a large region of reduced convection (maximum OLR) with a southwest – northeast orientation extends from the equator west of Indonesia to the mid-latitudes over the western North Pacific. A large anticyclonic anomaly (labeled as MA for monsoon anticyclone) is associated with this area of reduced convection. A large region of enhanced convection (minimum OLR) also with a southwest – northeast orientation extends from New Guinea to the dateline. A weak cyclonic anomaly (labeled as MC for monsoon cyclone) is associated with this area of enhanced convection. This coupled anticyclone – cyclone and associated OLR anomalies are indicative of the typical monsoon trough setup documented by Delk (2004) for phase 1 of the 15- to 25-day oscillation.

In the Southern Hemisphere, two anomalous cyclonic circulations (labeled C1 and C2) are oriented along 45°S south of Africa and southwest of Australia. These cyclonic anomalies are associated with the strong negative

index of the AAO (see curve A4 in Figure 3.24). Anomalous westerly (easterly) winds equatorward (poleward) of these cyclones indicate a more equatorward low-level jet. Two anomalous anticyclonic circulations (labeled A1 and A2 in Figure 3.26) are over southern Madagascar and southeastern Australia, respectively. These circulations signify a somewhat anomalous Mascarene High and Australian High at 850 hPa. Furthermore, circulations A1 and A2 are adjacent and northeast of the respective C1 and C2 circulations and may be related to Rossby-wave dispersion from the cyclonic anomalies that are a signature of the low AAO phase. This type of wave propagation is likely associated with the northwest – southeast tilt of eddies created by the shear of the anomalous westerlies of the equatorward low-level jet. Additionally, two anomalous cyclonic circulations (labeled C3 and C4) in the Southern Hemisphere east of the date line appear to be connected to Rossby-wave dispersion from the anticyclonic circulation (MA) associated with the maximum OLR anomalies in the monsoon trough region (Delk 2004).

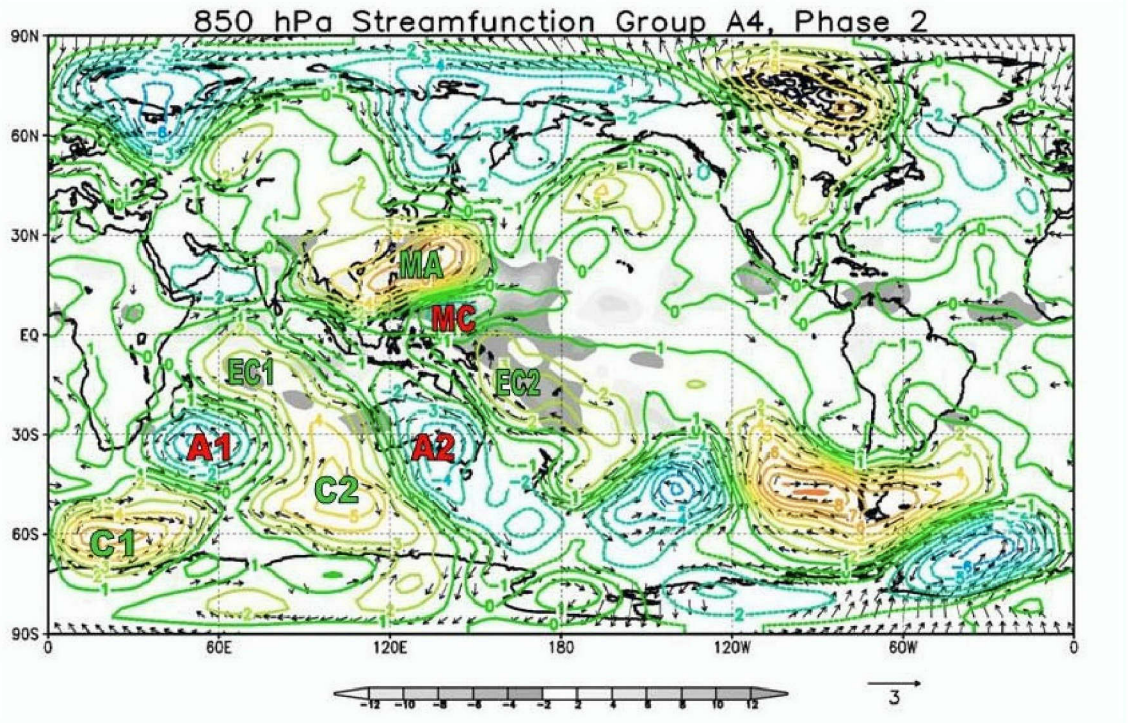


Figure 3.27 Phase 2 composite of 850 hPa streamfunction anomalies (contour interval, $10^6$ $m^2$ $s^{-1}$), significant wind anomalies (arrows) in m $s^{-1}$ (scale at bottom), and OLR anomalies (shaded) in W $m^{-2}$ for group A4.

*b. Phase 2*

In phase 2 (Figure 3.27), circulation MA has weakened and moved slightly poleward as anomalous easterly winds develop to the southeast. Positive OLR anomalies associated with reduced convection extend northeast from the equator south of India to the western North Pacific mid-latitudes. Circulation MC has developed southeast of circulation MA just north of the equator. Negative OLR anomalies associated with enhanced convection now straddle the equator from 130°E to the east of the dateline which indicates development of the enhanced phase of the monsoon trough due to an increase in equatorial westerlies.

In the Southern Hemisphere, the AAO begins to transition from a weak negative to a weak positive index, which begins a poleward shift in the low-level jet. Circulation A1 (Mascarene High) and circulation A2 (Australian High) remain nearly stationary and appear to strengthen. The strengthening of these two anticyclonic cells may be the result of wave dispersion to the northeast of circulations C1 and C2, and they also represent the poleward shift of the primary belt of westerly winds as the AAO shifts to a positive index. A secondary anomalous cyclonic circulation (labeled EC1) in the equatorial region northeast of Madagascar has developed downstream of circulation A1. A similar anomalous cyclonic circulation (labeled EC2) develops in the equatorial region northeast of circulation A2 apparently as a result of equatorward wave propagation as the Australian High continues to build with the strengthening AAO. Anomalous winds associated in the equatorward branch of circulation EC2 appear to contribute directly to the equatorward development of enhanced convection as a result of strong cross-equatorial low-level anomalous winds. The strengthening of circulation A2 and the presence of circulation EC2 are suggestive of a cold surge from the Southern Hemisphere mid-latitudes to the equatorial western North Pacific. Chang and Lau (1980) identified the planetary-scale effects of Northern Hemisphere cold surges during northern winter over the South China Sea. Love (1985) examined the impact of these northern winter surges on tropical cyclone formation.

From the evolution from phase 1 to phase 3 in the composites, it appears that a similar mechanism may occur during the Southern Hemisphere winter.

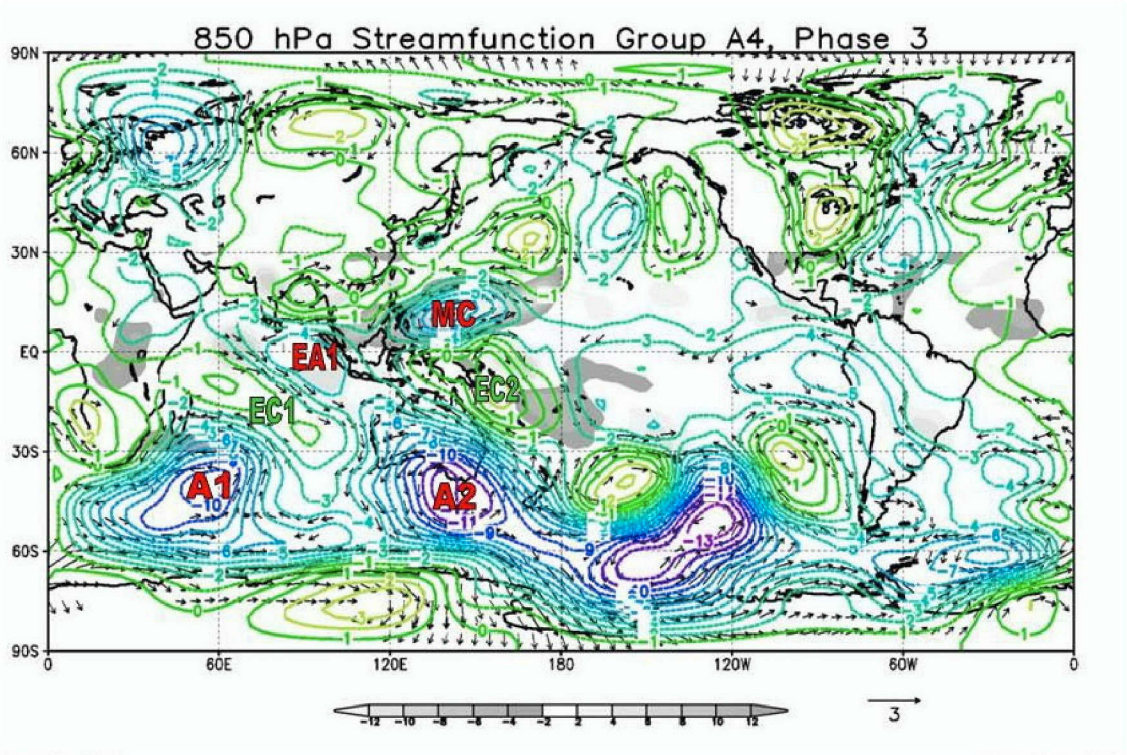


Figure 3.28 Phase 3 composite of 850 hPa streamfunction anomalies (contour interval, $10^6$ $m^2$ $s^{-1}$), significant wind anomalies (arrows) in m $s^{-1}$ (scale at bottom), and OLR anomalies (shaded) in W $m^{-2}$ for group A4.

*c. Phase 3*

In phase 3 (Figure 3.28), the region of reduced convection over the western North Pacific has decreased in overall extent as circulation MA has dissipated over eastern Asia. Circulation MC has strengthened over the Philippine Sea and negative OLR anomalies associated with enhanced convection now straddle the equator from 130°E to the dateline. This indicates development of the active monsoon trough due to an increase in equatorial westerlies. Finally, there is an apparent developing Rossby-wave train in the Northern Hemisphere that extends from the convection associated with circulation MC northeastward into the Gulf of Alaska. This wave train relates well with the findings of Delk (2004) who connected the development of new cyclonic

and anticyclonic anomalies in the equatorial monsoon trough region to downstream Rossby-wave trains.

In the Southern Hemisphere, the AAO is positive and strengthening, which continues a shift of the low-level jet poleward. Anticyclonic circulations A1 and A2 have strengthened in the mid-latitudes resulting in anomalous easterly winds along 30°S and anomalous westerly winds along 60°S. Anomalous cyclonic circulations C1 and C2 from the previous phase (Figure 3.27) have dissipated as a result of the building Mascarene High and Australian High. A developing anticyclonic anomaly (labeled EA1) in the equatorial Indian Ocean downstream of the building Mascarene High and circulation EC1 suggests a Rossby-wave response to the strengthening of the mid-latitude anticyclone associated with circulation A1. Anomalous southerly winds associated with circulation EA1 appear to support development of enhanced convection along the equator. Farther east, circulation EC2 strengthens over New Guinea as a result of the building Australian High. Anomalous westerlies along the equator are consistent with circulation EC2 which correspond with the area of developing convection of circulation MC. This equatorward development of circulation anomalies continues to suggest a Rossby-wave response similar to that described in the Indian Ocean.

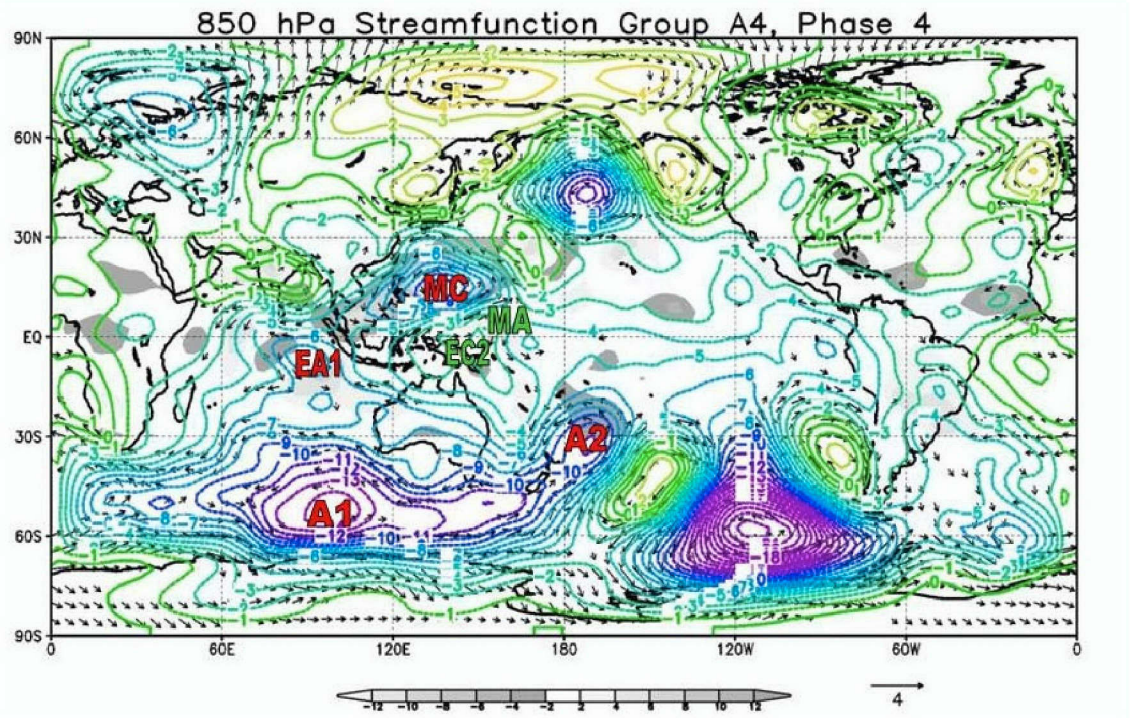


Figure 3.29 Phase 4 composite of 850 hPa streamfunction anomalies (contour interval, $10^6$ $m^2$ $s^{-1}$), significant wind anomalies (arrows) in m $s^{-1}$ (scale at bottom), and OLR anomalies (shaded) in W $m^{-2}$ for group A4.

*d. Phase 4*

In phase 4 (Figure 3.29), circulation MC has moved northwestward and strengthened over the Philippine Sea. The Rossby-wave train in the Northern Hemisphere continues to develop downstream of the developing convection associated with circulation MC. Negative OLR anomalies associated with the enhanced convection of circulation MC have increased and extend northeastward from the equator at 90°E to the western North Pacific mid-latitudes. A weak anomalous anticyclonic circulation (labeled MA) has developed along the equatorial western Pacific in the wake of circulation MC. This circulation coincides with an area of reduced convection associated with positive OLR anomalies near 140°E at the equator.

In the Southern Hemisphere, the AAO has reached its peak positive intensity (see curve A4 in Figure 3.24) and the low-level jet at 850 hPa has reached its most poleward latitude. Anomalous westerly winds associated with the poleward extent of the jet and anomalous easterlies in the subtropics

(30°S) have contributed to the development of circulation A1 into a broad anticyclonic circulation covering much of the mid-latitudes west of the dateline to south of Africa. As a result of this change throughout the mid-latitudes, the wave train activity suggested in the previous three phases has subsided. Circulation EA1 remains stationary and has strengthened west of Sumatra. Anticyclonic wind anomalies associated with this circulation correspond with the westward-most area of enhanced equatorial convection. Circulation EC2 has moved to the northwest and has weakened as it is now adjacent to the weak anticyclonic circulation (MA) in the Northern Hemisphere. Westerly wind anomalies along the equator are consistent with circulation EC2 and continue to contribute to the southern-most extension of enhanced convection associated with circulation MC. Circulation A2 has coupled with an apparent Rossby-wave train into the Southern Hemisphere mid-latitudes that is similar to the wave train in the Northern Hemisphere. The Southern Hemisphere wave response appears to originate from the enhanced convection of circulation MC and extends southeast to 120°W. It is noted that in this phase both the positive AAO index and the enhanced convection in the monsoon trough region are maximized.

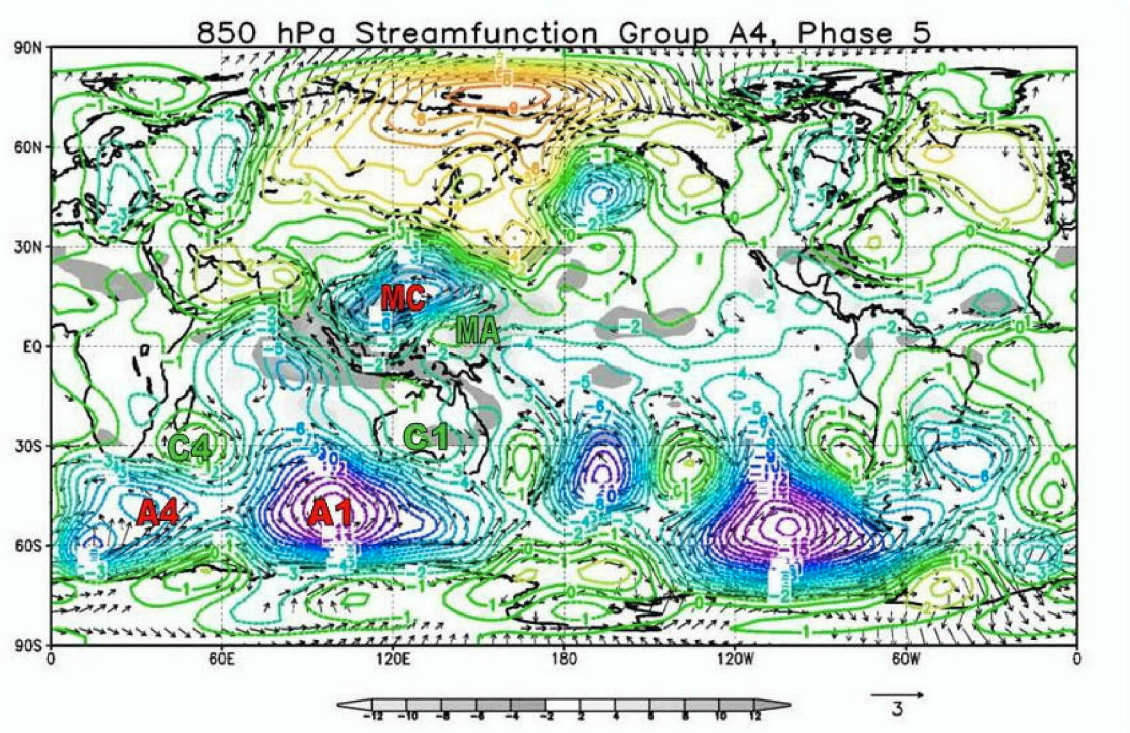


Figure 3.30 Phase 5 composite of 850 hPa streamfunction anomalies (contour interval, $10^6$ $m^2$ $s^{-1}$), significant wind anomalies (arrows) in m $s^{-1}$ (scale at bottom), and OLR anomalies (shaded) in W $m^{-2}$ for group A4.

*e. Phase 5*

In phase 5 (Figure 3.30), circulation MC moves northwestward over the Philippines and begins to weaken. Enhanced convection associated with circulation MC appears to maintain its intensity as negative OLR anomalies over the northern Philippines remain unchanged. This enhanced convection area has shifted westward and extends northeast from the equator at 75°E to the western North Pacific mid-latitudes. Circulation MA continues to develop along the equatorial western Pacific adjacent to circulation MC. The area of reduced convection associated with circulation MA has developed substantially and now extends northeastward from 130°E at the equator to the dateline. The Rossby wave in the Northern Hemisphere is still apparent but has weakened in response to the weakening of circulation MC in the tropics.

In the Southern Hemisphere mid-latitudes, circulation A1 continues to strengthen and extends northward into the central South Indian Ocean. A second anomalous anticyclonic circulation develops southeast of Africa (labeled

A4 in Figure 3.30). Two anomalous cyclonic circulations (labeled C4 and C1) develop to the northeast of circulations A4 and A1 respectively. Circulation C4 is over southern Madagascar and is associated with a weakening of the Mascarene High. Likewise, circulation C1 is over southern Australia and has led to a weakening of the Australian High. The structure of anomalous circulations in phase 5 appears to be opposite to that of phase 1 (Figure 3.26), in which the Mascarene High and Australian High are strengthening as a result of anticyclonic circulation anomalies overhead. The strengthening anticyclone – cyclone pairs in phase 5 appear to trigger another set of Rossby waves moving from the Southern Hemisphere mid-latitudes toward the equator. The northeastward flux of wave energy associated with circulation A1 and circulation C1 appears to interfere with and weaken the Southern Hemisphere Rossby-wave train that originated from circulation MC.

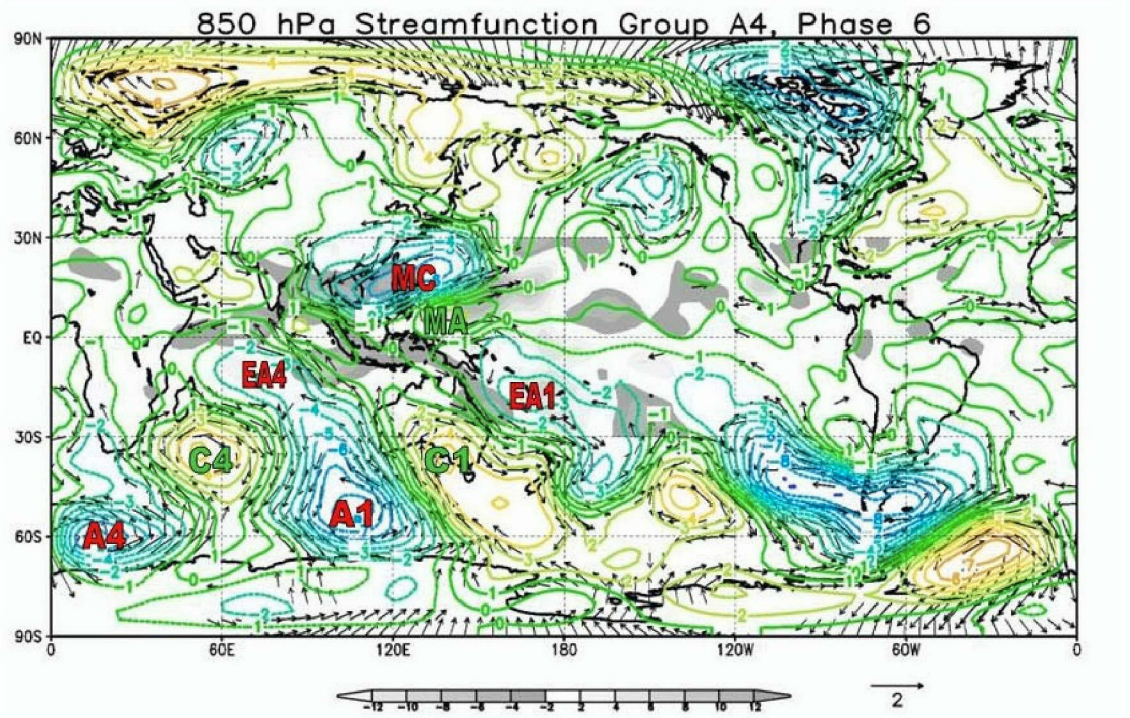


Figure 3.31 Phase 6 composite of 850 hPa streamfunction anomalies (contour interval, $10^6$ $m^2$ $s^{-1}$), significant wind anomalies (arrows) in m $s^{-1}$ (scale at bottom), and OLR anomalies (shaded) in W $m^{-2}$ for group A4.

*f. Phase 6*

In phase 6 (Figure 3.31), circulation MC weakens over the Philippines. Enhanced convection associated with this circulation extends westward from the South China Sea to eastern India where convection is enhanced by anomalous westerly winds. Circulation MA has moved westward and strengthened north of New Guinea. Reduced convection associated with this circulation extends from New Guinea northeastward to the dateline, which is consistent with anomalous easterly winds to the east. The Northern Hemisphere Rossby wave appears to have dissipated in response to the continued weakening of circulation MC.

In the Southern Hemisphere mid-latitudes, circulations A1 and A4 begin to weaken in response to the weakening AAO index (see curve A4 in Figure 3.24). At the same time, the weakening AAO is consistent with an equatorward shift in the low-level jet associated with the strengthening of circulations C4 and C1. Anomalous easterly (westerly) winds associated with the poleward (equatorward) branch of these cyclonic circulations have further weakened the Mascarene High and Australian High. Furthermore, anomalous anticyclonic circulations (labeled EA4 and EA1) have developed equatorward of the developing cyclonic circulations (C4 and C1). Circulation EA4 is in the central Indian Ocean south of the equator. Anomalous cross-equatorial southerly winds associated with this circulation correspond with enhanced convection along the equator west of 120°E. Circulation EA1 is northeast of Australia. Easterly wind anomalies associated with this circulation support reduced convection extending from the dateline northwest to circulation MA. This equatorward wave train structure in phase 6 appears to be opposite to that of phase 2 (Figure 3.27) in which the wave energy was transferred from weakening cyclonic circulations to developing anticyclonic circulations over the Mascarene High and the Australian High.

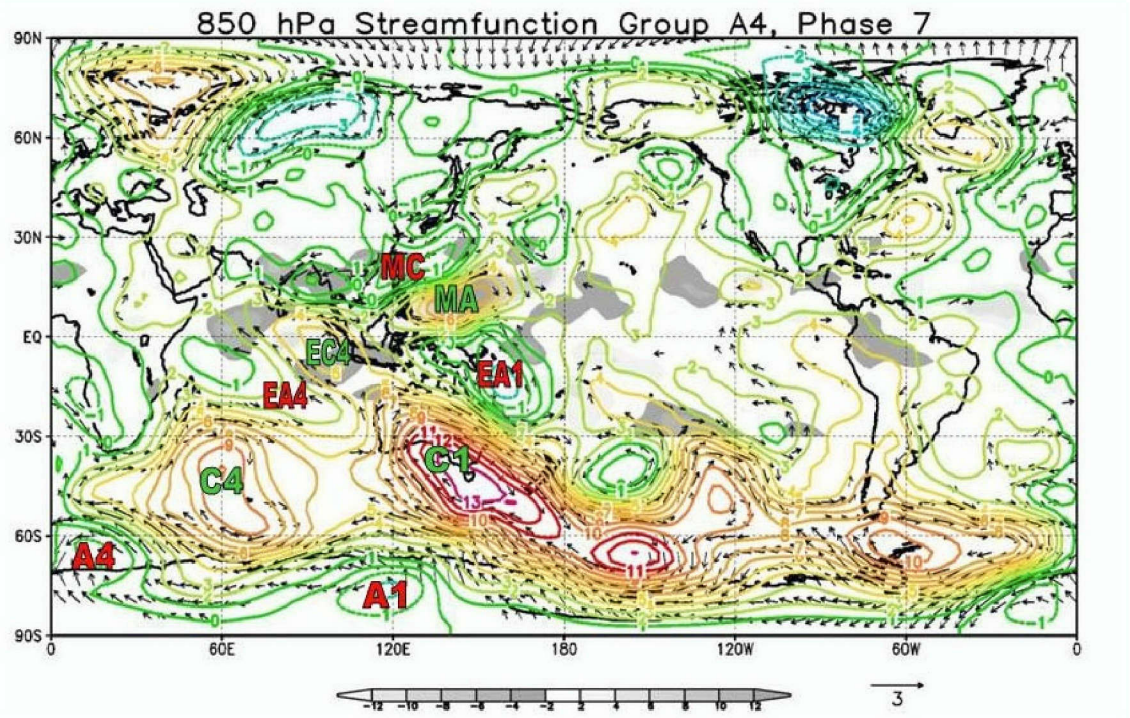


Figure 3.32 Phase 7 composite of 850 hPa streamfunction anomalies (contour interval, $10^6$ $m^2$ $s^{-1}$), significant wind anomalies (arrows) in m $s^{-1}$ (scale at bottom), and OLR anomalies (shaded) in W $m^{-2}$ for group A4.

*g. Phase 7*

In phase 7 (Figure 3.32), circulation MC weakens and moves northward over the Philippines. Enhanced convection associated with this circulation has reduced in coverage over the East China Sea. Circulation MA has developed to the southeast of circulation MC and has become the dominant anomalous circulation in the monsoon trough region. Reduced convection associated with this circulation is consistent with anomalous easterlies along the equator that extend from the central Indian Ocean to the mid-latitude dateline.

In the Southern Hemisphere, circulations C4 and C1 continue to strengthen as the AAO index becomes negative (curve A4 in Figure 3.24), and the low-level jet shifts toward the equator. Anomalous easterly winds along 60°S and anomalous westerly winds along 30°S are consistent with the strengthening of both cyclonic circulations C4 and C1 in the mid-latitudes. Anomalous anticyclonic circulations, A4 and A1 from the previous phase have weakened as a result of the weakening Mascarene High and Australian High,

respectively. Circulation EA4 has strengthened in response to the building cyclonic circulation (C4) and appears to have aided the development of a secondary cyclonic anomaly (labeled EC4) over the equator through Rossby-wave forcing. Anomalous westerlies along the equator are consistent with cyclonic circulation EC4, and connect with the area of enhanced convection of circulation MC. Circulation EA1 has developed in response to the strengthening cyclonic circulation (C1) over Australia. Anomalous easterlies associated with this anticyclonic circulation appear to be consistent with the area of reduced convection on the eastern edge of circulation MA. The equatorward wave train structure in phase 7 appears to be opposite to that of phase 3 (Figure 3.28), in which the dominant forcing was attributed to the development of anticyclonic circulations over the central Indian Ocean and Australia.

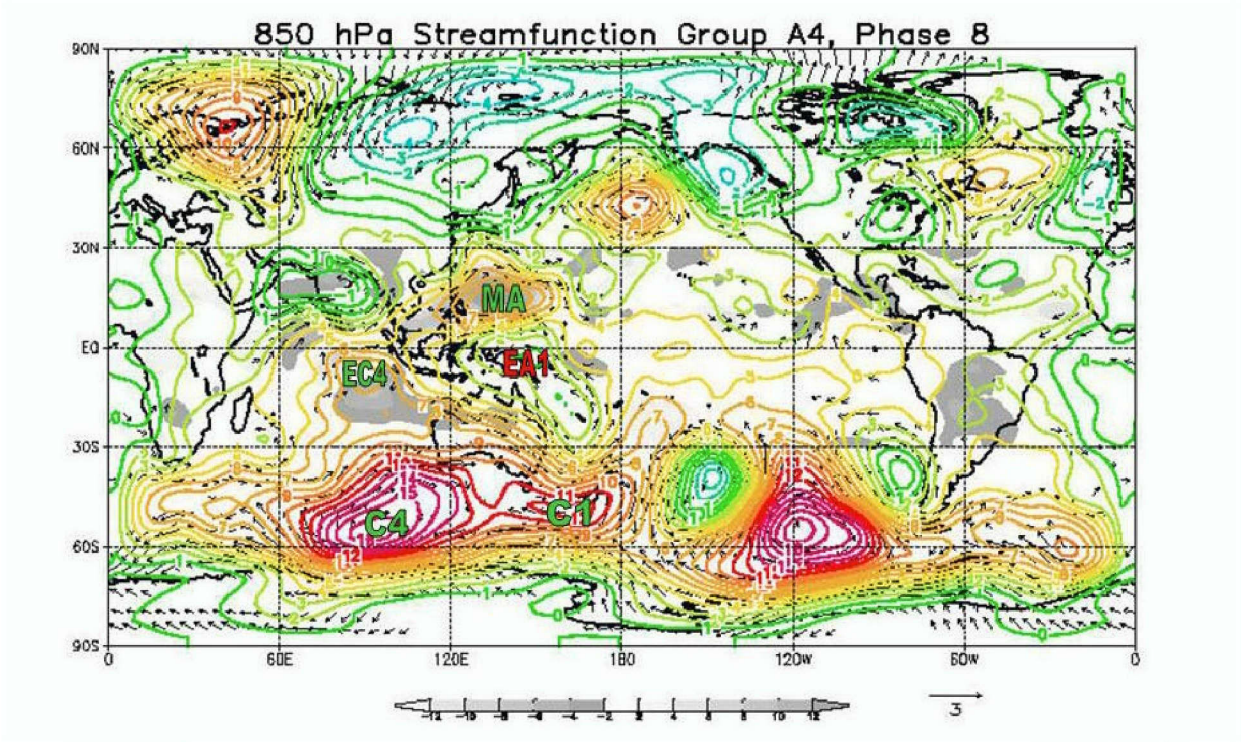


Figure 3.33 Phase 8 composite of 850 hPa streamfunction anomalies (contour interval, $10^6$ in $m^2$ $s^{-1}$), significant wind anomalies (arrows) in m $s^{-1}$ (scale at bottom), and OLR anomalies (shaded) in W $m^{-2}$ for group A4.

*h. Phase 8*

In phase 8 (Figure 3.33), circulation MC dissipates in a mid-latitude trough over northeast Asia. Circulation MA has reached peak intensity over the

Philippine Sea and covers most of the monsoon trough region of the western North Pacific. Reduced convection associated with this circulation is titled southwest – northeast from immediately south of the equator at 70°E to 170°E. Anomalous easterly winds along the equator continue to support higher OLR values (reduced convection) along the southern branch of circulation MA. A Northern Hemisphere Rossby-wave train extending into the Gulf of Alaska appears to be developing as a result of the development of circulation MA in the monsoon trough region.

In the Southern Hemisphere, the AAO index (curve A4 in Figure 3.24) has become increasingly negative and the low-level jet at 850 hPa has reached its equatorward-most latitude. The wave-train activity in the Indian Ocean has dissipated as circulation C4 has developed into a broad cyclonic circulation. Anomalous easterly winds associated with the weakening poleward jet and anomalous westerlies associated with the developing equatorward jet cover much of the mid-latitudes west of the dateline. The wave train activity originating over Australia has also dissipated as circulation C1 has coupled with an apparent Rossby-wave train in the Southern Hemisphere that is similar to that in the Northern Hemisphere. This Southern Hemisphere wave response appears to originate from the reduced convection area of circulation MA and extends southeastward to 90°W. Although circulation EC4 has remained stationary, it has amplified west of Sumatra. Cyclonic wind anomalies associated with this circulation correspond with the westward-most area of enhanced convection along the equator. Circulation EA1 has moved to the northwest and appears to be the favored cyclonic circulation to potentially develop behind circulation MA in the Northern Hemisphere. Easterly wind anomalies associated with this circulation along the equator correspond to the southern-most extension of reduced convection associated with circulation MA. Finally, the combination of circulations EA1, MA, EC4 and an unnamed cyclonic anomaly over India form a quadrapole set of circulations indicative of an equatorial Rossby-wave pattern.

The anomalous circulation structure of phase 8 is nearly opposite to that of phase 4 (Figure 3.29), in which the mid-latitudes were dominated by an

anomalous anticyclonic circulation. It is also noted the peak negative AAO index corresponds to the minimum convection in the western North Pacific monsoon trough region.

2. 200 hPa Winds and OLR (Group A4)

Selected phases of the 15- to 25-day mode at 200 hPa will be displayed to summarize the overall structure of the upper troposphere during the transition phases 3 and 6 (Figure 3.24). Changes in the anomalous circulation were examined and related to the upper-level jet structure that is driven by the AAO (Bals-Elsholz et al. 2001). Additionally, upper-level dynamics in the tropics associated with the AAO will be evaluated for significant impacts on the 15- to 25-day convective cycle of the monsoon trough documented by Delk (2004).

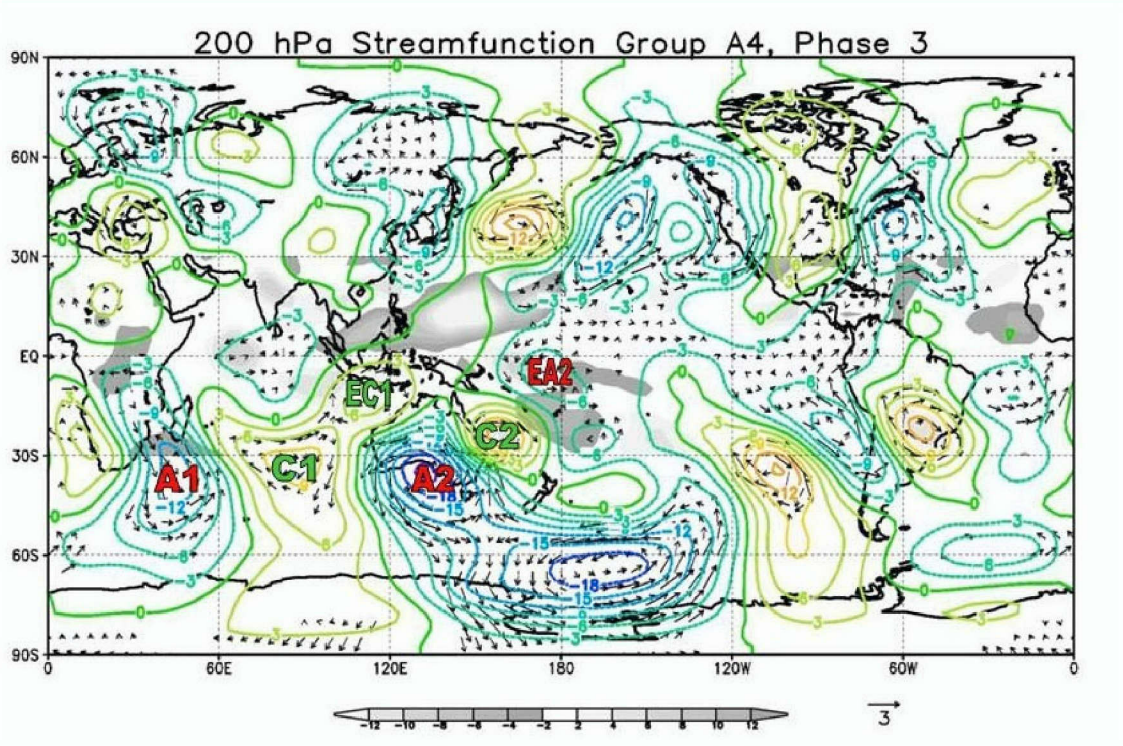


Figure 3.34 Phase 3 composite of 200 hPa streamfunction anomalies (contour interval, $10^6$ in $m^2$ $s^{-1}$), significant wind anomalies (arrows) in m $s^{-1}$ (scale at bottom), and OLR anomalies (shaded) in W $m^{-2}$ for group A4.

*a. Phase 3*

In phase 3 (Figure 3.34), anomalous 200 hPa westerly winds associated with a large anticyclonic circulation in the Southern Hemisphere over the dateline suggest a strengthening of the polar front jet (PFJ) from 150°E to

120°W. These anomalies correlate well with zonal wind anomalies for the AAO positive index displayed in Figure 3.13 (top). An apparent wave train in the eastern South Pacific develops in response to the meridional shear of the zonal wind downstream of the jet maximum with a northwest – southeast tilt that suggests equatorward propagation. This alignment is also favorable for poleward momentum transport, which is consistent with the shift from negative to positive AAO states (Lorenz and Hartmann 2001). Anomalous easterly winds associated with anomalous anticyclonic circulations labeled A1 and A2 south of Madagascar and Australia, respectively, indicate a poleward shift in the jet upstream of the subtropical jet (STJ) and PFJ split displayed in Figure 3.12 (top). Two weak equatorward wave trains are apparent in the exit regions of these anomalous westerlies of the jet. This wave structure resembles that of phase 3 for 850 hPa (Figure 3.28), which suggests an equivalent barotropic structure in the Southern Hemisphere. An anomalous anticyclonic circulation (labeled EA2) develops near the equator upstream of the circulation A2. Anomalous anticyclonic winds southeast of the monsoon trough region suggest that circulation EA2 is contributing to upper-level divergence in support of the enhanced convection associated with the start of the active monsoon trough phase. Finally, there is an equatorward propagating wave train over the Southeast Pacific Ocean at the exit region of the polar jet. The presence of equatorward-moving waves at the exit region of the three maxima in winds is consistent with the wave propagation pattern in the Southern Hemisphere defined by Ambrizzi et al. (1995).

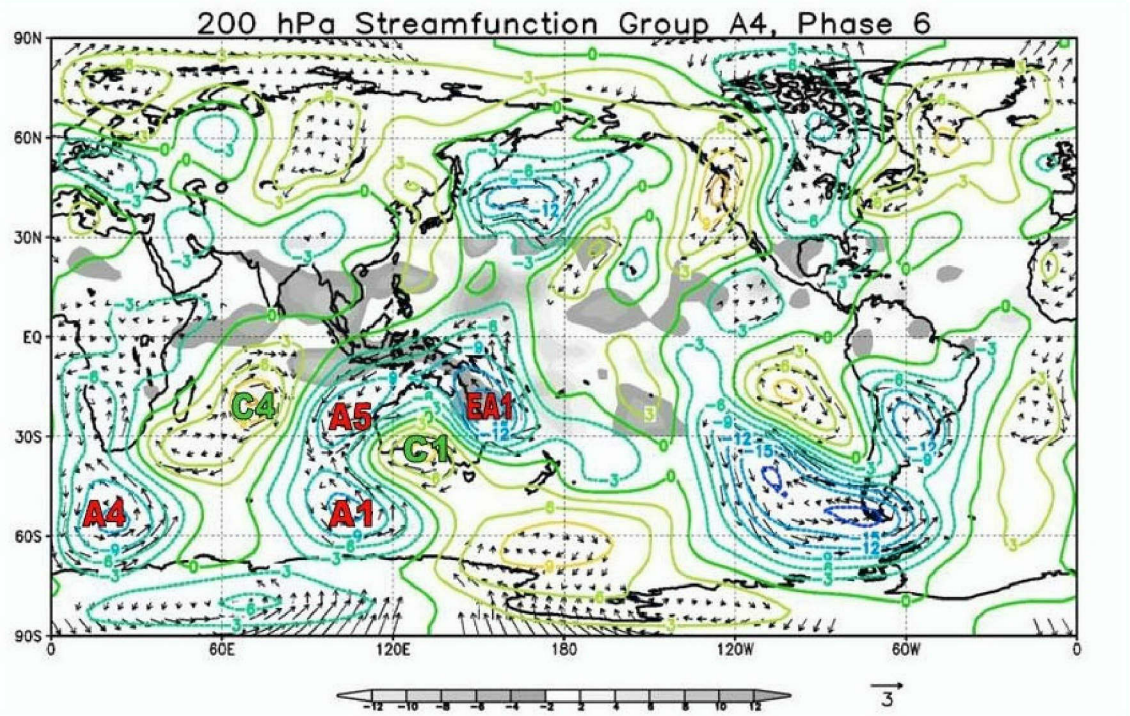


Figure 3.35 Phase 6 composite of 200 hPa streamfunction anomalies (contour interval, $10^6$ in $m^2$ $s^{-1}$), significant wind anomalies (arrows) in m $s^{-1}$ (scale at bottom), and OLR anomalies (shaded) in W $m^{-2}$ for group A4.

*b. Phase 6*

In phase 6 (Figure 3.35), the AAO is beginning a transition from a positive index to a negative index (curve A4 in Figure 3.24). Anomalous easterly winds associated with a large cyclonic circulation in the Southern Hemisphere over the dateline suggest a weakening of the polar branch of the split jet from 150°E to 120°W. These anomalies correlate well with zonal wind anomalies for the AAO positive index displayed in Figure 3.13 (bottom). An apparent wave train in the eastern South Pacific develops in response to meridional shear of the zonal wind downstream of the weakening jet maximum with a northwest – southeast tilt that is suggestive of equatorward propagation, which is out of phase with a similar wave train in phase 3 (Figure 3.34). Anomalous anticyclonic circulations A4 and A1 correspond to equivalent circulations at 850 hPa during phase 6 (Figure 3.31). A similar Rossby-wave pattern occurs from southwest to northeast of Australia as in phase 3 (Figure 3.34) but originates at higher latitudes in association with the positive phase of the AAO. As a result, an

anomalous upper-level anticyclonic circulation (EA1) exists northeast of Australia where an anomalous cyclonic circulation was found in Phase 3. Therefore, upper-level anomalous southerly winds are crossing the equator and contributing to confluence and reduced convection over the equatorial western Pacific.

3. Group C Composites

Group C defines instances of the 15- to 25-day mode that do not coincide with any significant AAO index. Selected composites for transition phases 2 and 6 of the 15- to 25-day mode will be displayed at both 850 hPa and 200 hPa to determine how the structure of the anomalous circulations of group C are related to the 15- to 25-day mode.

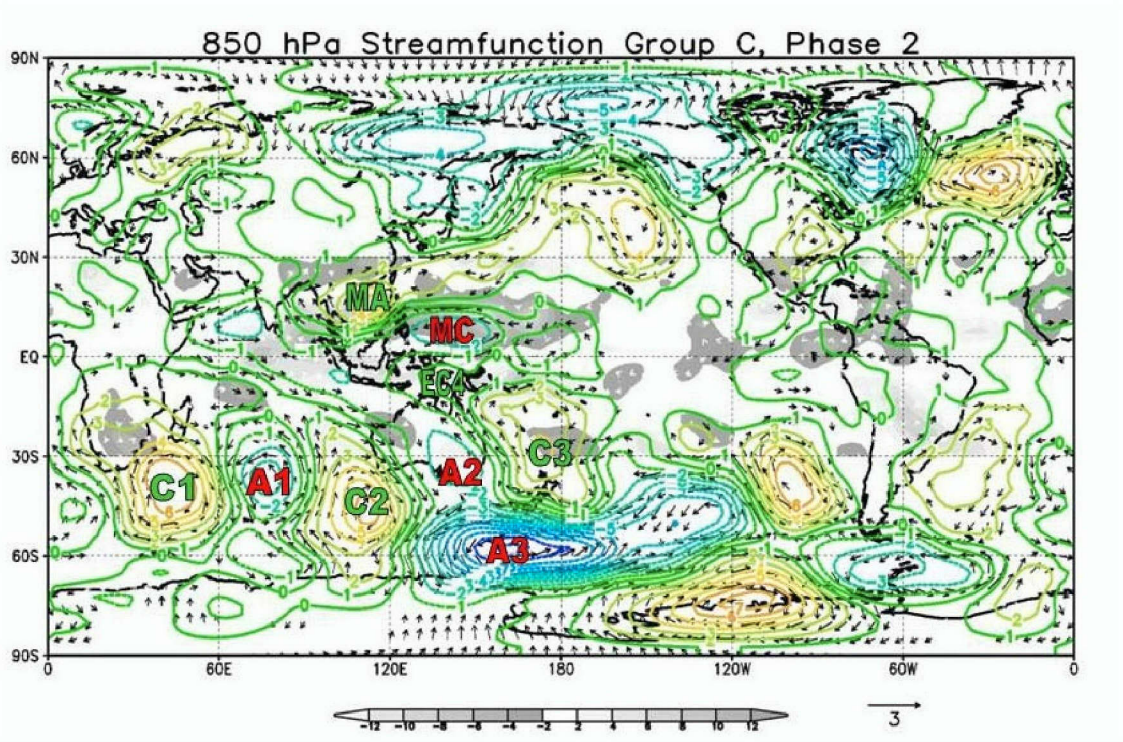


Figure 3.36 Phase 2 composite of 850 hPa streamfunction anomalies (contour interval, $10^6$ $m^2$ $s^{-1}$), significant wind anomalies (arrows) in m $s^{-1}$ (scale at bottom), and OLR anomalies (shaded) in W $m^{-2}$ for group C.

*a. Phase 2*

An anomalous anticyclonic circulation at 850 hPa (labeled MA in Figure 3.36) is over eastern China in phase 2. Positive OLR anomalies associated with reduced convection on both sides of the equator extend eastward from 60°E to Indonesia. An anomalous cyclonic circulation (labeled

MC) has developed east of the Philippines. Negative OLR anomalies associated with enhanced convection extend eastward along 20°N to the dateline indicating development of an enhanced phase of the monsoon trough due to an increase in equatorial westerlies.

In the Southern Hemisphere, a zonal wave pattern of anomalous cyclonic and anticyclonic circulations (labeled C1-A1-C2) extends eastward from southern Africa to 130°E. East of 130°E, the wave structure appears to split into two branches. In the equatorward branch, an anomalous anticyclonic circulation (labeled A2) that developed over southeastern Australia appears to aid the development of an anomalous cyclonic circulation (labeled C3) near the dateline at 30°S. This downstream development appears to result from Rossby-wave forcing in the exit region of the low-level jet maximum southeast of Australia depicted in Figure 3.14. The poleward branch of the wave spilt is dominated by a large anticyclonic anomaly (labeled A3) south of New Zealand and appears to represent the southward progression of the low-level jet east of 120°E displayed in Figure 3.14. Neither of these branches appear to have any significant connection to the tropics since most of their wave energy flux is directed along or poleward of 30°S. An anomalous cyclonic circulation (labeled EC4) over New Guinea appears to be part of an equatorial Rossby wave associated with the enhanced convection in the monsoon trough. Beyond the fact that the waves west of 130°E are aligned in a more zonal direction in phase 2 of group C (Figure 3.36) versus phase 2 of group A4 (Figure 3.27), there are several important differences between the two groups. In group A4, the strengthening Mascarene High and Australian Highs seem to partly be a response to the strong cyclonic cells (C1 and C2 in Figure 3.27) to the southwest. In group C this does not occur because of the zonal orientation. Consequently, the Mascarene High and Australian High do not get as intense in group C as they do in group A4.

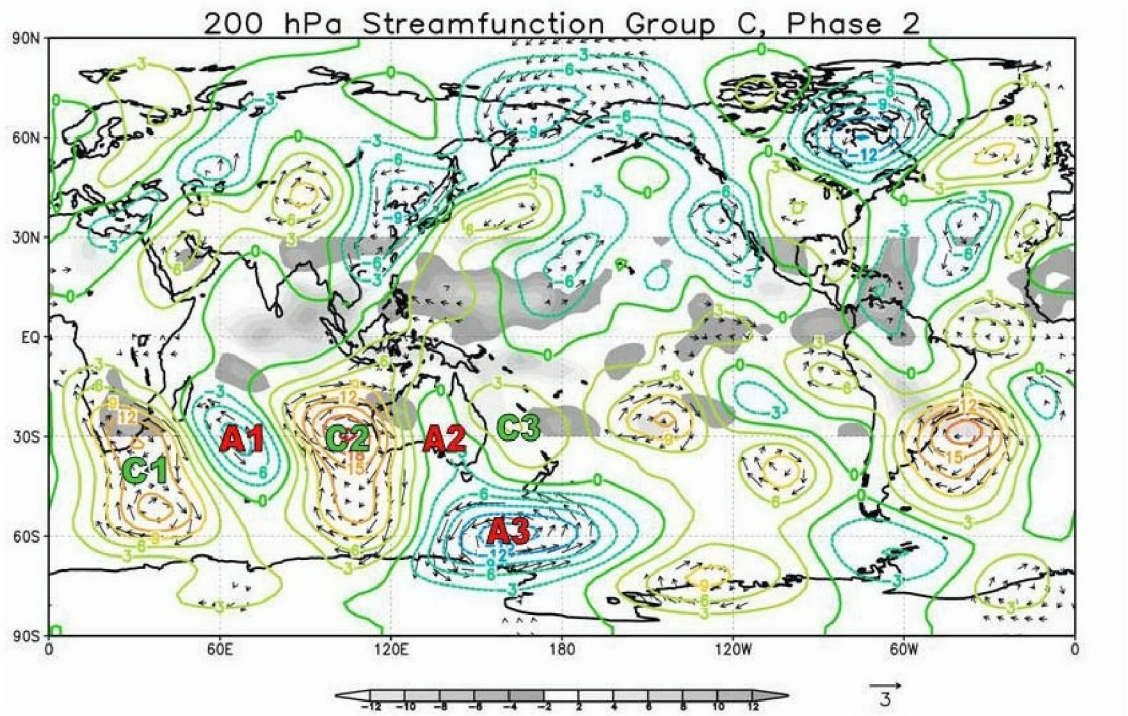


Figure 3.37 Phase 2 composite of 200 hPa streamfunction anomalies (contour interval, $10^6$ $m^2$ $s^{-1}$), significant wind anomalies (arrows) in m $s^{-1}$ (scale at bottom), and OLR anomalies (shaded) in W $m^{-2}$ for group C.

At 200 hPa (Figure 3.37), an equivalent barotropic structure of the Southern Hemisphere mid-latitudes is evident as the pattern of cyclonic and anticyclonic circulation anomalies is similar to that at 850 hPa (Figure 3.36). Again, no significant connection appears to exist between circulation centers in the mid-latitudes and enhanced convection in the tropics as the wave energy flux is directed eastward along 30° S.

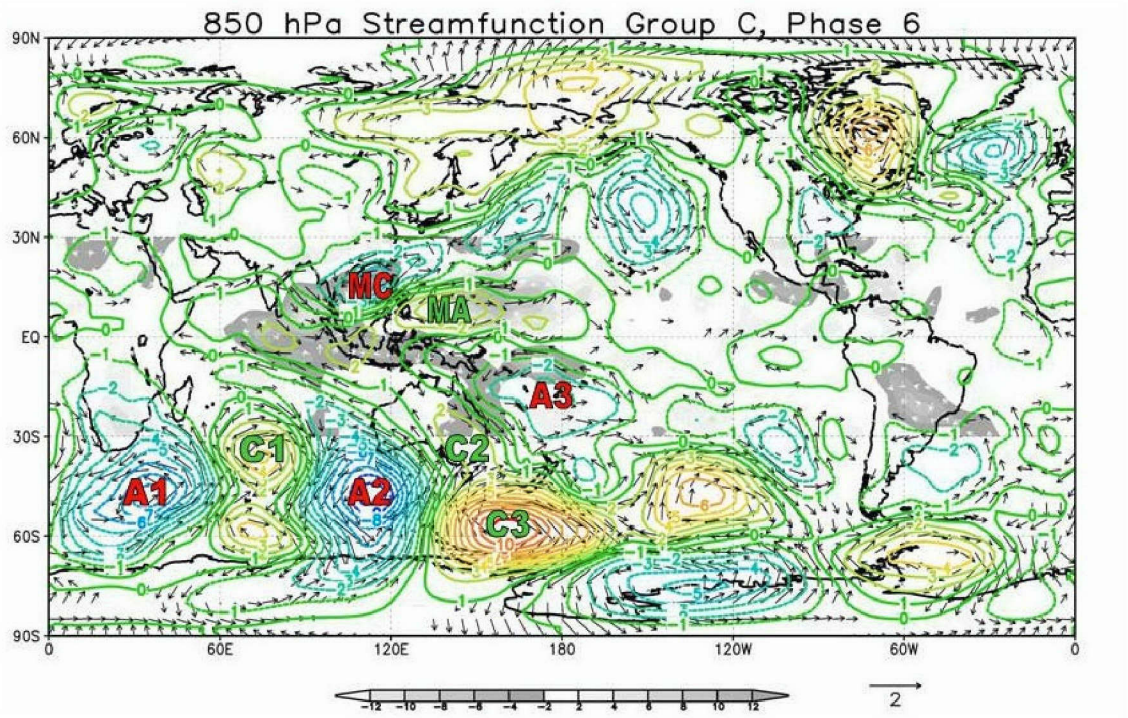


Figure 3.38 Phase 6 composite of 850 hPa streamfunction anomalies (contour interval, $10^6$ $m^2$ $s^{-1}$), significant wind anomalies (arrows) in m $s^{-1}$ (scale at bottom), and OLR anomalies (shaded) in W $m^{-2}$ for group C.

*b. Phase 6*

In phase 6, the anomalous circulation structure in the mid-latitudes is nearly opposite to that of phase 2. At 850 hPa (Figure 3.38), the cyclonic anomaly (labeled MC) in the monsoon trough is over eastern China. Convection associated with circulation MC appears to be enhanced by strong southwesterly winds originating over the Bay of Bengal. An anomalous anticyclonic circulation (labeled MA) east of the Philippines is consistent with reduced convection associated with the inactive phase of the monsoon trough. A nearly zonal wave pattern exists in the Southern Hemisphere west of 130°E with an equatorward and poleward deflection to the east. An anomalous cyclonic circulation C2 and then an anomalous anticyclonic circulation A3 is the most equatorward evidence of Rossby-wave energy that originates from the Southern Hemisphere mid-latitudes. Since this circulation is at 15°S and centered over the dateline, circulation MA appears to be consistent with reduced convection rather than enhanced convection in the Southern Hemisphere tropics.

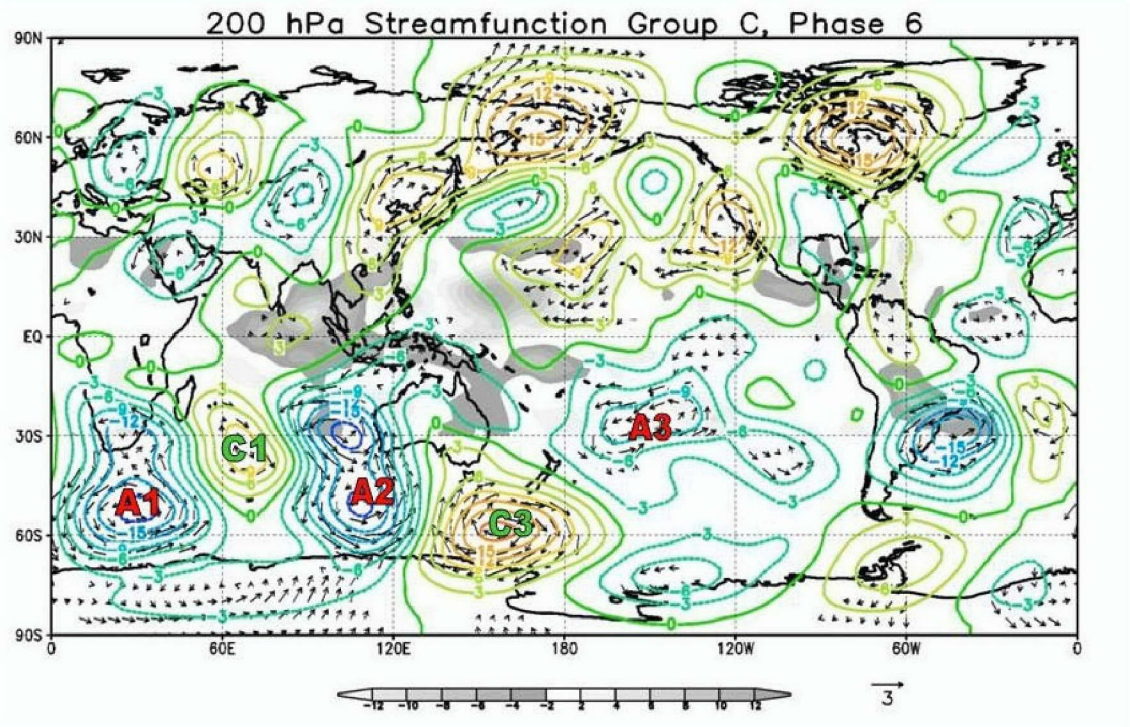


Figure 3.39 Phase 6 composite of 200 hPa streamfunction anomalies (contour interval, $10^6$ $m^2$ $s^{-1}$), significant wind anomalies (arrows) in m $s^{-1}$ (scale at bottom), and OLR anomalies (shaded) in W $m^{-2}$ for group C.

A similar zonal wave pattern is observed at 200 hPa (Figure 3.39). Except for anticyclonic circulation A3, the equivalent barotropic structure of the Southern Hemisphere mid-latitude circulations is again evident as the pattern of circulation anomalies is similar to that of 850 hPa (Figure 3.38). As in phase 2, no significant connection exists between 200 hPa circulation centers in the Southern Hemisphere mid-latitudes and enhanced convection in the tropics as the wave energy flux is along and then poleward of 30° S.

4. Group A5 Composites

Selected phases of the 15- to 25-day mode will be displayed at 850 hPa to summarize the overall structure of anomalous circulation in the mid-latitudes and its relation to the transition phases of the AAO. This structure will be compared to that of the group A4, which has been established above as a standard reference for the primary AAO-related circulations. Variations from the standard will be used to determine if the AAO of each case is connected to the 15- to 25-

day oscillation of the monsoon trough convection in the western North Pacific. Similar analyses will then be performed on groups B4, N, and P.

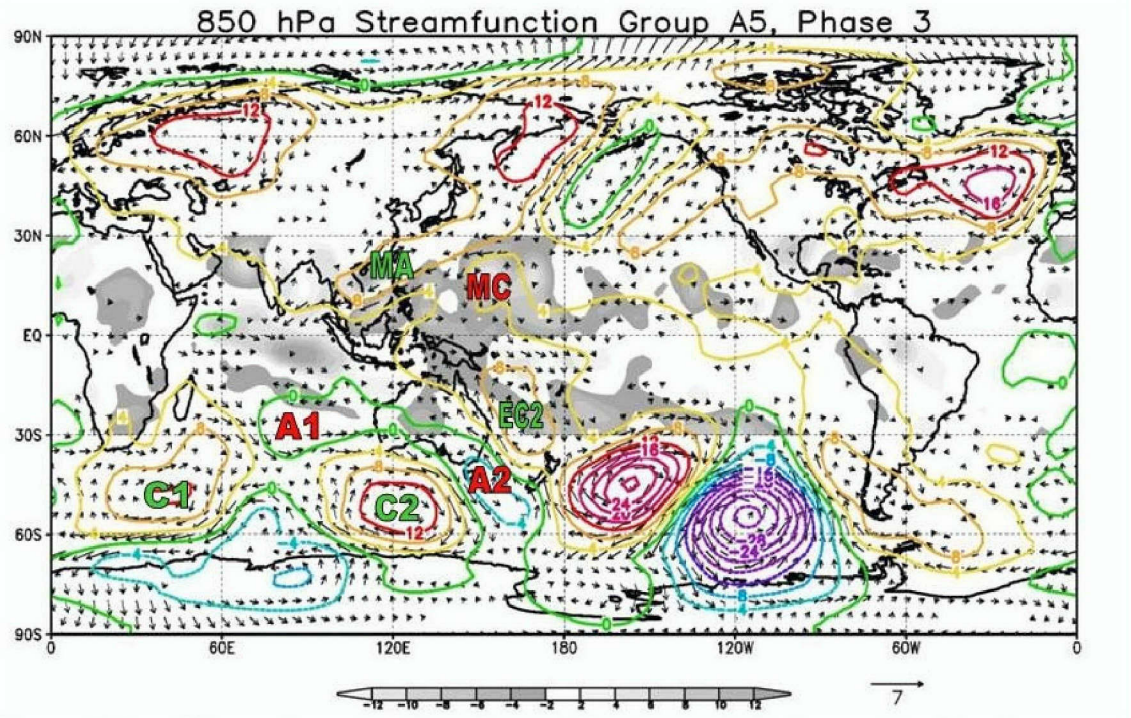


Figure 3.40 Phase 3 composite of 850 hPa streamfunction anomalies (contour interval, $10^6$ $m^2$ $s^{-1}$), significant wind anomalies (arrows) in m $s^{-1}$ (scale at bottom), and OLR anomalies (shaded) in W $m^{-2}$ for group A5.

*a. Phase 3*

In phase 3 (Figure 3.40), a weak cyclonic circulation (labeled MC) has developed east of monsoon trough region. Negative OLR anomalies associated with enhanced convection extend through tropical latitudes from west of the dateline to 120°E north of the equator. An anomalous anticyclonic circulation (labeled MA) near Hong Kong corresponds with reduced convection ahead of the monsoon trough.

In the Southern Hemisphere, the AAO is in a transition from a weak negative to a weak positive index (curve A5 in Figure 3.24), which is associated with a poleward shift in the low-level jet. Cyclonic anomalies (labeled C1 and C2) remain the dominant mid-latitude circulations west of the dateline in the Southern Hemisphere. Anomalous anticyclonic circulations (labeled A1 and A2) appear to be developing to the northeast of C1 and C2. A secondary anomalous cyclonic

circulation (labeled EC2) develops east of Australia apparently as a result of equatorward wave propagation as circulation A2 continues to build and circulation C2 continues to weaken during the transitioning AAO.

In comparison to phase 3 of group A4 (Figure 3.28), group A5 appears to have a delay in the development of the mid-latitude anticyclonic circulations A1 and A2. The above trend appears to be related to the delay in the transition phase of the stronger negative AAO for group A5 as suggested by curve A5 versus curve A4 in Figure 3.24. Furthermore, circulations A1 and A2 are east of their respective locations in group A4 (Figure 3.28) and do not correspond well with the strengthening of the Mascarene High or the Australian High. This shift in locations appears to be related to the average peak negative AAO index of group A5 that is nearly twice the magnitude of the average peak negative index of group A4 in Figure 3.24. With the stronger negative AAO index in group A5, anomalous westerlies associated with the low-level jet maximum in the mid-latitudes extend farther east. As a result, the wave propagation associated with these anomalous circulation cells shifts eastward and thus does not have a direct connection with the monsoon trough region in the western North Pacific as occurred with group A4.

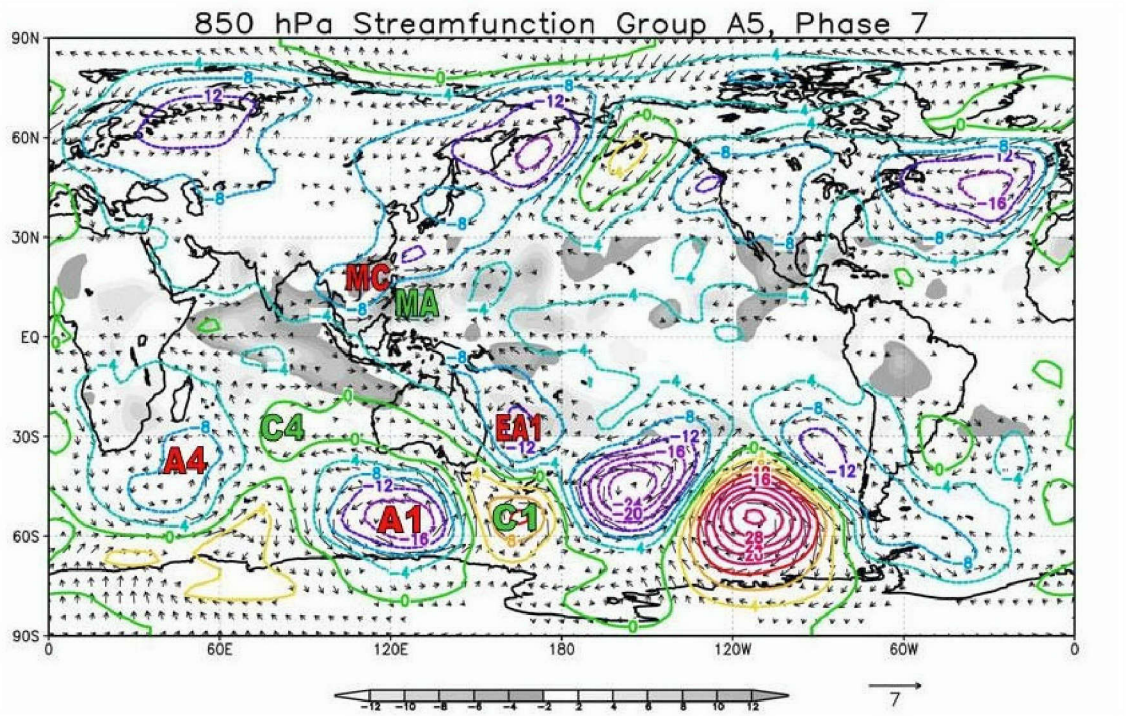


Figure 3.41 Phase 7 composite of 850 hPa streamfunction anomalies (contour interval, $10^6$ in $m^2$ $s^{-1}$), significant wind anomalies (arrows) in m $s^{-1}$ (scale at bottom), and OLR anomalies (shaded) in W $m^{-2}$ for group A5.

*b. Phase 7*

In phase 7 (Figure 3.41), an anomalous cyclonic circulation (labeled MC) near Hong Kong corresponds with the enhanced convection at the western end of the monsoon trough. However, a weak anticyclonic circulation (labeled MA) has developed east of the Philippines. Positive OLR anomalies associated with reduced convection extend through tropical latitudes west of the dateline to 100°E north of the equator. Thus, this phase corresponds to an inactive monsoon trough in the western North Pacific.

The AAO is now in a transition from a positive AAO index to a negative AAO index (curve A5 in Figure 3.24), which is associated with an equatorward shift in the low-level jet in the Southern Hemisphere mid-latitudes. Anticyclonic anomalies (labeled A4 and A1) are now weakening west of the dateline in response to the weakening positive AAO index. Anomalous cyclonic circulations (labeled C4 and C1) appear to be developing to the northeast of A4

and A1 with a secondary anomalous anticyclonic circulation (labeled EA1) developing east of Australia.

In summary, the Southern Hemisphere structure of phase 7 does not appear to be connected to the anomalous circulations in the monsoon trough region of the western North Pacific. Similar to reasoning given for phase 3 above, the delay in the transition of the AAO index from positive to negative (Figure 3.24) and the relative magnitude of the AAO index compared to group A4 results in a more eastward source of wave propagation that overshoots the monsoon trough region.

5. Group B4 Composites

*a. Phase 1*

In phase 1 (Figure 3.42), an anomalous anticyclonic circulation (labeled MA) is over of the South China Sea. Positive OLR anomalies associated with reduced convection are tilted southwest-northeast and extend northeast from 90°E at the equator to the western North Pacific mid-latitudes. An anomalous cyclonic circulation (labeled MC) is beginning to develop southeast of circulation MA just north of the equator. Negative OLR anomalies north of New Guinea are associated with enhanced convection and indicate the beginning of the enhanced phase of the monsoon trough.

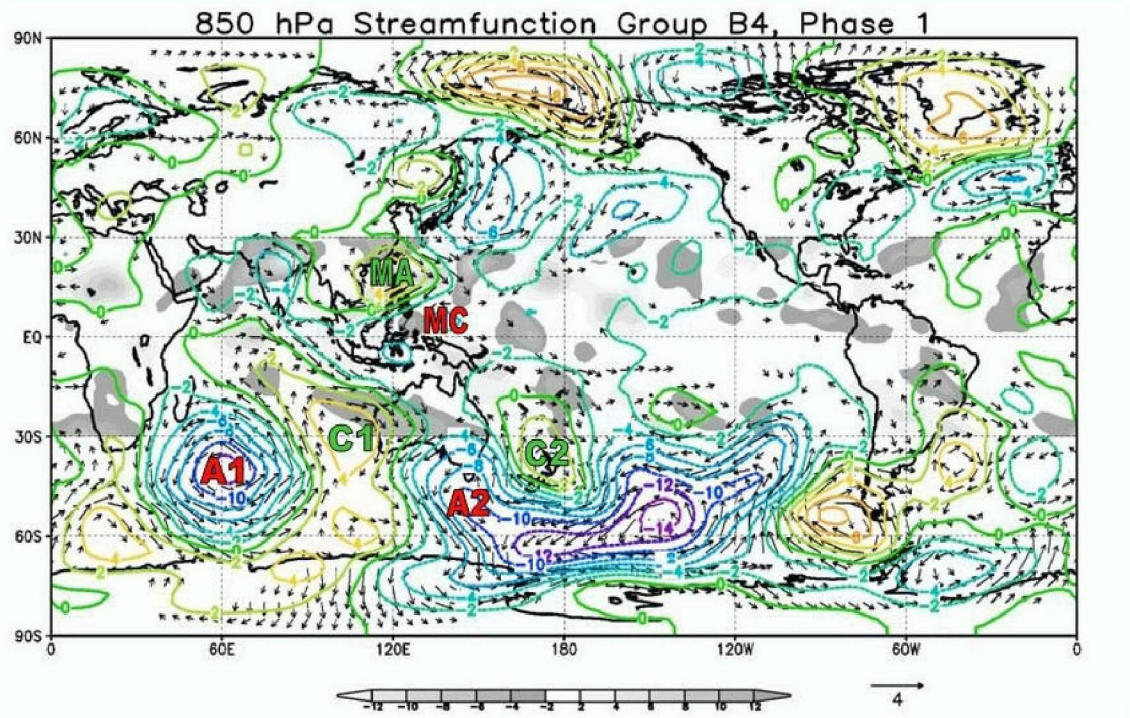


Figure 3.42 Phase 1 composite of 850 hPa streamfunction anomalies (contour interval, $10^6$ in $m^2$ $s^{-1}$), significant wind anomalies (arrows) in m $s^{-1}$ (scale at bottom), and OLR anomalies (shaded) in W $m^{-2}$ for group B4.

In the Southern Hemisphere, the AAO is transitioning from a weak positive to a weak negative index (curve B4 in Figure 3.25), which results in an equatorward shift in the low-level jet. Weakening anticyclonic anomalies (labeled A1 and A2) remain the dominant mid-latitude circulations west of the dateline in the Southern Hemisphere and are associated with the Mascarene High and Australian High. Anomalous cyclonic circulations labeled C1 and C2 northeast of circulations A1 and A2 appear to be connected to the Mascarene High and Australian High via Rossby-wave dispersion.

In comparison to phase 1 of group A4 (Figure 3.26), the equatorward wave propagation in group B4 appears to have already peaked since circulations A1 and A2 are weakening as the AAO index transitions from positive to negative. These tendencies are opposite to those in group A4 (curve A4 in Figure 3.24), in which the AAO index is positive and increasing and the Mascarene High and Australian High are strengthening and are sources of equatorward wave propagation from the mid-latitudes into the tropical regions. It

appears that the weaker forcing associated with the weakening Mascarene High and Australian High in group B4 limits the equatorward extent of wave energy propagation. Therefore, the AAO in group B4 does not appear to contribute to enhanced convection in conjunction with the development of the active phase of the monsoon trough in the western North Pacific.

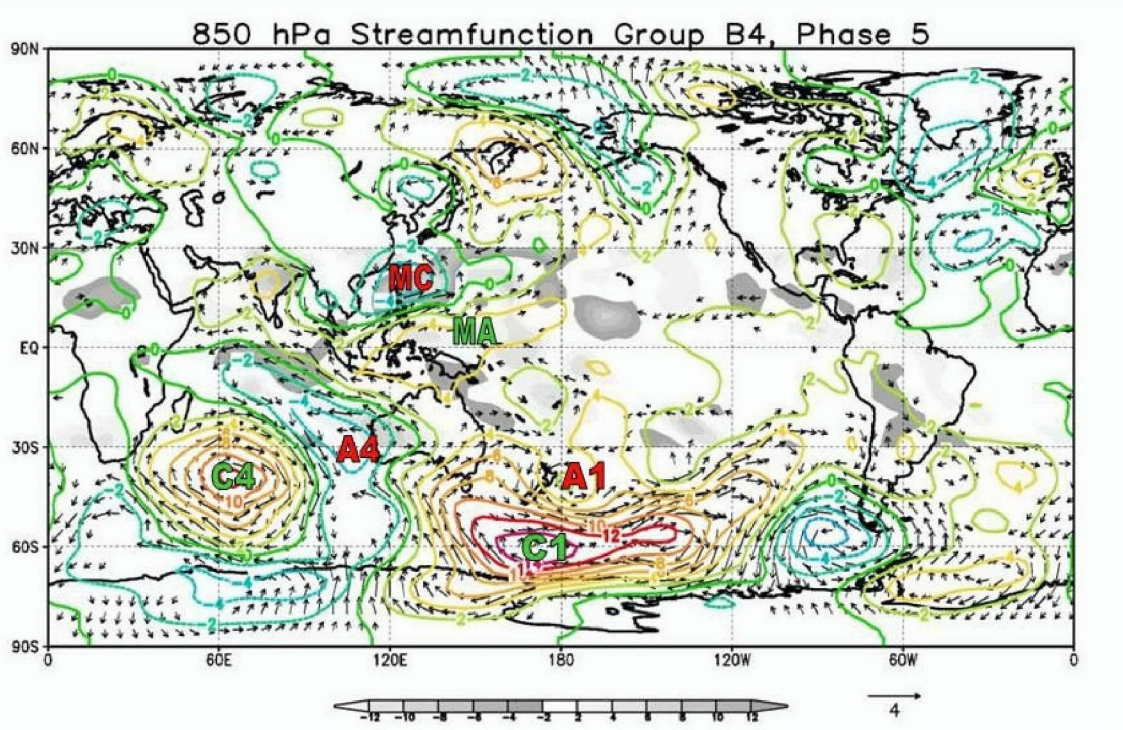


Figure 3.43 Phase 5 composite of 850 hPa streamfunction anomalies (contour interval, $10^6$ $m^2$ $s^{-1}$), significant wind anomalies (arrows) in m $s^{-1}$ (scale at bottom), and OLR anomalies (shaded) in W $m^{-2}$ for group B4.

*b. Phase 5*

In phase 5 (Figure 3.43), a weak anticyclonic circulation (labeled MA) has developed northeast of New Guinea. Positive OLR anomalies associated with reduced convection along the equator extend northeastward from Borneo through tropical latitudes to 170°E. An anomalous cyclonic circulation (labeled MC) over the Philippines corresponds with a region of enhanced convection of the monsoon trough.

In this phase, the AAO begins to transition from a negative index to a positive index (curve B4 in Figure 3.25), which corresponds with a poleward shift in the low-level jet. Cyclonic anomalies labeled C4 and C1 west of the

dateline are now weakening in response to the transition of the AAO index. Anomalous anticyclonic circulations labeled A4 and A1 appear to be developing to the northeast of C4 and C1, respectively, as expected from Rossby-wave dispersion.

However, these Southern Hemisphere circulations do not appear to have a significant connection to the anomalous circulations in the Northern Hemisphere monsoon trough region. Similar to reasoning given for phase 1 above, equatorward wave propagation peaks with the maximum AAO index well before the monsoon trough cycle has time to develop. It appears that the weaker forcing associated with Mascarene High and Australian High source regions limits the equatorward extent of potential wave energy flux from the Southern Hemisphere mid-latitudes and thus does not impact the early development of the inactive phase of the monsoon trough.

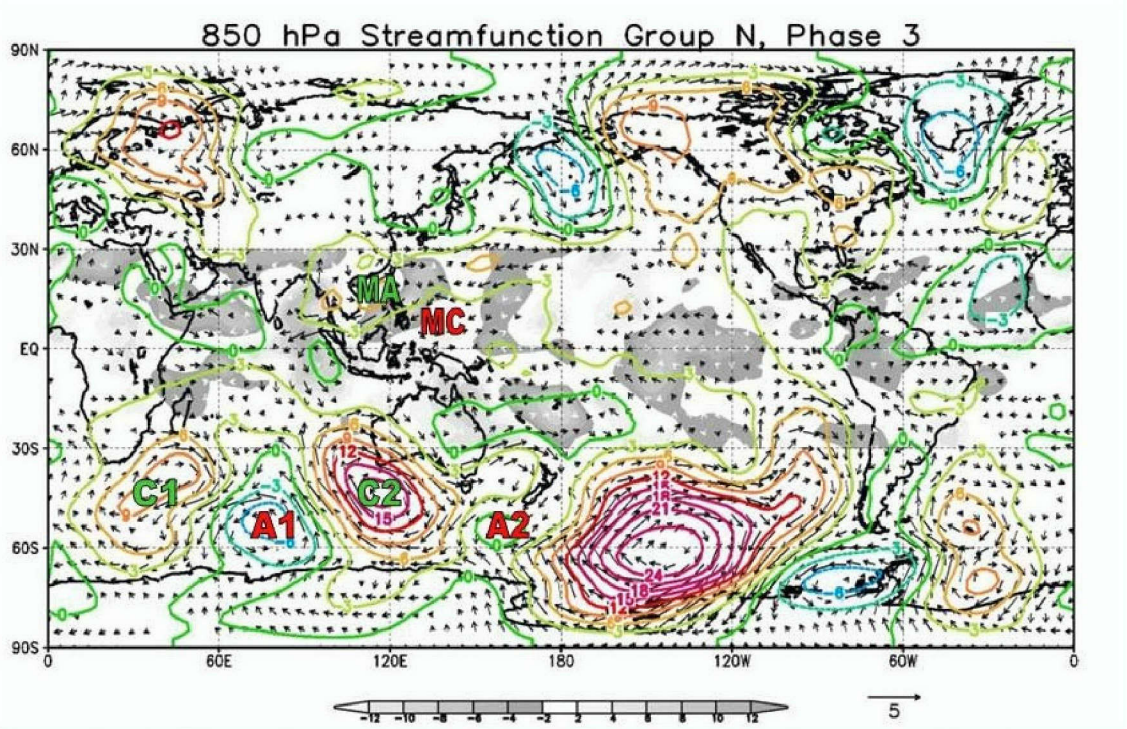


Figure 3.44 Phase 3 composite of 850 hPa streamfunction anomalies (contour interval, $10^6$ $m^2$ $s^{-1}$), significant wind anomalies (arrows) in m $s^{-1}$ (scale at bottom), and OLR anomalies (shaded) in W $m^{-2}$ for group N.

6. Group N Composites

*a. Phase 3*

In phase 3 (Figure 3.44), a weak anticyclonic anomaly (labeled MA) is over the South China Sea. Positive OLR anomalies associated with reduced convection extend westward into the Bay of Bengal and southwestward toward the equator. A weak cyclonic anomaly (labeled MC) has developed southeast of the Philippines at 10°N. Negative OLR anomalies associated with enhanced convection on the western half of this cyclonic circulation appear to be consistent with low-level convergence with the anticyclonic wind anomalies to the northwest. Enhanced convection associated with the eastern half of circulation MC is consistent with equatorial westerly winds in the lower troposphere north of the equator.

In the Southern Hemisphere, a more zonal wave pattern of anomalous cyclonic and anticyclonic circulations (labeled C1-A1-C2-A2) extends eastward from southern Africa to beyond the dateline. Anomalous cyclonic circulations appear to have reached their maximum intensity in conjunction with the peak negative AAO index (curve N in Figure 3.23), which indicates a more equatorward position of the low-level jet. This anomalous circulation in the Southern Hemisphere mid-latitudes has similar features to that of phase 1 of group A4 (Figure 3.30) in which strong cyclonic anomalies dominate the mid-latitudes and the AAO has reached its peak negative index (curve A4 in Figure 3.24). In the case of group A4, anomalous westerlies associated with cyclonic circulations C4 and C1 in Figure 3.30 are farther poleward near 40°S and strengthen the low-level jet maximum depicted in Figure 3.14 (bottom), which results in greater equatorward wave propagation (Hartmann and Lo 1998). In Figure 3.44, the anomalous westerlies associated with cyclonic circulations C1 and C2 are near 30°S in conjunction with a more equatorward shift in the jet. Anomalous easterly winds associated with circulations C1 and C2 are near 50°S and appear to weaken the low-level jet maximum and lead to a more zonal wave propagation (Hartmann and Lo 1998).

A wave pattern similar to that of phase 3 exists in phase six (Figure 3.45), which suggests that the Southern Hemisphere circulations in group N are again dominated by zonal wave propagation and do not appear to have any significant connection to the 15- to 25-day cycle of convection in the Northern Hemisphere monsoon trough region.

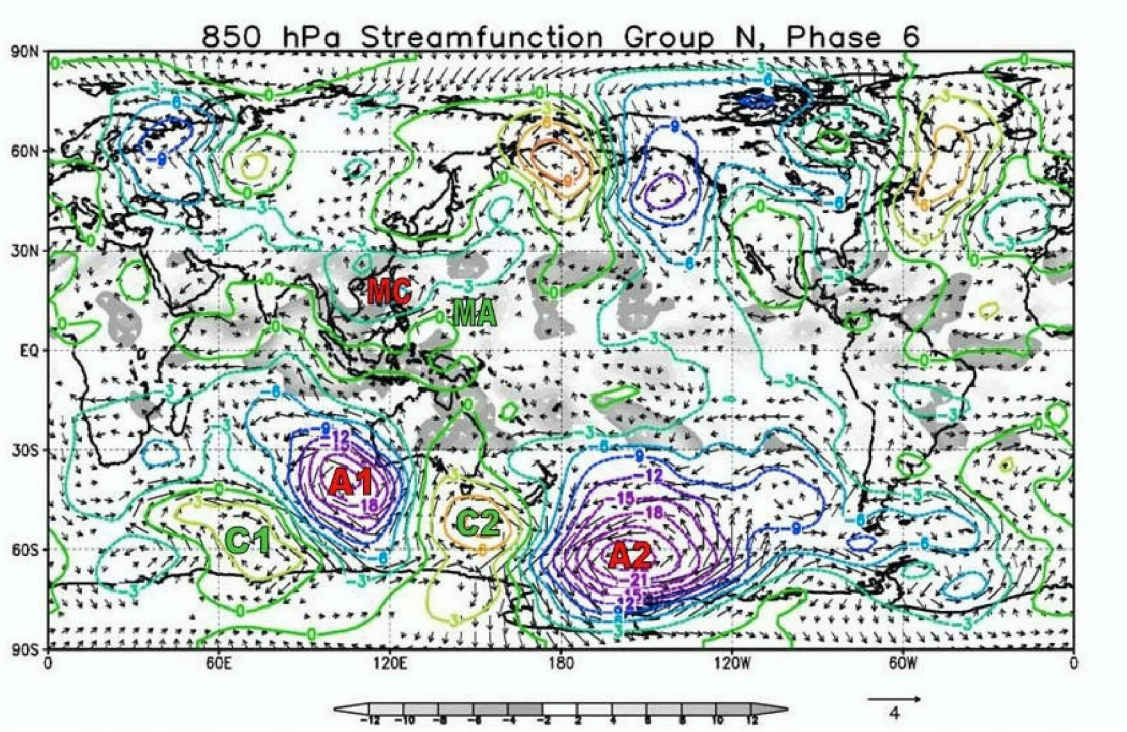


Figure 3.45 Phase 6 composite of 850 hPa streamfunction anomalies (contour interval, $10^6$ $m^2$ $s^{-1}$), significant wind anomalies (arrows) in m $s^{-1}$ (scale at bottom), and OLR anomalies (shaded) in W $m^{-2}$ for group N.

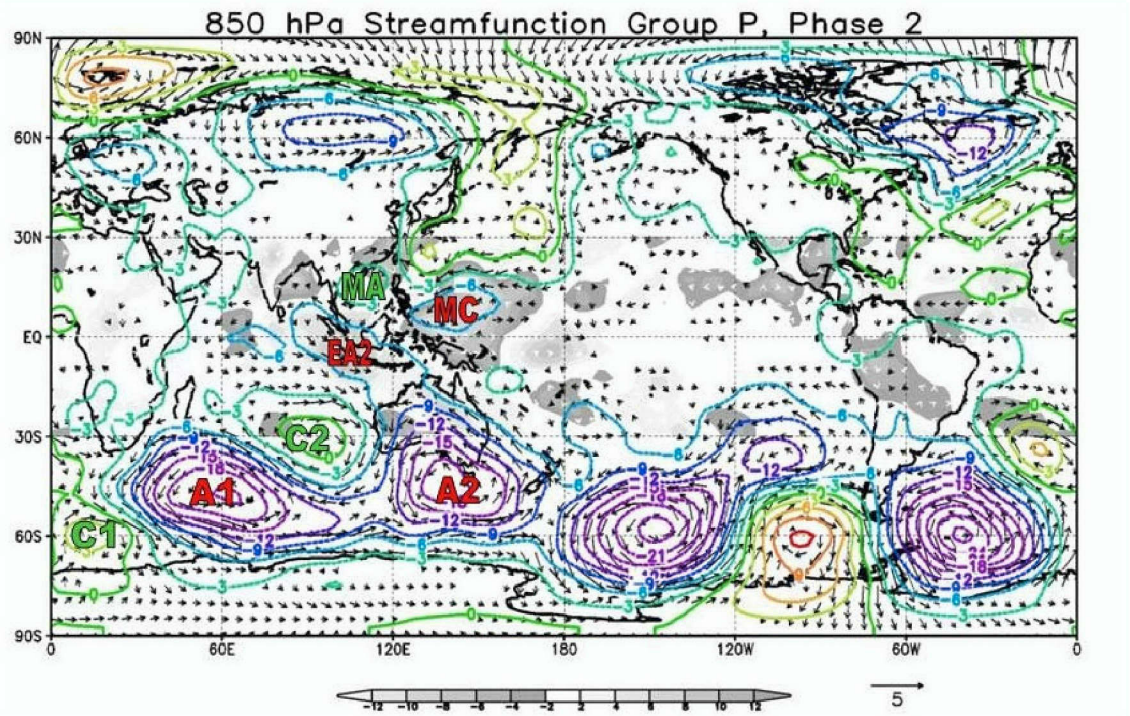


Figure 3.46 Phase 2 composite of 850 hPa streamfunction anomalies (contour interval, $10^6$ $m^2$ $s^{-1}$), significant wind anomalies (arrows) in m $s^{-1}$ (scale at bottom), and OLR anomalies (shaded) in W $m^{-2}$ for group P.

7. Group P Composites

*a. Phase 2*

In phase 2 (Figure 3.46), a large region of reduced convection is near the South China Sea and extends from the equator west of Indonesia to the Philippines. A large anticyclonic anomaly (labeled MA) is associated with this area of reduced convection and is consistent with equatorial easterlies west of 120°E. A large region of enhanced convection extends northeastward from New Guinea to west of the date line. A weak cyclonic anomaly (labeled MC) is associated with this area of enhanced convection and is consistent with equatorial westerlies east of the Philippines.

In the Southern Hemisphere, the AAO has reached its peak positive index (curve P in Figure 3.23), which indicates a more poleward placement of the low-level jet. Two anomalous anticyclonic circulations (labeled A1 and A2) are along 45°S and result in a strengthening of the Mascarene High and the Australian High. The anomalous cyclonic circulation (labeled C1)

southwest of circulation A1 at 60°S and the anomalous cyclonic circulation (labeled C2) is northeast of circulation A1 appear to be part of a Rossby-wave train. Even the secondary anomalous anticyclonic circulation (labeled EA2) in the equatorial region near Indonesia that has developed downstream of circulation C2 may or may not be part of that wave train. Anomalous easterly winds associated with circulation EA2 are consistent with reduced convection along the equator, and also the reduced convection that is associated with circulation MA.

The anomalous circulation pattern of group P during phase 2 of the 15- to 25-day cycle appears to have similar characteristics to that of group A4 for the same phase (Figure 3.27). Both groups have a stronger than normal Mascarene High and Australian High that appear to be sources of equatorward wave energy propagation from the mid-latitudes. The main difference between the two groups is related to the differing index of the AAO. For group A4, the AAO is transitioning from a weak negative index to an increasing positive index (curve A4 in Figure 3.24). For group P, the AAO has reached its maximum positive index and is beginning to weaken in subsequent phases of the 15- to 25-day cycle (curve P in Figure 3.23). Therefore, phase 3 will be examined for any significant differences in the Rossby-wave structure associated with the differing AAO indices between group A4 and group P.

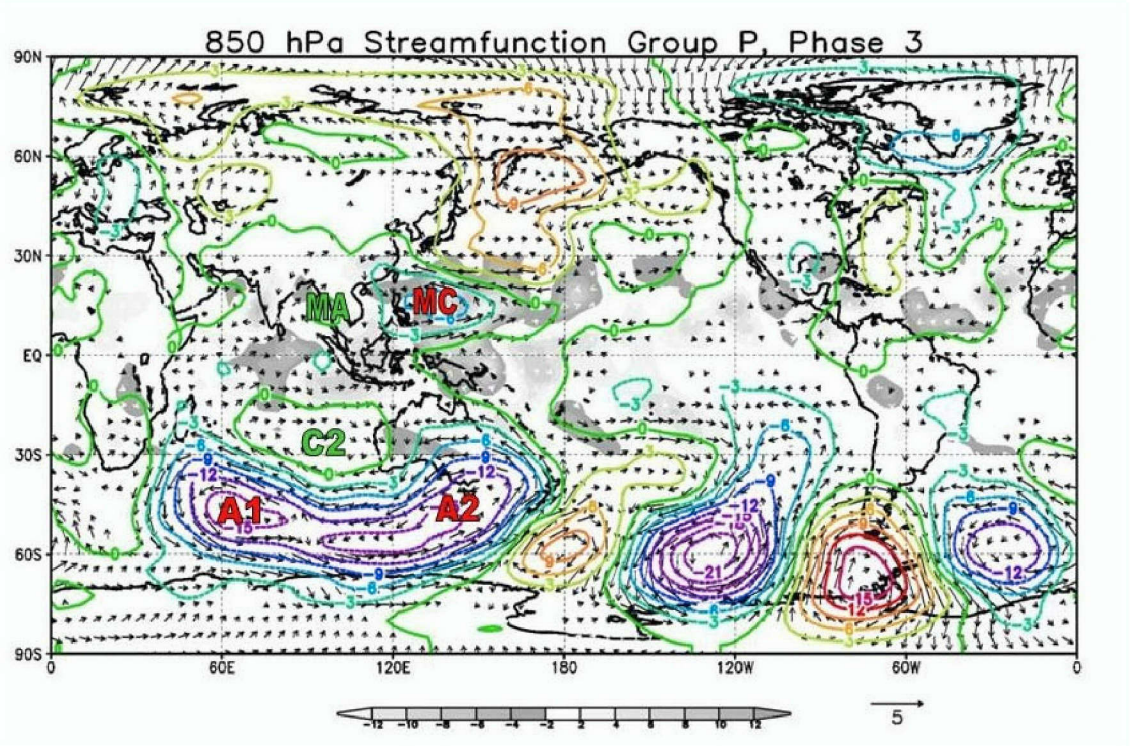


Figure 3.47 Phase 3 composite of 850 hPa streamfunction anomalies (contour interval, $10^6$ $m^2$ $s^{-1}$), significant wind anomalies (arrows) in m $s^{-1}$ (scale at bottom), and OLR anomalies (shaded) in W $m^{-2}$ for group P.

*b. Phase 3*

In phase 3 (Figure 3.47), circulation MA shifts westward over the Bay of Bengal. Reduced convection associated with this circulation extends from eastern India to east of the Philippines. Circulation MC has strengthened over the Philippine Sea. Enhanced convection associated with this circulation covers most of the tropics between the Philippines and the dateline and is consistent with anomalous westerly winds along the equator.

In the Southern Hemisphere, the AAO remains positive but has weakened relative to its maximum index during phase 2 of the 15- to 25-day cycle (curve P in Figure 3.23). In the mid-latitudes, circulations A1 and A2 begin to weaken in conjunction with the weakening AAO. Circulation EA2 has dissipated in the Southern Hemisphere tropics, and the apparent Rossby-wave train during phase 2 (Figure 3.46) appears to be weakening in the mid-latitudes, which leaves no discernible connection between the AAO and enhanced

convection associated with the developing active phase of the monsoon trough indicated by circulation MC.

THIS PAGE INTENTIONALLY LEFT BLANK

# IV. SUMMARY AND CONCLUSION

## A. SUMMARY

Delk (2004) determined that large-scale wave patterns in the western North Pacific that move southeast to northwest with an intraseasonal period of 15- to 25-days impact the frequency and location of tropical cyclone formation during Northern Hemisphere summer. She identified eight phases of this 15- to 25-day cycle and concluded that a peak in tropical cyclone formation was associated with anomalous convection and associated with equatorial westerly wind anomalies during the middle phases of the 15- to 25-day cycle. In the original pattern of low-level circulation anomalies associated with the 15- to 25-day variability, wave-like anomalies were also evident over the Southern Hemisphere mid-latitudes. The purpose of this study is to examine the characteristics of Southern Hemisphere wave activity over the mid-latitudes that appear to have a connection to the 15- to 25-day wave activity in the western North Pacific monsoon trough.

Empirical orthogonal function (EOF) analysis is used to identify the underlying structure of the Southern Hemisphere wave activity poleward of 20°S. The first EOF of 700 hPa geopotential height anomalies is identified as the leading mode of variability in the Southern Hemisphere and is defined as the AAO. The overall structure of the AAO is composed of an anomalous polar vortex surrounded by a ring of positive or negative height anomalies in the mid-latitudes. This structure is characteristic of a meridional seesaw of pressure anomalies between the polar region and the mid-latitudes that modulates the dominant zonal flow patterns.

Analysis of the daily variations in the AAO index identified significant spectral power at intraseasonal and interannual time scales. A 15- to 25-day filtered EOF analysis of the 700 hPa height anomalies indicates that an AAO signature is present on intraseasonal time scales that has a structure consistent with the unfiltered AAO structure. Principal components of the AAO EOF

analysis are used to define a 15- to 25-day AAO index capable of representing the magnitude and sense of the meridional pressure gradient represented by the AAO. Analysis of the filtered daily AAO indices identified periods of significant positive and negative AAO activity.

Composites of the zonal wind and zonal wind anomalies at 850 hPa and 200 hPa were then examined during both AAO positive index and AAO negative index periods. The upper-level composites of 15- to 25-day 200 hPa zonal winds indicate the presence of a split jet over the Indian Ocean in the Southern Hemisphere mid-latitudes. The equatorward branch of the jet is consistent with the STJ and the poleward branch of jet is consistent with the PFJ. Zonal wind anomalies at 200 hPa suggest that when the AAO index is positive the PFJ is strengthened and the STJ is weakened. An opposite relationship exists when the AAO index is negative. Composites of the 15- to 25-day 850 hPa zonal winds indicate a single mid-latitude zonal wind maximum over the central Indian Ocean. Low-level zonal wind anomalies suggest that when the AAO index is positive the 850 hPa jet is displaced poleward. When the AAO index is negative the low-level wind maximum is displaced equatorward.

Finally, temporal analysis of the daily AAO indices indicates that the maximum variability of the AAO has a seasonal dependence that coincides with the Northern Hemisphere summer months in which the 15- to 25-day cycle of monsoon trough convection is observed. Through Fourier analysis and filtered EOF analysis, the AAO has been demonstrated to have a significant contribution to intraseasonal variations on the order of 15- to 25-days in length.

## B. RELATIONSHIP OF THE AAO AND THE 15- TO 25-DAY OSCILLATION

The relationship between the variations in the wave activity in the western North Pacific monsoon trough and the AAO is examined first by means of a single event analysis of coinciding AAO and 15- to 25-day cycles. Each 15- to 25-day cycle of the monsoon trough is compared to anomalous circulations in the Southern Hemisphere that vary with the index of the AAO. Six distinct circulation patterns (A4, A5, B4, B6, P, and N) exist for significant AAO events occurring during the 15- to 25-day mode. Group A4 is the most common of these

occurrences and appears to have the greatest influence in modulating 15- to 25-day wave activity in the western North Pacific monsoon trough region.

In the case of group A4, the AAO is transitioning from a strong negative index to a strong positive index during the first four phases of the 15- to 25-day cycle (curve A4 in Figure 3.24). Cyclonic anomalies in the Southern Hemisphere mid-latitudes (labeled C1 and C2 in Figure 3.26) are consistent with the initially strong negative index of the AAO and begin to weaken with the poleward displacement of the low-level wind maximum. As the AAO continues to transition to a more positive index, anomalous anticyclonic circulations (labeled A1 and A2 in Figure 3.26) develop as a result of equatorward-directed Rossby-wave dispersion northeast of the weakening cyclonic circulations C1 and C2. Circulation A1 and A2 are consistent with a strengthened Mascarene High and Australian High at 850 hPa. As the AAO index becomes increasingly positive through phase 4 of the 15- to 25-day cycle, the low-level wind maximum continues to shift poleward and strengthens the anticyclonic anomalies associated with the Mascarene High and Australian High. The strengthening of the Mascarene High and Australian High results in the development of anomalous cyclonic circulations (labeled EC1 and EC2 in Figure 3.27) in the equatorial region of the Southern Hemisphere tropics. Cross-equatorial westerly and southerly winds associated with circulation EC2 are consistent with enhanced convection in the western North Pacific monsoon trough and appear to have significant impacts on the development of the active phase of the 15- to 25-day wave. In phase 4 of the 15- to 25-day cycle, the AAO reaches its peak positive index and this coincides with the peak convection associated with the active phase of the 15- to 25-day wave activity in the monsoon trough.

In the final four phases of group A4, the AAO index transitions from a strong positive index to a strong negative index (curve A4 in Figure 3.24). Anticyclonic anomalies in the Southern Hemisphere mid-latitudes (labeled A4 and A1 in Figure 3.30) in conjunction with the peak AAO index of phase 4 begin to weaken as the low-level wind maximum shifts equatorward. Anomalous cyclonic circulations (labeled C4 and C1 in Figure 3.30) develop as a result of

equatorward wave propagation northeast of the weakening anticyclonic circulations. Circulation C4 and C1 are consistent with a weakening of the Mascarene High and Australian High at 850 hPa. As the AAO index becomes increasingly negative through phase 8 of the 15- to 25-day cycle, the low-level wind maximum continues to shift equatorward and strengthen cyclonic anomalies C4 and C1, respectively. Wave dispersion from C4 and C1 results in the development of anomalous anticyclonic circulations (labeled EA4 and EA1 in Figure 3.31) in the equatorial region of the Southern Hemisphere tropics. Cross-equatorial northerly winds associated with circulation EA1 are consistent with reduced convection in the western North Pacific monsoon trough during the latter phases of the 15- to 25-day wave.

Composite analysis of anomalous streamfunction, OLR, and winds of the 15- to 25-day mode at 200 hPa suggests an equivalent barotropic wave structure in the Southern Hemisphere. In the upper troposphere, the AAO is the dominant forcing mechanism of circulation variability and modulates the upper-level split jet structure. A positive (negative) AAO index results in a strengthening (weakening) of the PFJ and a weakening (strengthening) of the STJ. Wave activity similar to that in the low-level circulation develops in response to the meridional shear of the transitioning zonal jet maximum with a northwest – southeast tilt that suggests equatorward energy propagation. This alignment is also favorable for poleward momentum transport, which is consistent with the shift between positive and negative AAO states. The pattern of these low-frequency anomalies are qualitatively similar to those of high-frequency eddies during transition between high and low AAO periods that were identified by Shiogama et al. (2004).

Group C was defined as a pattern in which the AAO had no statistically significant variations during the 15- to 25-day events. Composite analysis of anomalous streamfunction, winds, and OLR at 850 hPa and 200 hPa indicates that when the Southern Hemisphere was void of any significant forcing from the AAO, wave activity associated with the low- and upper-level jet structure is more

zonal, disconnected from tropical latitudes, and has no apparent connection to 15- to 25-day wave activity of the western North Pacific monsoon trough.

The five remaining circulation patterns (A5, B4, B6, P, and N) for significant AAO events that occur during the 15- to 25-day mode have some similarities with the Southern Hemisphere mid-latitude circulation of group A4, but are ultimately out of phase with the 15- to 25-day wave activity in the monsoon trough region. For instance, the anomalous circulation pattern of group P during phase 2 of the 15- to 25-day cycle appears to have similar mid-latitude circulations as those in group A4 for the same phase (Figure 3.27). Both groups have a strengthening Mascarene High and Australian High that appear to be sources of equatorward wave energy from the mid-latitudes. In group P, the AAO has reached its maximum positive index in phase 2 and begins to weaken in subsequent phases of the 15- to 25-day cycle (curve P in Figure 3.23), which is not synchronized with the peak of the active phase of 15- to 25-day monsoon trough activity during phase 4.

## C. HOW THE AAO NEGATIVE TO POSITVE TO NEGATIVE INDEX COINCIDES WITH THE 15- TO 25-DAY WAVE EVENT

The state of the initial AAO index in relation to the onset of the 15- to 25-day cycle is critical in developing sufficient equatorward wave energy flux from the Southern Hemisphere mid-latitudes that can reach the monsoon trough region north of the equator. Furthermore, it is the transition phases of the AAO that appear to have the most significant impact on the anomalous wave structure in the Southern Hemisphere mid-latitudes west of the dateline.

The process by which equatorward wave propagation connects the Southern Hemisphere mid-latitude circulation related to the AAO to the 15- to 25-day convective activity in the western North Pacific monsoon trough is summarized in Figure 3.48. In phase 1, strong westerly wind anomalies exist in the subtropics and strong easterly wind anomalies exist in the polar latitudes. These zonal wind anomalies are consistent with an anomalously weak anticyclone equatorward of the westerly wind anomaly and a strong cyclonic anomaly in the mid-latitudes associated with meridional shear of the anomalous

wind maxima. As the AAO index evolves from negative to positive in phases 1-3 of the 15- to 25-day cycle (Figure 3.48 top), anomalous westerly winds shift poleward and modulate the structure of the low- and upper-level wind maxima. In the low levels, a poleward shift in anomalous westerlies is consistent with a poleward shift in the low-level wind maximum. In the upper levels, a poleward shift in anomalous westerlies is consistent with a strengthening of the PFJ. As the AAO index continues to become more positive in phase 3 (Figure 3.48 top), the anomalous wind structure becomes nearly opposite to that of phase 1. Strong easterly wind anomalies now exist in the subtropics and strong westerly wind anomalies exist in the polar latitudes. Meridional shear of the anomalous wind maxima results in a strengthening of the mid-latitude anticyclonic anomaly and the development of an anomalous cyclonic circulation south of the equator (labeled EC in Figure 3.48 top). Cross-equatorial southerly wind anomalies associated with circulation EC are consistent with enhanced convection related to the active phase of the 15- to 25-day monsoon trough in the western North Pacific.

A nearly opposite connection exists as the AAO transitions from positive to negative in phases 5-7 of the 15- to 25-day cycle (Figure 3.48 bottom). In phase 5, strong easterly wind anomalies exist in the subtropics and strong westerly wind anomalies exist in the polar latitudes. A weak cyclonic anomaly equatorward of the westerly wind anomalies and a strong anticyclonic anomaly in the mid-latitudes are associated with meridional shear of these anomalous wind maxima. As the AAO becomes increasingly negative (phase 7 in Figure 3.28), anomalous easterly winds shift poleward and the anomalous wind structure becomes nearly opposite to that of phase 5. Strong westerly wind anomalies now exist in the subtropics and strong easterly wind anomalies exist in the polar latitudes. Meridional shear of the anomalous wind maxima results in a strengthening of the mid-latitude cyclonic anomaly and the development of an anomalous anticyclonic circulation south of the equator (labeled EA in Figure 3.48 bottom). Cross-equatorial northerly wind anomalies associated with

circulation EA are consistent with reduced convection during the inactive phase of the 15- to 25-day monsoon trough.

Based on these results, nearly one half of the significant 15- to 25-day monsoon trough variations coincide with a transition of the AAO from a significant negative to positive index. The remaining instances either occur when the AAO is not significantly varying or when the AAO varies such that AAO transitions do not match 15- to 25-day transitions. This variation is because the 15- to 25-day variability also involves a Northern Hemisphere component (Delk 2004). Therefore, identification of 15- to 25-day variability together with AAO activity could help identify periods of monsoon trough variability on intraseasonal scales.

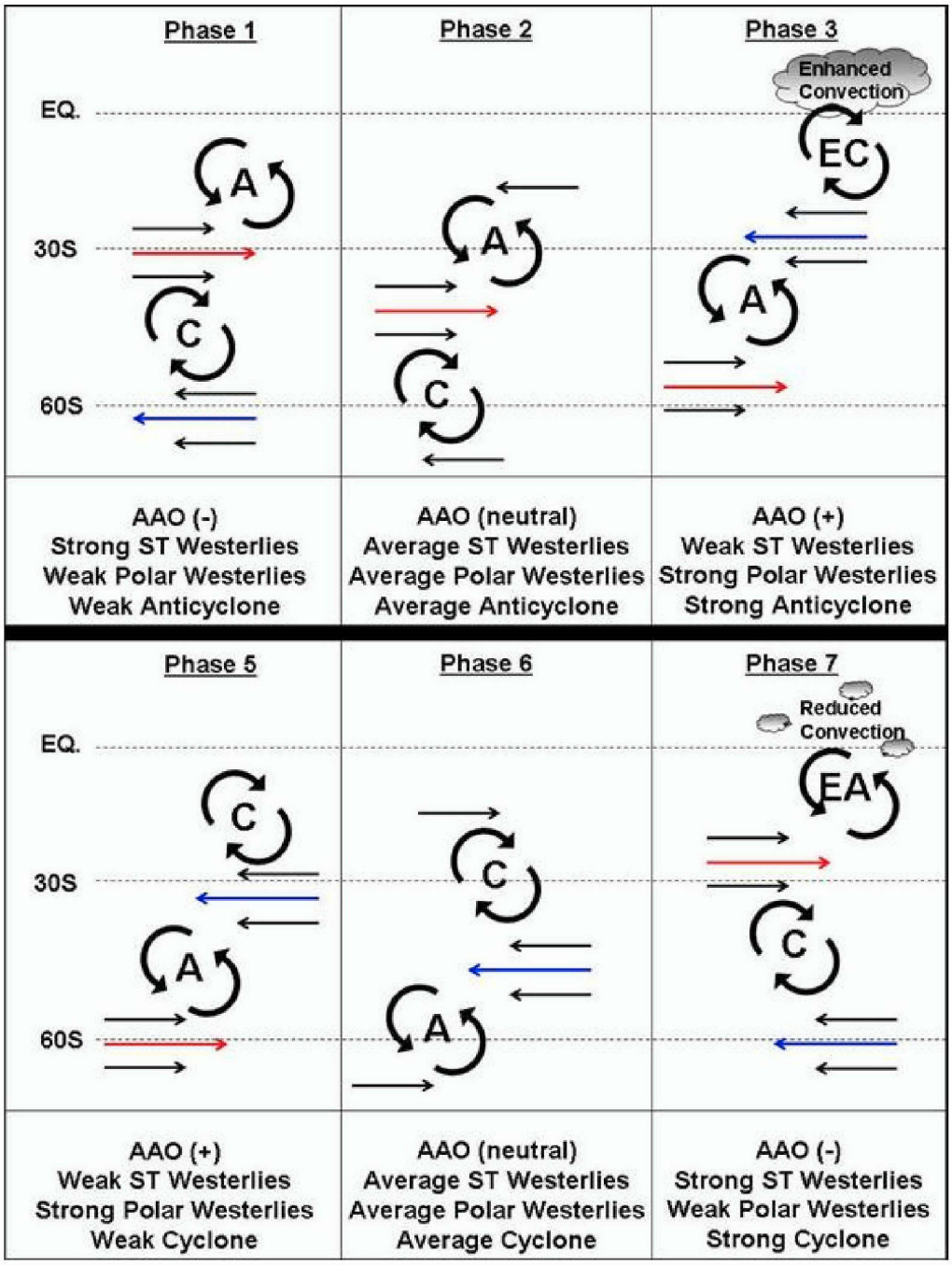


Figure 3.48 Schematic of anomalous wave activity with equatorward propagation in the Southern Hemisphere related to the AAO transition from a negative to positive index (top) during phases 1-3 of the 15- to 25-day cycle and from a positive to negative index (bottom) during phases 5-7 of the 15- to 25-day cycle. This evolution is representative of group A4. Vector lengths indicate relative strength of the anomalous zonal winds in the subtropics (ST) and polar regions. Maximum westerly anomaly is highlighted in red and maximum easterly anomaly is highlighted in blue.

## D. FUTURE STUDY

Based on this study, a significant connection exists between the Southern Hemisphere mid-latitude circulation variations related to the AAO and the 15- to 25-day wave activity in the western North Pacific monsoon trough. This connection is most evident when AAO has a peak negative index that coincides with the initial phase of the 15- to 25-day wave oscillation and then transitions to a peak positive index during phase 4 of the 15- to 25-day mode. Furthermore, the above phase relationship between the AAO and the 15- to 25-day oscillation is related to periods of enhanced convection in the western North Pacific monsoon trough.

Based on the above relationship, areas for future research should include studies on the operational use of the combined AAO index and the 15- to 25-day mode and its potential value to long-term forecasting of tropical cyclone development in the western North Pacific monsoon trough. A valuable extension would be to examine the potential mechanisms that induce transitions of the AAO between positive and negative indices since recent studies related to the AAO fail to address this topic.

THIS PAGE INTENTIONALLY LEFT BLANK

# APPENDIX

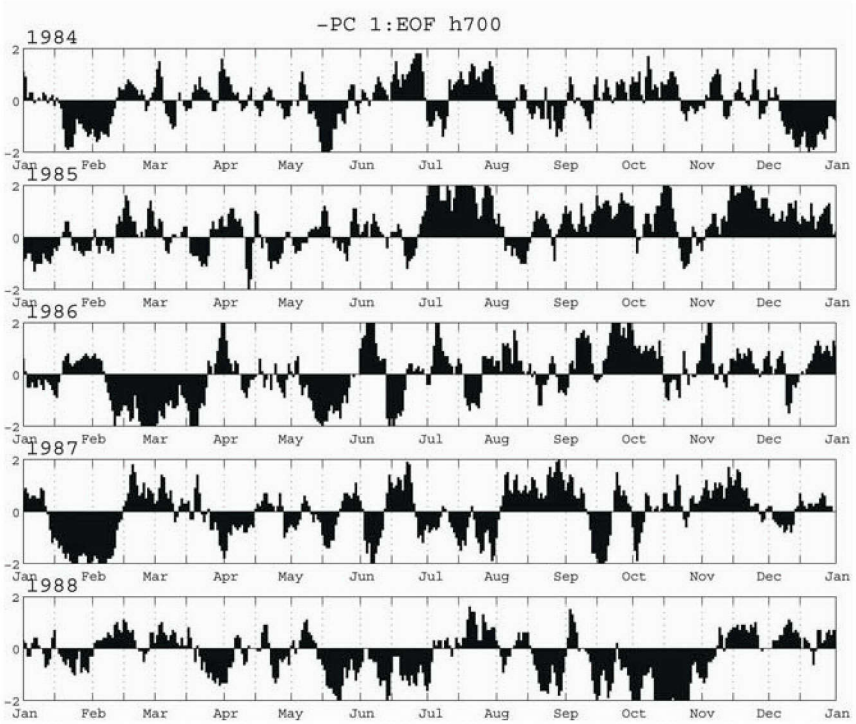


Figure A1 Daily time series from 1984-1988 of the AAO index defined as the leading PC of the 700 hPa height anomaly EOF analysis.

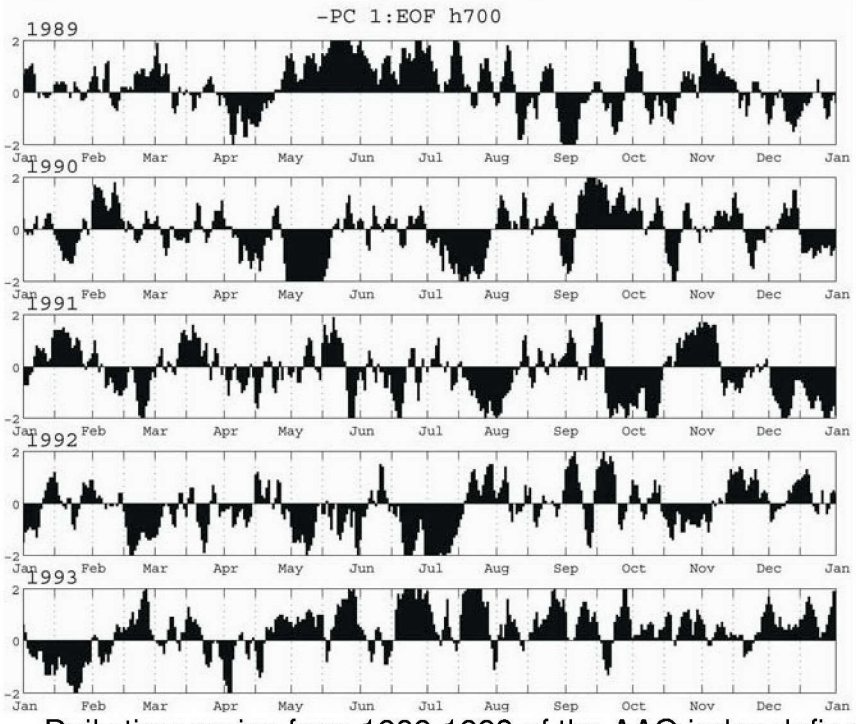


Figure A2 Daily time series from 1989-1993 of the AAO index defined as the leading PC of the 700 hPa height anomaly EOF analysis.

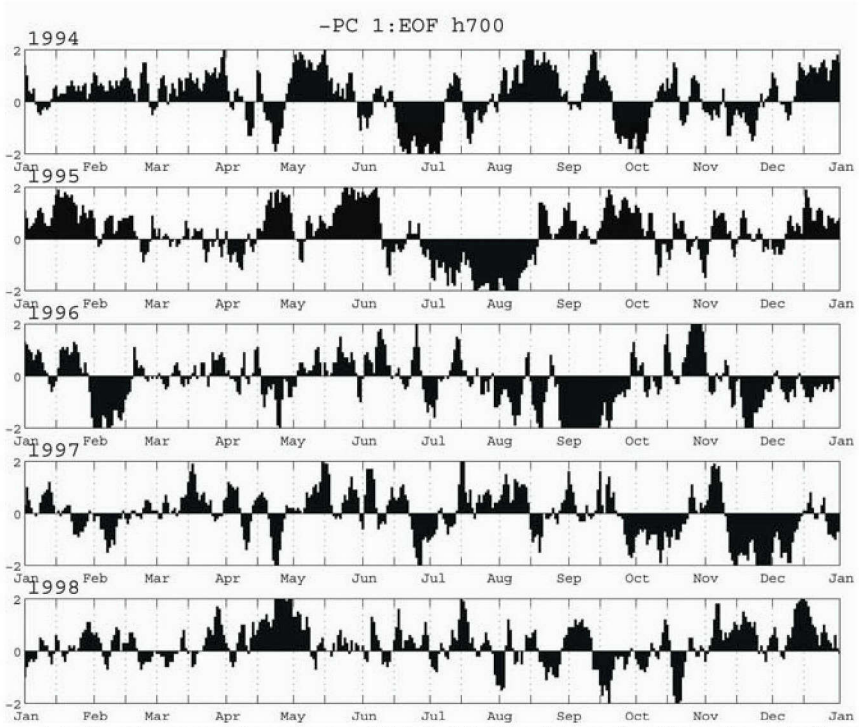


Figure A3 Daily time series from 1994-1998 of the AAO index defined as the leading PC of the 700 hPa height anomaly EOF analysis.

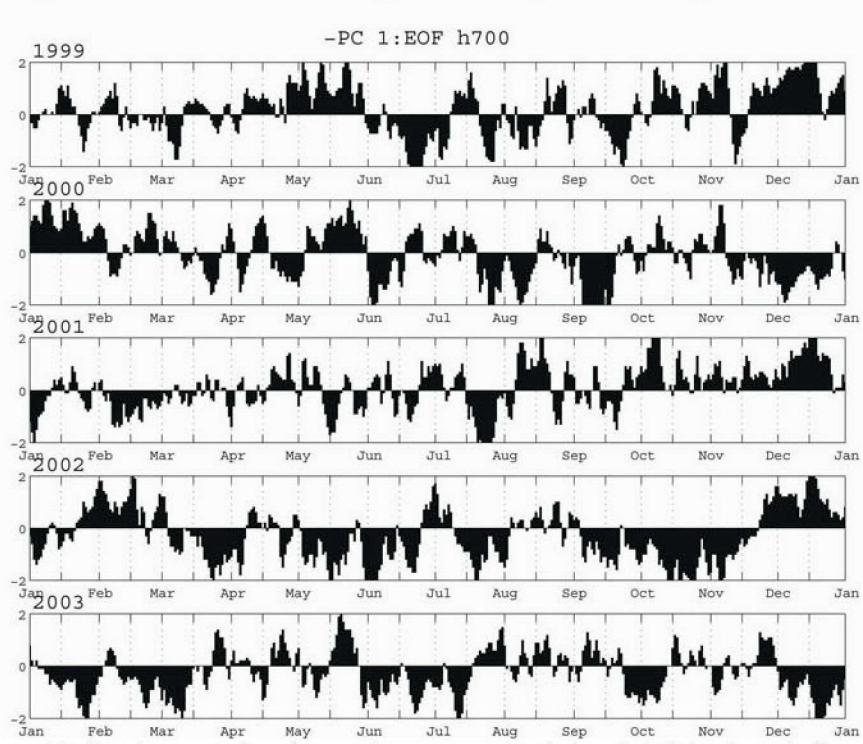


Figure A4 Daily time series from 1999-2003 of the AAO index defined as the leading PC of the 700 hPa height anomaly EOF analysis.

# LIST OF REFERENCES


Air Force Weather, 2004: AFW transformation: Strategic plan and vision FY2008-2032, U.S. Air Force distribution, 18 pp.

Ambrizzi, T., B. J. Hoskins, and H. -H. Hsu, 1995: Rossby wave propagation and teleconnection patterns in the austral winter. *J. Atmos. Sci.,* 52, 3661-3672.

Bals-Elsholz, T. M., and Co-Authors, 2001: The wintertime Southern Hemisphere split jet: Structure, variability and evolution. *J. Climate,* 14, 4191-4215.

Bretherton, C. S., C. Smith, and J. M. Wallace, 1992: An intercomparison of methods for finding coupled patterns in climate data. *J. Climate,* 5, 541-560.

Chang, C.-P., and K. M. Lau, 1980: Northeasterly cold surges and near-equatorial disturbances over winter MONEX area during December 1974. Part II: Planetary-scale aspects. *Mon. Wea. Rev.*, 108, 298-312.

Delk, T. L., 2004: Intraseasonal, large-scale circulations and tropical cyclone activity over the western North Pacific during boreal summer. M.S. Thesis, Naval Postgraduate School, Monterey, CA, 76 pp.

Duchon, C. E., 1979: Lanczos filtering in one and two dimensions. *J. Appl. Meteor.,* 18, 1016-1022.

Hartmann, D. L., and F. Lo, 1998: Wave-driven zonal flow vacillation in the Southern Hemisphere. *J. Atmos. Sci.,* 55, 1303-1315.

Kalnay, E., and Co-Authors, 1996: The NCEP/NCAR 40-year Re-analysis Project. *Bull. Amer. Meteor. Soc.,* 77, 437-471.

Kiladis, G. N., and K. C. Mo, 1998: Interannual and intraseasonal variability in the Southern Hemisphere. *Meteor. Monographs*, 27, 307-336.

Liebmann, B., and C. A. Smith, 1996: Description of a complete (interpolated) outgoing long-wave radiation dataset. *Bull. Amer. Meteor. Soc.,* 77, 1275-1277.

Lorenz, E. N., 1956: Empirical Orthogonal Functions and statistical weather prediction. *Sci. Rep. 1,* Statistical Forecasting Project, Dept. of Meteor., MIT (NTIS AD 110268), 49 pp.

Lorenz, V., and D. L. Hartmann, 2001: Eddy-zonal feedback in the Southern Hemisphere. *J. Atmos. Sci.,* 49, 3312-3327.

Love, G., 1985: Cross-equatorial interactions during tropical cyclogenesis. *Mon. Wea. Rev.*, 113, 1499-1509.

Madden, R. A., and P.R. Julian, 1994: Observations of the 40-50 day tropical oscillation--a review. *Mon. Wea. Rev.*, 122, 814-837.

Maloney, E. D., and D. L. Hartmann, 2000: Modulation of eastern North Pacific hurricanes by the Madden-Julian Oscillation. *J. Climate*, 13, 1451-1460.

--, 2001: The Madden-Julian Oscillation, barotropic dynamics and North Pacific tropical cyclone formation. Part I: Observations. *J. Atmos. Sci.*, 58, 2545-2558.

Miller, A. J., S. Zhou, and S.-K. Yang, 2003: Relationship of the Arctic and Antarctic Oscillations to the Outgoing Longwave Radiation. *J. Climate*, 16, 1583-1592.

Richman, M. B., 1986: Rotation of principal components. *J. Climate*, 6, 293-335.

Shiogama, H., T. Terao, and H. Kida, 2004: The role of high-frequency eddy forcing in the maintenance and transition of the Southern Hemisphere annular mode. *J. Meteor. Soc. Japan,* 82, 101-113.

Thompson, D. W. J., and J. M. Wallace, 2000: Annular modes in the extratropical circulation. Part I: Month-to-month variability. *J. Climate*, 13, 1000-1016.

--, D. J. Lorenz, 2004: The signature of the annular modes in the tropical troposphere. *J. Climate,* 17, 4340-4342.

Wilks, D. S., 1995: *Statistical methods in the atmospheric sciences.* Academic Press, New York, 467 pp.

Xue, F., H. Wang, and J. He, 2004: Interannual variability of Mascarene High and Australian High and their influences on east Asian summer monsoon. *J. Meteor. Soc. Japan,* 82, 1173-1186.

# INITIAL DISTRIBUTION LIST

1. Defense Technical Information Center
   Ft. Belvoir, Virginia

2. Dudley Knox Library
   Naval Postgraduate School
   Monterey, California

3. Dr. M. Steven Tracton
   Office of Naval Research
   Arlington, Virginia

4. Superintendent
   Naval Research Laboratory
   Monterey, California

5. Commanding Officer
   Fleet Numerical Meteorology and Oceanography Center
   Monterey, California

6. Professor Russell Elsberry
   Naval Postgraduate School
   Monterey, California

7. Professor Patrick Harr
   Naval Postgraduate School
   Monterey, California

8. Professor Tom Murphree
   Naval Postgraduate School
   Monterey, California

9. Director, Joint Typhoon Warning Center
   Naval Pacific Meteorology and Oceanography Center
   Pearl Harbor, Hawaii

10. Captain Kenneth Burton
    25th Operational Weather Squadron
    Davis Monthan AFB, Arizona